AN INHERENTLY SAFER APPROACH FOR NONTRADITIONAL DUST EXPLOSION RISK REDUCTION

by

Md Nur Hossain

Submitted in partial fulfilment of the requirements

for the degree of Doctor of Philosophy

at

Dalhousie University

Halifax, Nova Scotia

June 2016

This thesis is dedicated to the memory of my father, Md. Abdus Sattar whose unfailing support has always been the key to my success.

TABLE OF CONTENTS

List of Tables

List of Figures

Abstract

Dust explosions continue to occur in industrial processes that handle combustible powders. Considerable research is therefore conducted with the objectives of both preventing the occurrence and mitigating the consequences of such events. But, most of the research conducted in relation to dust explosion is based on traditional fuel/air system (e.g., micron-sized powder, spherical shape powder and fuel with single component). Due to the increased demand, nanotechnology and its applications; textile industries and other flock manufacturing plants; and pharmaceutical industries are growing rapidly day by day. Such industries can generate severe risk of explosions associated with nontraditional dusts (the term 'nontraditional' has been used in the current study as: (i) nano-sized powder rather than micron-sized (e.g., nano-sized Ti powder); (ii) flocculent materials characterized by a length-to-diameter ratio rather than a particle diameter (e.g., polyamide 6.6 and polyester fibers); and (iii) hybrid mixtures consisting of a combustible dust and a flammable gas or solvents rather than single component (e.g., lactose admixed with methanol)). A generalized Quantitative Risk Management Framework (QRMF) for dust explosions has been applied in the current work to integrate the above three nontraditional categories of dust explosions. Experimental results have been used as input to the quantitative risk management framework so as to provide a comprehensive procedure to analyze, assess, and control the likelihood and consequences of explosions associated with nontraditional dusts. Risk management strategies have been developed through a synthesis of experimental findings and a comprehensive literature review. Use of the QRMF for the three nontraditional fuel/air systems has been ensured with each system being considered from the key perspectives of hazard characterization, hazard identification, risk assessment, and risk control (along with other aspects of the quantitative risk management sequence). Explosion prevention and mitigation measures have been taken in an inherently safer approach which start with inherent safety measures at beginning, then passive and active engineered devices, and procedural measures in an hierarchical manner. The findings of this research can facilitate industrial facilities in Canada and worldwide with safer operations by preventing and mitigating explosions associated with the aforementioned nontraditional dusts.

List of Abbreviations and Symbols Used

Abbreviations:

2D view	Two Dimensional View
3D view	Three Dimensional View
ALARP	As Low As Reasonably Practicable
ATM	Atmospheric
atm	Atmospheric
ATM Condition	Atmospheric Condition
CASD	Computer Aided Scenario Design
CCPS	Center for Chemical Process Safety
CFD	Computational Fluid Dynamics
Conc.	Concentration
CSB	US Chemical Safety and Hazard Investigation Board
CV	Control Volume
DESC	Dust Explosion Simulation Code
DL	Dispersion Limitation
DustEx	Dust Explosion
E	Ethanol
ESC	Equivalent Social Cost
F	Frequency (Y^{-1})
FAR	Fatal Accident Rate
FLACS	Flame Acceleration Simulator
FLACS-DustEx	Flame Acceleration Simulator-Dust Explosions
FV	Finite Volume
I	Ignition
IE	Ignition Energy
Ind.	Inductance
IPA	Iso-propanol/ Iso-propyl Alcohol
ISD	Inherently Safer Design
ISIR	Individual Specific Individual Risk

Lactose + Ethanol (ATM)	Lactose Admixed with Ethanol in Atmospheric Condition
Lactose + Ethanol (PW)	Lactose Admixed with Ethanol in Pre-wetting Condition
Lactose + Iso-propanol (ATM)	Lactose Admixed with Iso-propanol in Atmospheric Condition
Lactose + Iso-propanol (PW)	Lactose Admixed with Iso-propanol in Pre-wetting Condition
Lactose + Methanol (ATM)	Lactose Admixed with Methanol in Atmospheric Condition
Lactose + Methanol (PW)	Lactose Admixed with Methanol in Pre-wetting Condition
LFL	Lower Flammable Limit
LOC	Limiting Oxygen Concentration
M	Methanol
MCC	Micro Crystalline Cellulose
MCC + Ethanol (ATM)	MCC Admixed with Ethanol in Atmospheric Condition
MCC + Ethanol (PW)	MCC Admixed with Ethanol in Pre-wetting Condition
MCC + Iso-propanol (ATM)	MCC Admixed with Iso-propanol in Atmospheric Condition
MCC + Iso-propanol (PW)	MCC Admixed with Iso-propanol in Pre-wetting Condition
MCC + Methanol (ATM)	MCC Admixed with Methanol in Atmospheric Condition
MCC + Methanol (PW)	MCC Admixed with Methanol in Pre-wetting Condition
MEC	Minimum Explosible Concentration
MIE	Minimum Ignition Energy
MIT	Minimum Ignition Temperature
MOC	Management of Change
MP	Metal Particle
N	Number of Fatalities
ND	Not Determined

NFPA	National Fire Protection Association
NI	No Ignition
NIOSH	National Institute of Occupational Safety And Health
OH&S	Occupational Health and Safety
OSHA	Occupational Safety & Health Administration
PET	Polyethylene Terephthalate
PHA	Process Hazard Analysis
PP	Pressure Panel
PS	Particle Size
PSD	Particle Size Distribution
PSM	Process Safety Management
PW	Pre Wetting
QRM	Quantitative Risk Management
QRMF	Quantitative Risk Management Framework
Relex	Reliability Excellence
ROD	Rate Of Death
SEM	Scanning Electron Microscope
SMS	Safety Management System
USD	Us Dollar
Vol.	Volume

Symbols:

$(dP/dt)_m$	Maximum rate of pressure rise due to an explosion test (bar/s)
$(dP/dt)_{max}$	Maximum rate of pressure rise (bar/s)
f_i	Frequency of incident outcome, case i (yr^{-1})
N_i	The number of fatalities resulting from outcome, case i
P_{ovr}	Overpressure (N/m^2)
P_T	Total predetermined population for average risk
$P_{x,y}$	Number of people at location x, y
$R_{Ind} = IR$	Individual risk
IR_{AV}	Average individual risk in the exposed population (yr^{-1})
$IR_{x,y}$	The total individual risk of fatality at geographical location x, y (yr^{-1}).
$IR_{x.y,i}$	Individual risk at location x, y (yr^{-1})
$p_{f,i}$	Probability of fatality
°C	Degrees celsius
A_{V0}	Total calculated area of pressure panels (m^2)
C_2H_5OH	Ethanol
C_3H_7OH	Iso-propanol
CH_3OH	Methanol
D_{eq}	Equivalent characteristic size of the flocks
d_f	Diameter of a flock
Dtex or decitex	A unit of measuring the linear density of fibers
E_s	Statistic energy
F_S	Frequency of scenarios (y^{-1})
g/cm^3	Gram per cubic centimeter
g/m^3	Gram per cubic meter
IE	Ignition occurred at energy level IE
k	Constant
K	Turbulent Kinetic energy

K_1, K_2	Probit correlation causative variables
kg/m^3	Kilogram per cubic meter
kJ	Kilojoules
kJ/mol	The kilojoule per mole
kPa	Kilopascal
K_{st}	Dust deflagration index (dust cloud explosion violence) (bar•m/s)
L	Liter
m	Meter
m^2	Square meters
m^3	Cubic meter
mg	Milligram
mH	Millihertz
micro Ti	Micron-sized titanium
mJ	Millijoule
ml	Milliliter
mm	Millimeter
ms	Millisecond
N	Number of trials conducted
N_2	Nitrogen
Nano Ti	Nano-sized titanium
N_F	Total number of fatalities
N_I	Number of combustions successfully induced
NIE	No ignition was observed at energy level IE
N_L	Average number of people at the location
nm	Nano (10^{-9}) meters
P	Pressure (N/m^2)
P	Probability
P_m	Maximum pressure reached due to an explosion test (bar)
P_{max}	Maximum explosion pressure (bar)
P_{red}	Reduced pressure after explosion venting (bar(g))
P_{stat}	nominal static burst pressure of pressure panels (bar(g))

R	Risk
S	Severity of consequences
t	Time (s)
t_{exp}	Total explosion time
TiO_2	Titanium dioxide
t_v eff	Effective time delay
t_v set	Set time delay
V	Enclosure volume
W	Watt
Y	Probit variable (unit-less)
μm	Microns (10^{-6}) meters
p	Risk aversion power factor

Acknowledgments

It is a pleasure to acknowledge sincere gratitude to my research supervisor, Dr. Paul Amyotte, for his encouragement, guidance, support and friendly advice throughout the course of this study. I am truly grateful to have him as my Ph.D. supervisor and also as mentor, philosopher and guardian for more than the last 4 years of my life.

I would also like to express my honest appreciation to others who helped:

To the other members of my examining committee, Dr. M.J. Pegg, Dr. Faisal Khan and Dr. Jan Haelssig , for their assistance in the preparation of this document;

To the Chemical Engineering Department of the Dalhousie University which provided financial support in the form of a teaching assistantship;

To the Natural Sciences and Engineering Research Council of Canada (NSERC), for their financial support in the form of a full-time graduate research scholarship;

To the Gexcon AS, for their support by providing the license of FLACS-DustEx (FLame ACceleration Simulator—Dust Explosions);

To my colleagues Meftah Abuswer, Yuan Chunmiao, Ivan Iarossi, Morgan Mackenzie, Chris Cloney, Martin Clouthier, Simon Boilard, Vincent Boilard, Kalie Symington and Ben Smith, for their assistance with huge support and helping during my study and experimental work;

To Mr. Matt Kujath for his help in procedure development for explosibility testing of nanotitanium powder.

To my wife, Iffat Jahan, for her love, support and kind understanding;

To my friends and neighbors from the Bangladeshi Community in Halifax, Sharif bhai and Liza apu, Rupok bhai and Rinku apu, Mushfiq bhai and Tithi bhabi, Murad and Fahria, Ashif and Sifat, Fatmi and Nitol, Bappy, Shakil, Sabbir, Avijit, Rusho and Robin for their friendly support during my study.

To my mother, Momtaz Begum and the rest of my family for their support and patience throughout the course of this study.

Chapter 1 Introduction

A brief introduction to dust explosions, and the motivation, scope and objectives of the current research are given in Chapter 1.

1.1 Introduction

Dust explosion risk reduction has been the subject of intensive research for several decades now. However, there remains a strong need for continued research on dust explosions—especially for dusts that may be termed nontraditional when compared with the more common and frequently tested micron-sized, spherical particles comprising a single-fuel powder.[1] The specific fuel/air systems studied here fall into three nontraditional categories: (i) micron-and nano-sized titanium powders, (ii) flocculent polyamide 6.6 and polyester, and (iii) hybrid mixtures of lactose and microcrystalline cellulose dusts admixed with methanol, ethanol and isopropanol solvents. The relevant industrial applications are the handling of metallic nano-powders, fabric and textile processing, and pharmaceutical manufacturing, respectively.

Recent advancements in material science and engineering technology have resulted in a corresponding increase in the number of nanoscale products. An investigation into accidental explosions in Taiwan has revealed that metal dust explosions occur most frequently among the various types of dust explosions.[2] As a consequence, "nano-safety" has emerged as a new area of concern, especially for nano-sized metal powders.[3] Dust explosion is a common hazard encountered in the metal processing industry because most combustible metals can be as energetic and hazardous as organic fuels.[4] Explosibility parameters are important considerations for dust explosion prevention, and they have been

well documented for metallic particles in the micron range.[5,6] The unique physical and chemical properties of nano-sized metal powders increase the explosion potential.[7–10]

Flocculent materials are fibrous (non-spherical in shape). Flocculent fibers cannot be well characterized by diameter only, and are better described by length-to-diameter ratio. Flocculent materials, for example cotton, acrylic, and polyester are used in many industrial applications. Due to increasing demand of flocculent materials in industries, using such materials may present explosion hazards similar to spherical dusts, and they should be handled with adequate protection and safety measures. There was a severe explosion in 1995 involving nylon flock fibers at the Malden Mills facility in Massachusetts, USA, which injured 37 people and destroyed the entire facility.[11] Managers at the Malden Mills facility did not consider flock fibers as a potentially combustible dust prior to the accident.[11] Explosions associated with flocculent materials continue to occur in many facilities that handle fibrous products. Continued research is therefore needed to prevent the occurrence of, and mitigate the consequences of, such events associated with flocculent materials.

Hybrid mixtures consist of a flammable gas/liquid and a combustible dust and are common in many situations that occur in the pharmaceutical industry. A typical example of a hybrid fuel system is methane gas and coal dust in underground coal mines.[12] Explosions associated with hybrid mixtures continue to occur in many industrial processes that handle combustible dust and flammable gases or liquids. Explosion scenarios of hybrid mixtures have been studied with three possible approaches: (i) gaseous solvent at room temperature existing in the combustion atmosphere prior to dust dispersal, (ii) liquid solvent at room temperature requiring flashing-off for admixture to the combustion atmosphere prior to dust dispersal, and (iii) liquid solvent at room temperature admixed as a liquid with the dust prior to dust dispersal. The introduction of flammable solvents in either liquid or

gaseous form can significantly enhance the explosibility parameters of excipients (non-pharmaceutically active dusts) alone. The influence of the co-presence of a flammable gas on the explosibility parameters of a fuel dust alone is a well-established fact, as noted by Amyotte & Eckhoff[13]. However, due to the vast expanse of the subject matter and its wide range of industrial applications, continued research on hybrid mixtures is still needed, as seen in recent studies.[14–21]

In the current work, a generalized Quantitative Risk Management Framework (QRMF) for dust explosions as described by Abuswer et al.[22], has been adapted to the three aforementioned nontraditional categories of particulate fuel/air systems in order to assess and control the risks. Use of the QRMF for the three nontraditional fuel/air systems is ensured, with each system being considered from the key perspectives of hazard characterization, risk (consequence and likelihood) assessment, and risk control (along with other aspects of the quantitative risk management sequence).

1.2 Motivation for the Current Research

The current research is motivated by the occurrence of dust explosion scenarios in nanotechnology and its applications; textile industries and other flock manufacturing plants; and pharmaceutical industries and other industries that deal with hybrid mixtures. Risks associated with these three types of particulate fuel/air systems can be prevented and mitigated by comprehensive assessment and application of the strategies of controlling risks, as addressed in the current work. Consequently, this research has been conducted to protect people, assets, production, and the environment.

1.3 Research Scope and Objectives

The scope of the research is the prevention and mitigation of explosions associated with nontraditional dusts. The primary goals are to assess explosion risks associated with three categories of nontraditional fuel/air systems and to develop strategies by which nontraditional dust explosions can be prevented and their consequences mitigated. In order to achieve these goals, the objectives of the current research are summarized as follows:

- To provide explosion likelihood and explosion severity data acquired through best-practice testing methodologies using standardized apparatus.
- to investigate the influence of liquid and vapourized solvent (methanol, ethanol, and isopropanol at a concentration 80% of its lower flammability limit) on explosion severity and explosion likelihood parameters of pharmaceutical-grade MCC (microcrystalline cellulose) and lactose powder.
- to examine the inerting effect of nano-sized TiO_2 powder on the minimum ignition energy (MIE) of nano- and micron-sized Ti powders.
- to investigate the inerting effect of nano-sized TiO_2 powder on the minimum ignition temperature (MIT) of nano- and micron-sized Ti powders.
- to investigate the influence of fiber length on the explosibility parameters of polyamide 6.6 computationally.
- to investigate the influence of solvent admixture on the explosibility of pharmaceutical-grade MCC at laboratory- and industrial-scale computationally.
- to incorporate inherently safer design (ISD) principles in managing explosion risk associated with the three categories of nontraditional fuel/air systems investigated.

1.4 Original Contributions of the Research

Limited studies in the field of dust explosion research have dealt with nontraditional dust explosion and risk reduction. The current research provides an inherently safer approach to prevent and mitigate explosions associated with the three aforementioned nontraditional categories of particulate fuel/air systems. Based on the hierarchy of controls (inherent, engineered, and procedural safety), this approach can effectively help various constituencies (e.g., research laboratories, test facilities, design engineers and industrial practitioners) in understanding prevention and mitigation strategies for nontraditional dust explosions.

The influence of the solvents (methanol, ethanol and isopropanol) on explosibility parameters of MCC (micro crystalline cellulose), and lactose in the pre-wetting mode (liquid solvent at room temperature admixed as a liquid with the dust prior to dust dispersal) as determined in the current research is critically important wherever the process of premixing flammable solvents into powder is utilized. The results provide a useful input in assessing risks for situations having such explosive atmospheres in industrial applications.

In the current research, the effectiveness of using nano-sized TiO_2 powder as a solid inertant in prevention and mitigation of explosion risks associated with micron- and nano-sized titanium powder has been investigated. The outcomes of this research finding can provide an approach for reducing ignition sensitivity of nano Ti powder to electric sparks and in contact with hot surfaces.

The Computational Fluid Dynamics (CFD) tool FLACS-DustEx (FLame ACceleration Simulator—Dust Explosions), which was previously marketed as DESC (Dust Explosion Simulation Code), has been used to simulate explosion scenarios in an industrial-scale for

nontraditional dust (flocculent polyamide 6.6 and polyester, and hybrid mixtures of MCC dust admixed with methanol, ethanol and isopropanol solvents). The simulation results can be useful to predict possible explosion scenarios and to estimate the explosibility parameters in practical industrial applications.

1.5 Outline of the Thesis

This thesis comprises six chapters, which are organized as follows. The first chapter provides a brief introduction to the research topic and states the motivation and objectives of the study. The fundamentals of dust explosions and relevant background knowledge are described in the second chapter. A review of the pertinent literature is presented in the third chapter. This review provides a brief summary of completed research in the investigation of explosions associated with the three categories of nontraditional fuel/air systems studied here. Chapter four describes experimental results. The content of the fifth chapter is based on an adaptation of QRMF to the three aforementioned nontraditional categories of particulate fuel/air systems. In addition, chapter five describes strategies for risk reduction of nontraditional dust explosions. Chapter 4 and 5 contain experimental and simulation results as following a series of technical papers that have been published in peer reviewed journals and conference proceedings.

Finally, the sixth chapter presents the conclusions of the research work and provides recommendations for future research. Figure 1-1 summarizes the overview of the thesis described above.

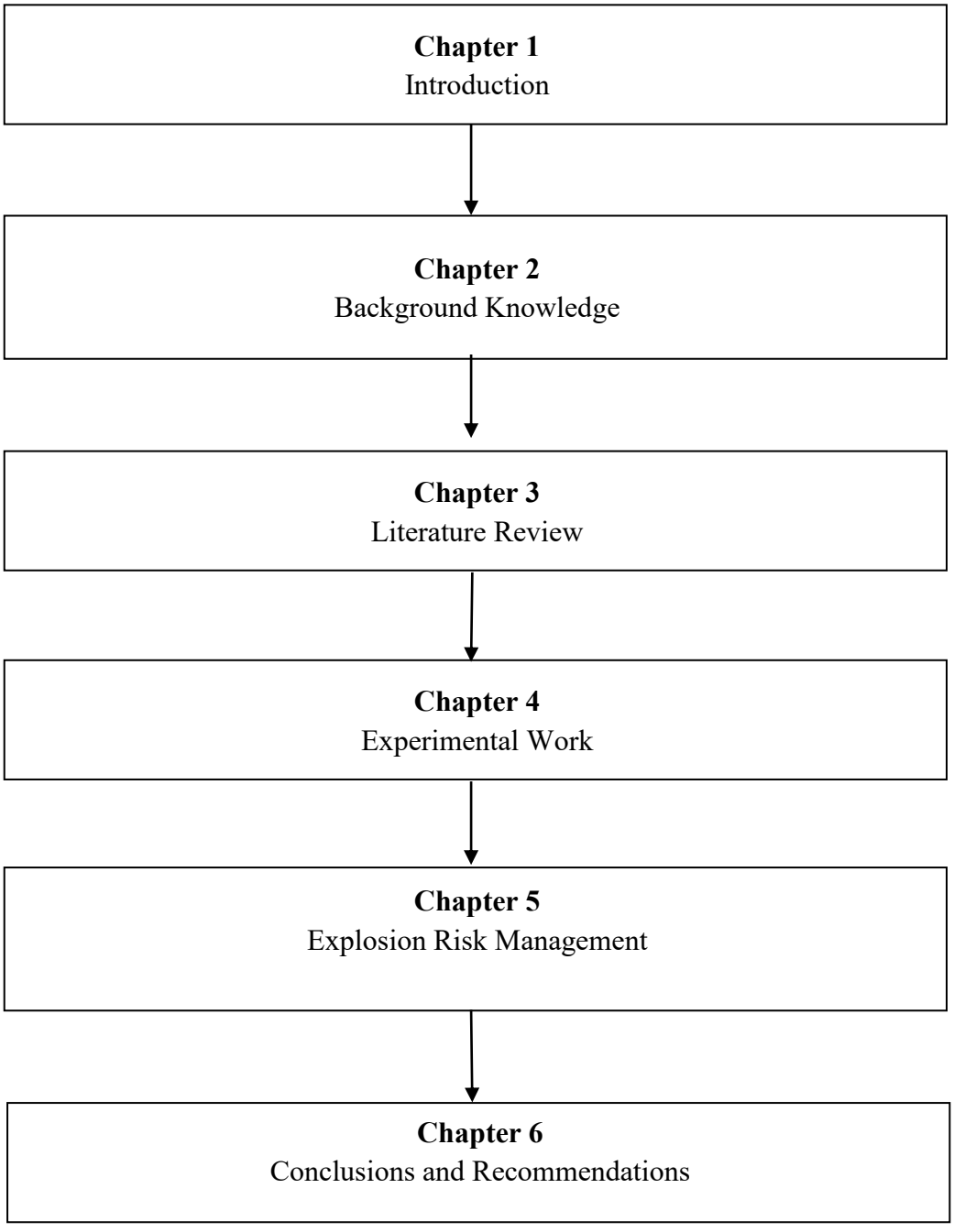

Figure 1-1 Thesis overview.

Chapter 2 Background Knowledge

The fundamentals of dust explosions and relevant background knowledge are described in this Chapter.

2.1 Fundamentals of Dust Explosions

Dust is comprised of small particles in the atmosphere, usually found as particulate solid material suspended in air. The U.S. National Fire Protection Agency (NFPA) has produced several definitions of combustible dust over the years. According to their most recent definition, combustible dust is a solid which has the ability to explode and cause a fire or deflagration hazard when suspended in air or some other oxidizing medium over a range of concentrations, regardless of particle size and shape.[23] Particle size distribution is one of the main concerns in efforts aimed at preventing dust explosions and mitigating consequences. Another important issue is the shape of the dust, which is characterized by its structural arrangement of the particles. Particle size, distribution, and shape determine the amount of total exposed surface. Surface area controls the reactivity of the dust in the combustion process. Higher surface area exposes more reactant to participate in the combustion process and subsequently generate explosions with greater severity and likelihood.

A dust fire occurs when the combustible dust (fuel) is exposed to heat (an ignition source) in the presence of oxygen (air). These elements constitute the fire triangle, which is required to satisfy the conditions for a possible fire. However, the requirements for a dust explosion demand two additional factors: dispersion of dust particles (mixing) and confinement[6]. The dust explosion pentagon is formed when all five of these elements are present, as shown in Figure 2-1.[13] Dispersed dust burns rapidly and confinement allows

pressure to build. Without the presence of dispersion (mixing) and some degree of confinement, an explosion cannot occur.

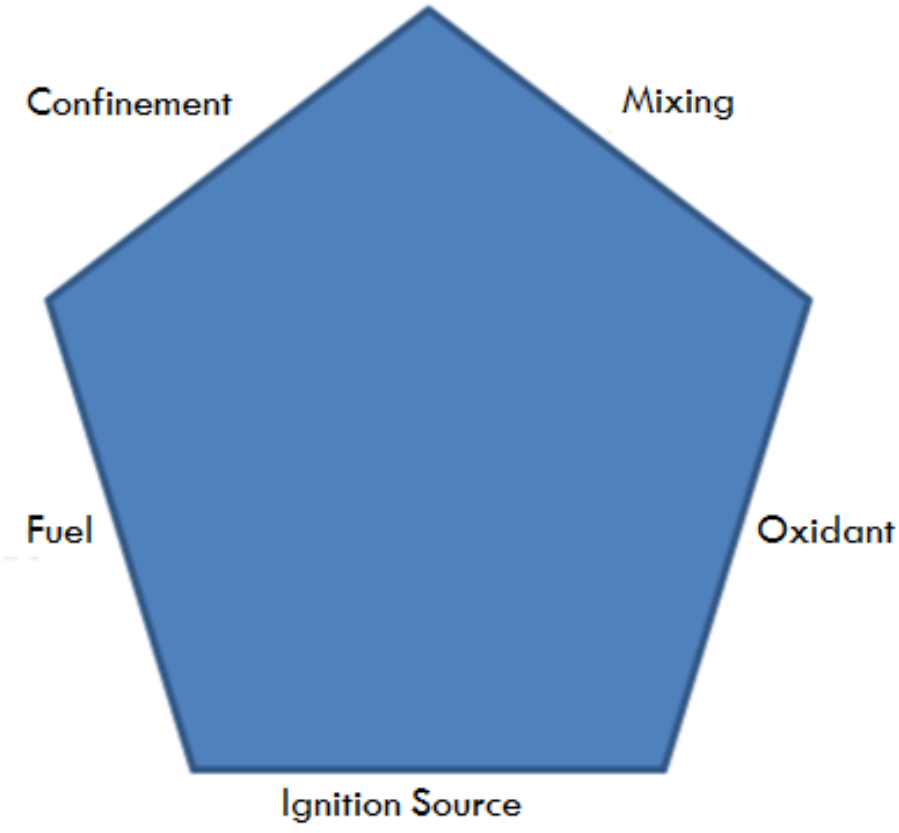

Figure 2-1 Dust explosion pentagon.[13]

Both the fire triangle and explosion pentagon still hold for nontraditional-dust explosions but the concentration, particle size, particle shape and mixing requirements could provide increased severity and likelihood of an explosion. Many types of ignition sources can cause dust explosions. An ignition source needs to be sufficiently energetic in order to cause the dust to ignite. Common ignition sources are:[6]

- Smouldering or burning dust.

- Open flames (welding, cutting, matches, etc.).
- Hot surfaces (hot bearings, dryers, heaters, etc.).
- Heat from mechanical impacts
- Electrical discharges and arcs.

The dust particles are suspended in air when a dust cloud is produced. In this phase, the finest particles will remain in suspension while the coarser particles settle. Typical stages of a dust explosion scenario are illustrated in Figure 2-2.[9]

Most organic materials and many metals, and even some non-metallic inorganic materials, if finely divided and dispersed into air with an adequate concentration will burn or explode in the presence of an ignition source.[6] Combustible dust includes metals (such as aluminum and magnesium), wood, coal, plastics, sugar, paper, soap, dried blood, candy, spice, starch, flour, feed and certain textiles.[6] Combustible dust may also exist in a variety of industrial facilities, including grain, tobacco, pulp, rubber, furniture, pesticides, pharmaceuticals, dyes, coal, and fossil fuel power generation. Table A.1 (Appendix A) lists major chemical industries that may have combustible dusts. The types of combustible dusts play a strong role in the explosion severity and likelihood as the composition of the material dictates the combustion process that takes place.

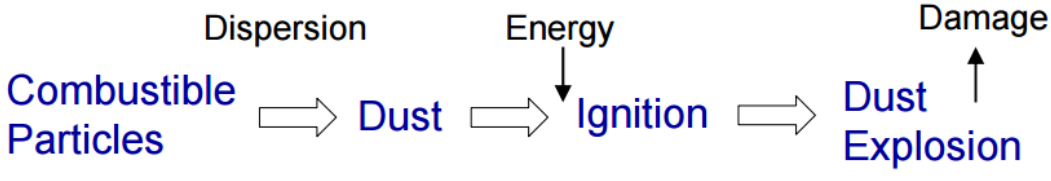

Figure 2-2 Dust explosion scenario.[9]

A dust cloud can be generated when a combustible material is handled in industrial facilities. Such a dust cloud also can be generated due to segregation of the particles as the process evolves.[6] Explosion potential is high if the dust particles are fine and oxidize easily. A dust cloud, when ignited, can produce deflagrations, which are flame fronts that move at speeds below the speed of sound. Combustible particles absorb heat by an ignition source, after which, some types of dusts (e.g., polymeric dusts) melt before devolatilize; and others (e.g., most organic dusts) gasify rather than melt as a result of heating. Once vapor is formed, it reacts and combusts as a gas in the combustion reaction zone, and the flames start to propagate, as shown in Figure 2-3.[9]

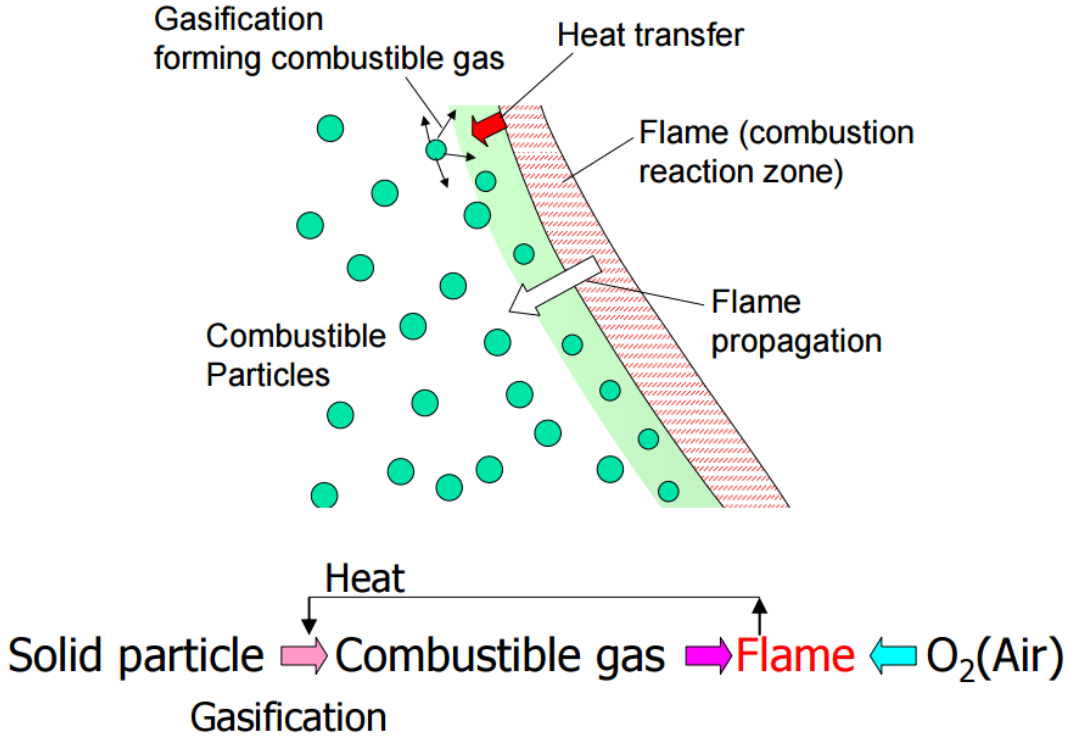

Figure 2-3 Process of dust explosion.[9]

Dust explosions may have two distinct stages, primary and secondary explosions. The distinction between primary and secondary explosions can be so close together that

they may be heard as one explosion, or a series of explosions. The primary explosion is caused by a confinement of airborne dust in contact with a heat source that ignites the dust. These explosions commonly occur within process equipment (mills, mixers, grinders, dryers, etc.).[6] Secondary explosions as explained in Figure 2-4 occur outside of the equipment in the process area and are fueled by dust deposits being disturbed by a primary explosion.[24] Secondary explosions can result in damage that is more severe than the primary explosion due to increased concentration and amount of combustible dust.

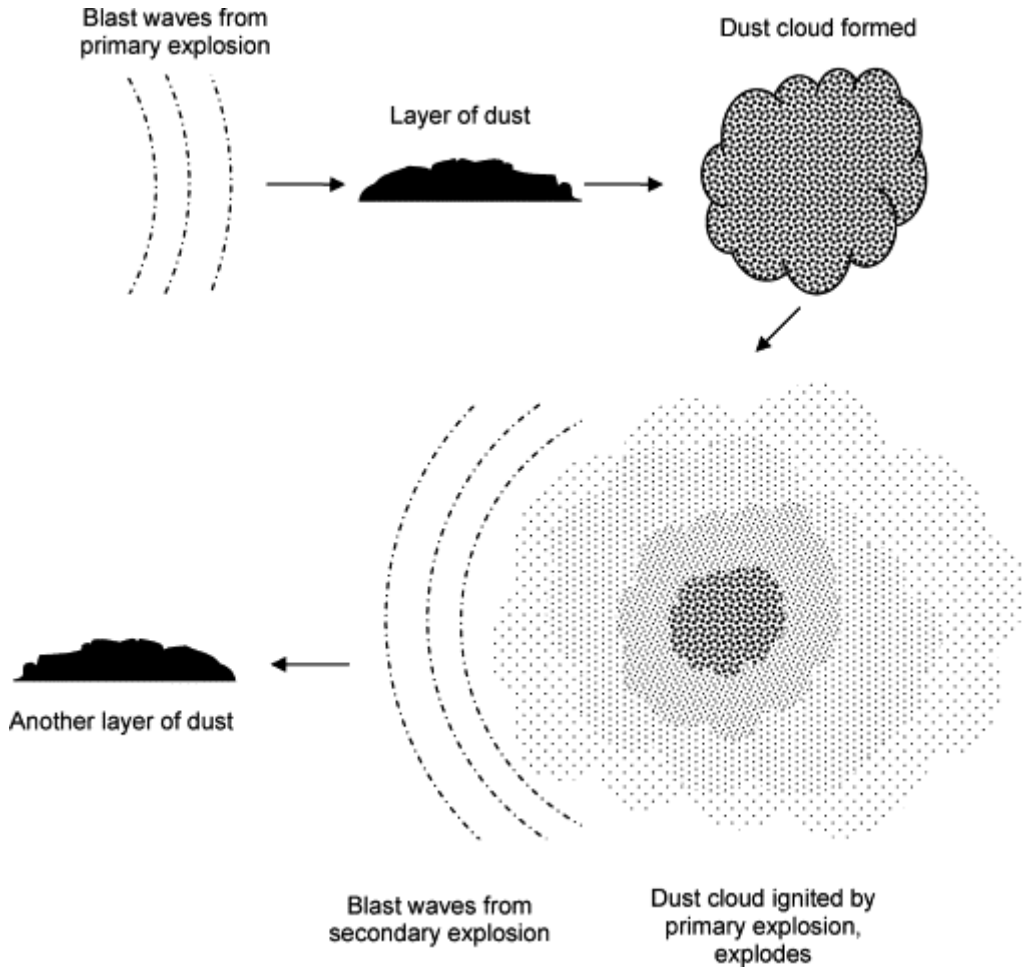

Figure 2-4 Primary and secondary explosions.[25]

2.2 Nontraditional Dusts as Potential Hazards

In the current work, nontraditional dust is considered as: (i) nano-sized titanium powders, as compared to traditional micron-sized; (ii) flocculent or fibrous, as compared to traditional spherical shape; and (iii) hybrid mixtures, as compared to single fuel powder. Industries that produce these types of nontraditional powder are growing rapidly for their many commercial uses. For example, nanomaterials are widely used in mechanical and chemical polishing, magnetic recording tapes, sunscreens, automotive catalyst supports, bio-labelling, electro-conductive coatings and optical fibers.[26] The biomedical and pharmaceutical fields, electronics, metallurgy, agriculture, textiles, coatings, cosmetics, energy and catalysts are other sectors with growing applications of nanomaterials.[26] Due to the size of nanoparticles, both physical and chemical change can occur that may influence the severity and likelihood parameters of dust explosions.[7] A few examples of flocculent materials and their application are plastic/polymers production and associated products (e.g., polyamide, polyester, linen flax, cotton, wood, etc.).[13,27] Hybrid mixtures can be generated by the addition of solvents into powders such as catalysts, pigments, and other reactants in a reactor, hopper or large container within the process industry, especially in pharmaceutical industries.[28] Nontraditional dust over a range of concentrations is capable of exploding and causing a fire or deflagration hazard when suspended in air or some other oxidizing medium. There can be increasingly potential hazards and risks as the production and use of nanomaterials, flocculent materials, and hybrid mixtures continue to grow.

2.3 Past Accidents in the Literature

Learning from past industrial accidents will lead the development of safety measures and establish required standards and guidelines that can be used to prevent and mitigate explosions associated with nontraditional dust.

Abbasi and Abbasi[25] compiled a comprehensive summary of dust explosions that occurred around the world from 1785 to 2004. Some of the accidents mentioned in their report are associated with metal powders, fibrous materials, and hybrid mixtures, deepening the demand for continued research in the area of nontraditional dust explosions. Table B.1 (Appendix B) provides a tabulated review of dust explosion incidents between 1911 and 2004.[29]

A few past industrial explosions are mentioned below:

In 1973, at a slurry explosive factory in Norway, a massive explosion occurred in a batch mixer when fine aluminum flakes, sulfur, and other ingredients were being mixed. Five workers were killed and a substantial part of the plant was destroyed.[25] Another fatal dust explosion occurred at a textile plant in China in 1987.[25] The explosion took place in the dust-collecting unit, possibly ignited by an electrostatic spark, killing 58 workers and injuring another 177. In 2002, five workers died from a severe explosion at Rouse Polymeric International Inc., a rubber recycling plant in Mississippi.[25] In 2003, an explosion occurred with fibrous polyethylene dust at West Pharmaceuticals, Kinston, NC. As a consequence, six workers died and 38 others were injured.[30]

Upon reopening of a nano titanium bag of 100 g (not under nitrogen due to handling difficulties) the titanium spontaneously ignited as reported by Boilard[24]. A similar incident (nano-titanium spontaneously ignited) occurred at the University of Wisconsin-

Madison when the researcher was using a spatula to remove 2 g of powder.[31] Other than these two lab incidents, no industrial cases have been reported for nano-titanium. However, like many metal powders, a few industrial incidents have occurred associated with micron-sized titanium powder resulting in severe injuries and, in some cases, fatalities. For example, A fire erupted at a metal recycling plant in Los Angeles where titanium was ignited on July 13, 2010.[32] Firefighters responded to the scene as soon as the accident happened and water was used to extinguish the flame. Seven firefighters were injured and the total damages were estimated at 5 million USD.[33,34]

An explosion of hybrid mixture occurred in East Rutherford, New Jersey at the US Ink/Sun Chemical Corporation on October 9, 2012 is reported in a completed investigation report by the US Chemical Safety and Hazard Investigation Board (CSB)[35] This explosion occurred in the ink mixing room after a loud 'thump' was heard from the newly installed dust collection system.[35]

These examples and the proliferation of dust explosions serve to increase the demand for further study and ongoing research in this field.

2.4 Basic Explosion Characteristics

Basic explosion characteristics of a combustible dust for both perspectives of explosion severity and likelihood are given below.

2.4.1 Explosion Severity

The maximum explosion overpressure, P_{max}, and the maximum rate of pressure rise, $(dP/dt)_{max}$, characterize the explosion behavior of a combustible dust in a closed system. These parameters are determined by dispersing a dust into an explosion chamber (e.g., Siwek 20-L chamber), and igniting the dust cloud at a predefined delay time after dust dispersion. Tests are conducted over a range of dust concentrations using a standardized protocol to determine the maximum of the explosion pressure parameters. As the rate of pressure rise is dependent on the volume of the specific chamber used for testing, a size-normalized maximum rate of pressure rise, K_{St}, is calculated by the following cubic relationship as shown in Equation (1).

$$K_{St} = (dP/dt)_{max} V^{1/3} \quad (1)$$

where

V is the volume of the apparatus.

Maximum explosion pressure and size-normalized maximum rate of pressure rise are required to predict explosion scenarios and to ensure adequate safety measures for preventing and mitigating dust explosions.[36]

2.4.2 Likelihood of Occurrence

Likelihood of occurrence is evaluated mainly through determining the minimum ignition energy (MIE), minimum ignition temperature (MIT), and minimum explosible concentration (MEC). Limiting oxygen concentration (LOC) and other ignition sensitivity parameters can also be considered.

The minimum ignition energy (MIE) of a dust cloud is defined as the lowest energy spark required to ignite a dust/air mixture. MIE is often determined using the MIKE 3 apparatus, which consists of a 1.2-L transparent cylindrical glass tube with a dust dispersion cup at the base. A spark of known energy at specified energy levels is generated at a set time delay after dust dispersion.

The minimum ignition temperature (MIT) is the lowest temperature of a hot surface that will cause a dust cloud to ignite and spread flames and is determined using an apparatus such as the BAM oven. This test is intended to determine the ignition temperature of airborne dust on a hot surface. The lowest temperature of the heated impact plate at which the dust ignites is identified as the minimum ignition temperature. Hot surfaces capable of igniting dust clouds may exist in a number of circumstances in industrial facilities, such as in furnaces and burners, as well as in dryers of various kinds. If an explosible dust cloud is generated in an uncontrolled way within the confined space of a hot surface at a temperature above the minimum ignition temperature, the result can be a dust explosion.[37] Therefore, it is essential to know the minimum ignition temperature of combustible dust. Precautions and safety measures should be taken to ensure that temperatures of hot surfaces always remain below the minimum ignition temperature.

The minimum explosible concentration (MEC) corresponds to the smallest concentration that will explode when dispersed in air and is typically determined using the 20-L apparatus. The MEC of a dust can be used to define prevention methods against explosions associated with that dust. The limiting oxygen concentration (LOC) is the lowest oxygen concentration below which combustion is not possible, and is usually determined using the 20-L apparatus.

In the experimental work, ASTM International standards[38–41] were followed using standardized dust explosibility test equipment: (i) Siwek 20-L explosion chamber for P_{max}, K_{St} and MEC, (ii) MIKE 3 apparatus for MIE, and (iii) BAM oven for MIT. The first two of these parameters (P_{max} and K_{St}) are related to explosion severity, while the latter four (MEC, MIE, LOC and MIT) provide information on the explosion likelihood.

Typical units, description, and addressed risk components of the above explosion parameters are given in Table 2-1.[13] The higher the value of the K_{St}, the more severe the dust explosion is.

Table 2-1 Explosibility parameters and risk components.[13]

Parameter	Typical Units	Description	Risk Component Addressed
P_{max}	bar(g)	Maximum explosion pressure in constant-volume explosion	Consequence severity
$(dP/dt)_{max}$	bar/s	Maximum rate of pressure rise in constant-volume explosion	Consequence severity
K_{St}	bar.m/s	Size- or volume-normalized maximum rate of pressure rise in constant-volume explosion	Consequence severity
MEC	g/m^3	Minimum explosible dust concentration	Likelihood of occurrence
MIE	mJ	Minimum ignition energy of dust cloud (electric spark)	Likelihood of occurrence
MIT	°C	Minimum ignition temperature of dust cloud	Likelihood of occurrence
(LOC)	volume %	Limiting oxygen concentration in the atmosphere for flame propagation in dust cloud	Likelihood of occurrence

2.5 Risk Management Framework

Quantitative Risk Management (QRM) has gained extensive recognition as a powerful tool to identify and assess significant sources of risk and to measure the effectiveness of different risk controls. The generalized framework shown in Figure 2-5

described by Abuswer et al.[22] has been adapted to the three aforementioned nontraditional categories of particulate fuel/air systems in order to assess and control risks.

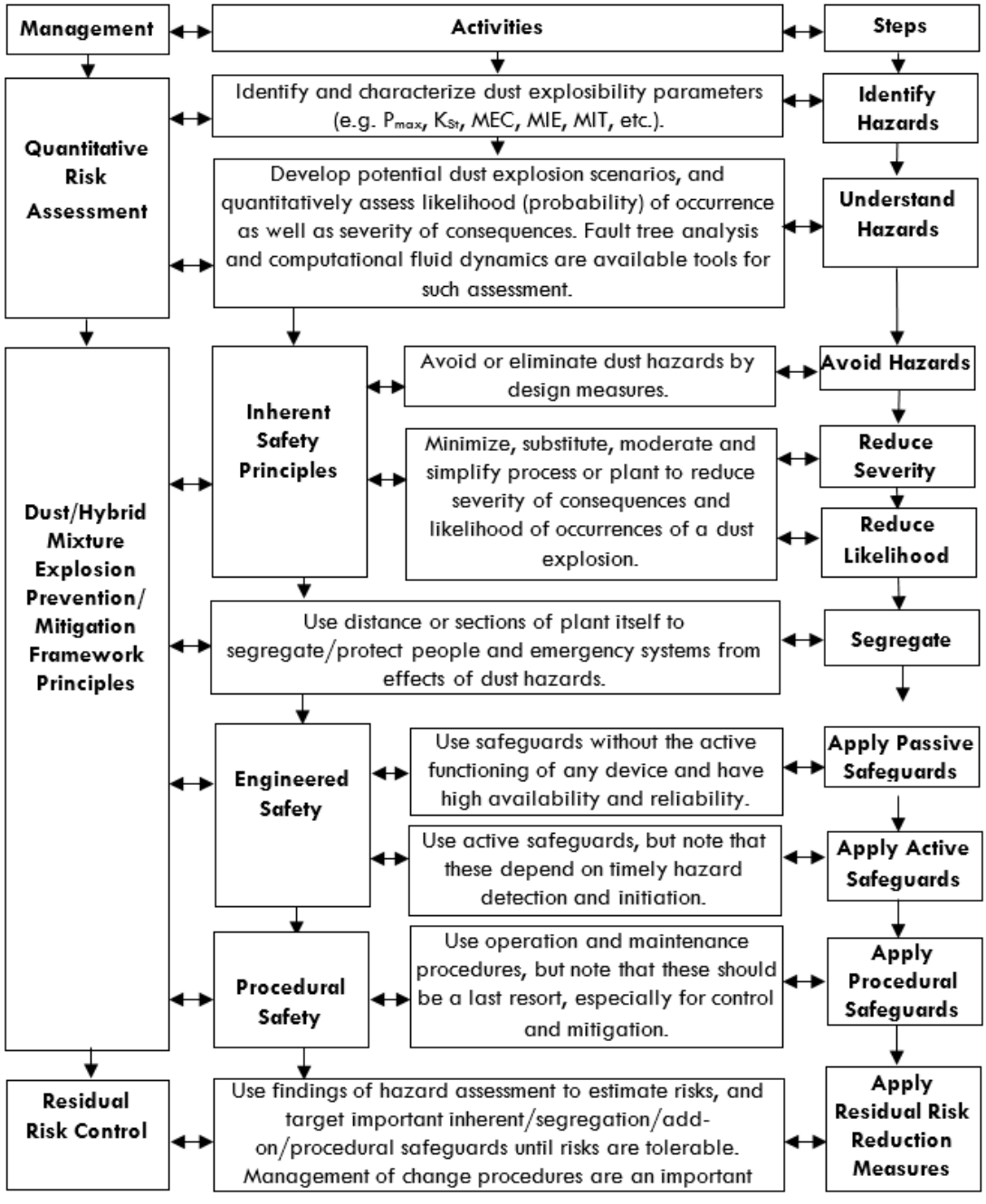

Figure 2-5 Generalized risk management framework for dust explosions.[22]

Some key steps and associated components for quantitative risk management are discussed below.

2.5.1 Hazard Identification and Characterization

Combustible dusts need to be characterized by determining their explosibility parameters (e.g., P_{max}, K_{St}, MEC, MIE, MIT), and considering the influences of several factors (e.g., particle size and agglomeration, moisture content, solvents in case of hybrid mixtures, inert content, etc.) on the explosibility parameters.

2.5.2 Risk Assessment

There is a need to analyze what risks may be present after all potential hazards have been identified. Risk should be determined on the basis of how often an event, or incident, is likely to occur (frequency), and what the consequences are from that event. Total risk can be determined by Equation (2).[42]

$$R = S * P \tag{2}$$

where

R = total risk.

S = severity of consequences.

P = likelihood of occurrence.

2.5.2.1 Severity of Consequences

Two steps are required to determine explosion consequences. First, explosion scenarios should be created for areas threatened by a combustible powder. FLACS-DustEx (FLame ACceleration Simulator—Dust Explosions) software is capable of predicting

explosibility parameters in the affected locations. Explosion overpressure (P_{max}), as determined by FLACS-DustEx, is the most important parameter needed to calculate damage. Then the effects after explosion, such as deaths, injuries, and structural damage, can be measured depending on the number of causative variables (K_1, K_2) by Equation (3).[43]

$$Y = K_1 + K_2 \ln (\mathrm{P_{ovr}}) \quad (3)$$

where

Y = Probit variable (unit-less).

$\mathrm{P_{ovr}}$ = overpressure (N/m^2).

2.5.2.2 Likelihood of occurrence

The QRMF uses Fault Tree Analysis (FTA) to estimate the likelihood or probability of a dust explosion for a given scenario. FTA is an analytical tool to determine the probability of occurrence of an undesired event by means of a series of "AND & OR" logic gates. FTA is also capable to determine various possible causes that can lead to the top event or accident.

2.5.3 Risk Control

Risk reduction strategies for nontraditional dusts have been structured according to three categories of control measures (inherent, engineered and procedural safety). The provision of considering inherent safety and other safety measures to prevent or mitigate nontraditional dust explosions is explained below according to the hierarchy of controls, starting from the most effective inherent safety measure to the least effective procedural

safety measure. The definitions of the four safety measures according to the hierarchy of controls as given in CCPS[44] are captured here as follows:

Inherent: Eliminating the hazard by using materials and process conditions that are non-hazardous; i.e., substituting water for a flammable solvent;

Passive: Minimizing the hazard through process and equipment design features that reduce either the frequency or consequence of the hazard without the active functioning of any device; i.e., providing a diked wall around a storage tank of flammable liquids;

Active: Using controls, alarms, safety instrumented systems, and mitigation systems to detect and respond to process deviation from normal operation; i.e., a pump which is shut off by a high level switch in the downstream tank when the tank is 90% full. These systems are commonly referred to as engineering controls, although human intervention is also an active layer;

Procedural: Using policies, operating procedures, training, administrative checks, emergency response, and other management approaches to prevent incidents, or to minimize the effects of an incident; i.e., hot work procedures and permits. These approaches are commonly referred to as administrative controls.

The difference between inherent safety and the other two categories (engineered and procedural safety) is that inherent safety seeks to eliminate the hazard at the source as opposed to accepting the hazard and looking to prevent its occurrence or mitigate its effects.[13] Unlike the other controls for risk reduction, inherent safety is mainly applied for removing the hazard in the design stage of the process.

2.5.3.1 Inherent safety

The four key principles of inherently safer design: minimization, substitution, moderation, and simplification, as stated by Amyotte and Eckhoff[13] are summarized as follows in Table 2-2.[13]

Table 2-2 Principles of inherently safer approach.[13]

Principle	Description
Minimization	Use smaller quantities of hazardous materials when the use of such materials cannot be avoided or eliminated. Perform a hazardous procedure as few times as possible when the procedure is unavoidable.
Substitution	Replace a substance with a less hazardous material or processing route with one that does not involve hazardous material. Replace a hazardous procedure with one that is less hazardous.
Moderation	Use hazardous materials in their least hazardous forms or identify processing options that involve less severe processing conditions.
Simplification	Design processes, processing equipment, and procedures to eliminate opportunities for errors by eliminating excessive use of add-on safety features and protective devices.

2.5.3.2 Passive engineered safety

Passive engineered safety measures perform their function independently without the active functioning of devices. Explosion relief vents are good example of such passive add-ons which release explosion pressure when the pressure rises.[13]

2.5.3.3 Active engineered safety

Engineered safety add-on devices that require mechanical activation are referred to as active devices. These devices require failure detection and subsequent mechanical activation to perform their function. Active engineered devices are less reliable than passive devices; therefore, they must be properly maintained and tested to limit the possibility of failure. Examples of such active devices include explosion suppression systems, active block valves, etc.

2.5.3.4 Procedural safety

From most of the past investigations of dust explosions by the US Chemical Safety Board (CSB), it has been found that some accidents could have been prevented and their effects could have been reduced if proper procedural safety measures had been in place. Some common procedural safety measures are discussed below.

Procedural safety measures are recommended policies, operating procedures, training, administrative checks, emergency response, and other management approaches to prevent explosions, or to minimize the effects of an explosion. Adequate procedural safety measures are required for controlling accumulations of nontraditional dusts on floors, elevated platforms, and other areas in the facility. Safe work procedures (e.g., hot work permit) for nontraditional dusts are vital to avoid ignition sources. In addition, implementing a preventive maintenance program for leak detection and leak mitigation procedures for flammable gas piping and gas processing equipment applied to certain industrial applications (especially in the case of hybrid mixtures) are some other important procedural safety measures.

An overall hierarchical view in relation to dust explosions is given in Table 2-3.[13]

Table 2-3 A hierarchical view of various means of preventing and mitigating dust explosions.[13]

EXPLOSION PREVENTION		**EXPLOSION MITIGATION**
Preventing Explosible Dust Clouds	**Preventing Ignition Sources**	
Process design to prevent undesired generation of dust clouds and particle size reduction and segregation *Inherent Safety – Minimization, Substitution, Moderation, Simplification*	Smouldering combustion in dust, dust fires *Procedural Safety – may also involve aspects of Inherent Safety or Engineered Safety*	Good housekeeping (dust removal/cleaning) Mitigation with respect to secondary dust explosions; prevention with respect to primary dust explosions *Inherent Safety – Minimization*
Keeping dust concentration outside explosible range *Inherent Safety – Minimization*	Other types of open flames (e.g. hot work) *Procedural Safety – may also involve aspects of Inherent Safety or Engineered Safety*	Explosion-pressure resistant construction *Inherent Safety – Simplification*
Inerting of dust cloud by adding inert dust *Inherent Safety – Moderation*	Hot surfaces (electrically or mechanically heated) *Procedural Safety – may also involve aspects of Inherent Safety or Engineered Safety*	Explosion isolation (sectioning) *Inherent Safety – Moderation (e.g., unit segregation, product choke, etc.) if not using mechanical devices. If mechanical devices are used to isolate plant sections, classification would be Engineered Safety – Passive in the case of physical barriers, or Engineered Safety – Active in the case of isolation valves.*
Intrinsic inerting of dust cloud by combustion gases *Engineered Safety – Active*	Heat from mechanical impact (metal sparks and hot-spots) *Procedural Safety – may also involve aspects of Inherent Safety or Engineered Safety*	Explosion venting *Engineered Safety – Passive*
Inerting of dust cloud by N_2, CO_2 and rare gases *Engineered Safety – Active*	Electric sparks and arcs and electrostatic discharges *Procedural Safety – may also involve aspects of Inherent Safety or Engineered Safety*	Automatic explosion suppression *Engineered Safety – Active*
		Partial inerting of dust cloud by inert gas *Engineered Safety – Active*

Chapter 3 Literature Review

A review of the relevant literature is presented in this chapter. This review provides a brief summary of research in the investigation of explosions associated with the three nontraditional categories of specific fuel/air systems studied here.

3.1 Experimental Work on Dust Explosions

While dust explosion research associated with nontraditional dust has been limited, some research has already been conducted with various materials, as discussed below.

3.1.1 Nanomaterials

One of the key concerns that needs to be addressed is whether nano-sized particles present an enhanced dust explosion risk as compared to the risk presented by micron-sized particles. Dufaud et al.[10] found increased maximum explosion pressure and maximum rate of pressure rise for nano-sized aluminium powders as compared to micron-sized powders. Similarly, the experimental results of Wu et al.[45] demonstrate that 40 μm aluminium powder can produce a P_{max} of 5.9 bar (g), whereas 35 nm aluminium powder can generate a P_{max} of 7.3 bar (g). The same research has revealed that the value of $(dP/dt)_{max}$ in a 20-L chamber for the 35 nm aluminium powder is 4.5 times that for the 40 μm aluminium powder.

The experimental testing conducted by Mittal[46] for magnesium powder indicates a significant increase in explosion severity parameters as particle size decreases from 125 to 1μm as shown in Figures 3-1 and 3-2. This trend has not been observed for nano-sized magnesium powder. Many researchers have previously confirmed that micron-sized powders have shown an increasing trend in explosion severity with decreasing particle

diameter.[9,10,46,47] This trend might suggest the extrapolation of explosion severity data for micron-sized powders down to the nano-range. In reality, extrapolation would not yield the expectation of extreme explosion overpressures and rates of pressure rises because a decreasing trend in explosion severity is seen at particle diameters below 1µm as illustrated in Figure 3-3.[46] A similar trend has been shown to exist for carbon black samples.[48] Possible factors for the observed plateau in explosion severity data include particle agglomeration, pre-ignition of the dust during dispersion, increased oxide content, and wall-quenching.

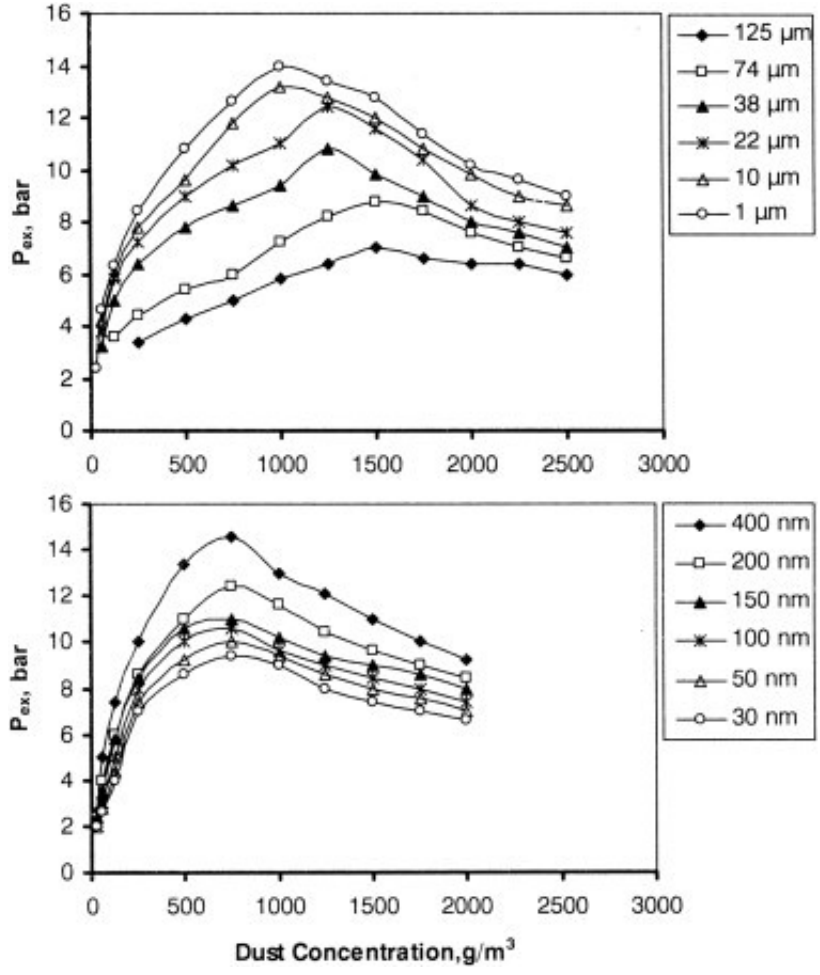

Figure 3-1 Variation of explosion pressure, P_{ex}, with dust concentration for micron- and nano-sized magnesium powder.[46]

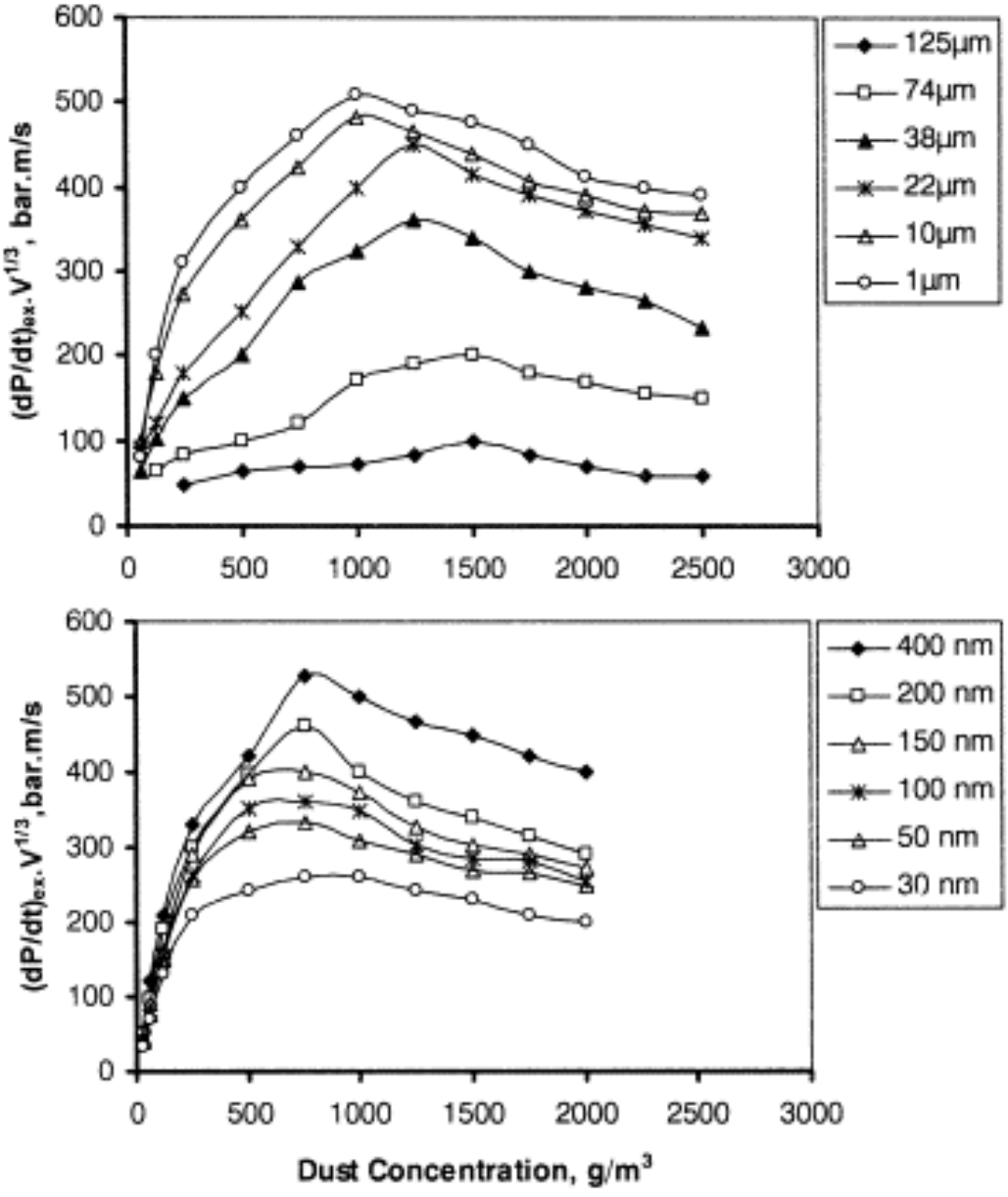

Figure 3-2 Variation of size normalized rate of explosion pressure-rise, $(dP/dt)_{ex}.V^{1/3}$, with dust concentration for micron- and nano-sized magnesium powder.[46]

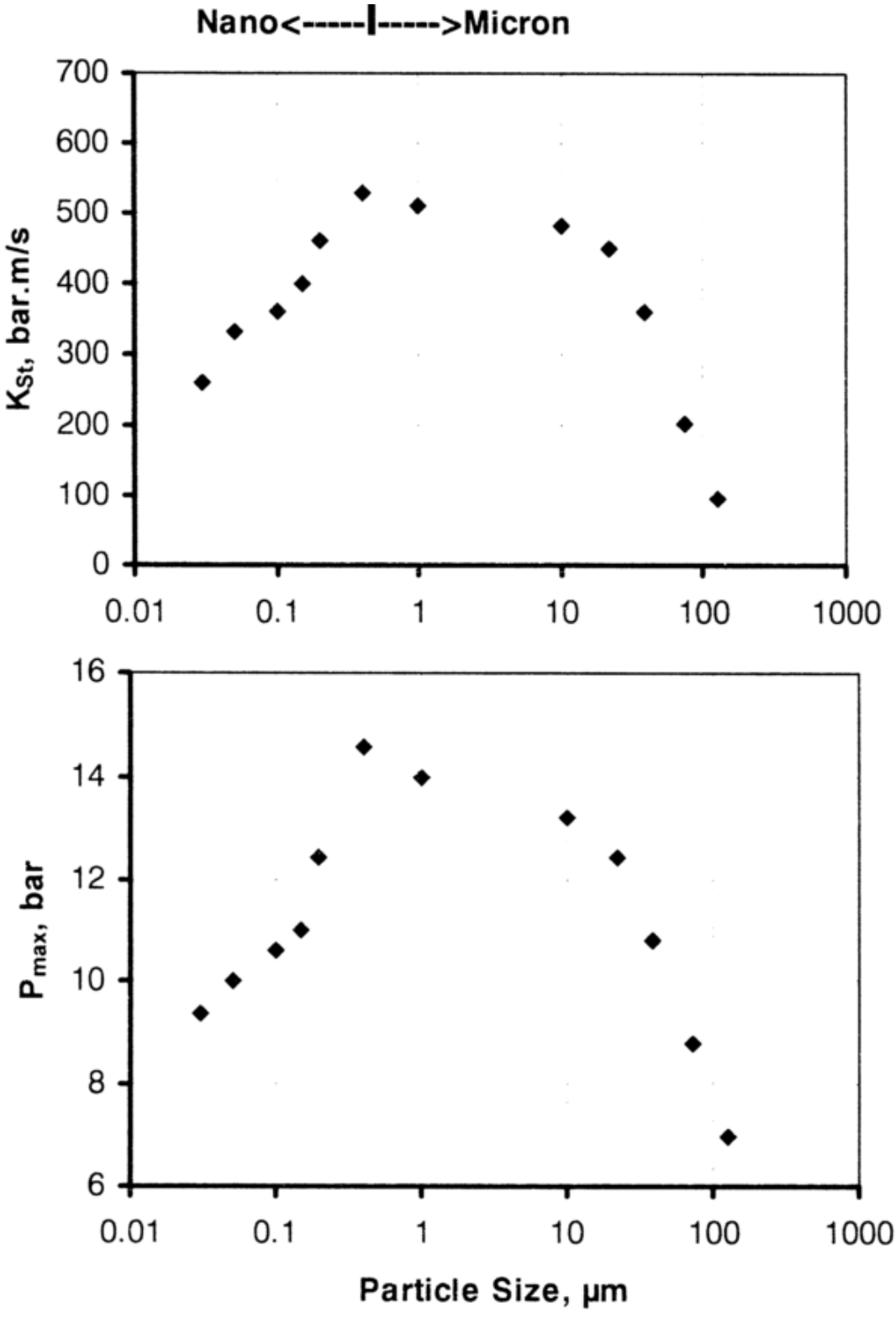

Figure 3-3 Effect of moving from micron- to nano-sized particles on explosion severity data, K_{St} and P_{max}, for magnesium powder.[46]

Agglomerates are a collection of particles held loosely together by inter-particle forces, while aggregates are a collection of particles that are strongly bonded, and cannot be separated through dispersion. As particle diameter is decreased, inter-particle forces become more dominant, and powders exhibit a higher propensity to coagulate. Eckhoff[6] has stated that agglomerates consisting of small particles behave as a single particle with a diameter equal to the agglomerate. In a study by Wu et al.[49], the differences in explosion severity behaviour between the tested 35 nm and 100 nm aluminium samples were significant (100 nm aluminium powder has a P_{max} of 12.5 bar (g) which is 1.7 times that of 35 nm aluminium powder) – even with the agglomeration diameters of the two samples being similar (161.3 nm and 167.5 nm, respectively).

In dust explosion testing of nanopowders, pre-ignition during dispersion has been observed in the literature (Boilard et al.[7]; Dufaud et al.[10]; Mittal[46]), meaning the powders were ignited by frictional or static sparking during the dispersion process before activation of the ignition source (typically a chemical ignitor). There would thus be an overlap in the pressure rises due to both dispersion and explosion of the nanopowders.

In an attempt to prevent pre-ignition during 20-L testing of nano-sized titanium, Boilard et al.[7] used nitrogen to disperse the dust into an atmosphere containing an elevated oxygen concentration (so that upon mixing, the resulting atmosphere at the time of ignition would contain the usual 21% oxygen). Explosions still occurred prior to the activation of the chemical ignitor. The biggest issue arising from this pre-ignition is the possible underestimation of the explosion severity data obtained from nano-sized powders; hence the results are not directly comparable to the explosion severity data of the micron-sized powder. Reduced oxygen concentration can eliminate the pre-ignition behaviour, which has been observed in the experiments conducted by Mittal[46] with magnesium nanopowders.

The 150 nm sample pre-ignited at 21 % oxygen but not at 12 % oxygen; the 20 µm sample did not pre-ignite at either oxygen concentration as shown in Table 3-1.[46]

Table 3-1 Explosion severity of magnesium powders at different oxygen concentrations.[46]

Particle Diameter	Oxygen Concentration [%]	P_{max} [bar(g)]	$(dP/dt)_{max}.V^{1/3}$ (bar.m/s)
150 nm	12	7.2	260
150 nm	21	11.0	400
20 µm	12	8.8	260
20 µm	21	12.4	450

Boilard et al.[7] and Mittal[46] observed in their experiments that the optimal dust cloud concentrations for nanopowders to produce maximum overpressures and rates of pressure rise are lower than for micron-sized powders. Boilard et al.[7] found the optimal dust concentration for 150 nm titanium as approximately 500 g/m^3, while micron-sized titanium did not reach its maximum rate of pressure rise until concentrations around 1500 g/m^3. Similar results were observed for testing with magnesium by Mittal[46]; micron-sized magnesium powders produced the highest rates of pressure rise in the range of 1000 – 1500 g/m^3, while for particle sizes below 1µm, the optimal concentration was 750 g/m^3. The reason for such behaviour is that lower concentrations of nanopowders result in the same reactive surface area as higher concentrations of larger diameter dust.[46]

For micron-sized metal powders, MIE trends to lower values for decreasing particle diameters, making the powder more sensitive to spark ignition.[6,50] Recent research work on MIE of metallic nanopowders has shown similar trends which continue to hold when moving

from the micron to nanometer range.[7,10,45–47,49] Many of the powders in both the micron and nano range tested had ignition energies below 1mJ, the lower limit of the MIKE 3 apparatus. Nanopowder can also ignite at significantly lower dust concentrations than micron-sized dust.[7,46]

Moving from micron-sized to a nano-sized range, the ignition sensitivity continues to increase and is not seen as a decreasing trend as observed for the case of explosion sensitivity. The extremely high temperatures of the electric sparks compared to the temperature of the dust cloud flame could be a reason for the observed phenomenon. Particle agglomerates may remain intact similar to the case of explosion severity, while the initial spark may shatter the agglomerates into primary particles.[3,51]

For micron-sized aluminium powders, minimum ignition temperature (MIT) has been shown to decrease with decreased particle size due to an increase in the reactive surface area.[52] A similar trend of decreasing MIT with decreasing particle diameter has been observed when moving into the nanometer range for metallic dust.[7,46]

Boilard et al.[7] found that for 150 µm titanium powders, ignition did not occur at a temperature of 590 °C (the highest temperature attainable with the apparatus used); titanium powders of 150-nm diameter ignited at a temperature of 250 °C. Boilard et al.[7] found similar ignition temperatures of 240-250 °C for other titanium samples with even lower particle diameters between 60-80 nm and 40-60 nm. Similarly, minimum ignition temperature has been shown to decrease with decreased particle size for magnesium powders tested by Mittal[46].

Minimum explosible concentration (MEC) is generally independent of particle diameter for fine powders having a narrow size distribution. In the results obtained by Boilard et al.[7], the MEC for titanium was between 40 and 50 g/m^3 for a particle size of 150 nm, 50 g/m^3 for a particle size ≤ 20 µm, and 60 g/m^3 for particle sizes < 45 µm and < 150 µm. Similarly, for magnesium samples Mittal[46] found that the MEC was 20 g/m^3 for particle sizes 30-150 nm, and 30 g/m^3 for particle sizes of 200 nm, 400 nm and 1µm.

Different powders with various flammability values frequently become mixed together in process industries.[53] Mixing an inert solid compound with a combustible dust is an application of the moderation principle of inherent saafety.[54,55] Such mixing can effectively decrease the ignition sensitivity of micron-sized metallic powders (Mintz et al.[56]; Myers[57]), thereby allowing use of the hazardous material in a less hazardous form.[58] For example, the MIE of aluminium dust clouds significantly increased with the addition of flame retardant, from 34 mJ to 452 mJ.[57] Therefore, such a solid inertant technology may also have the potential to increase the MIE of nano-sized metal powders. Also, previous work on Al metal particle (MP) combustion indicated lower minimum ignition energy as observed with the addition of nano-scale thermites.[59]

Mintz et al.[56] found that between 70 and 75% by weight, fine MgO dust could completely quench the explosibility of a 50:50 Al-Mg alloy dust. The solid inertant technology effectively reduced the explosion hazard of micron-sized metallic powders and allowed the use of these hazardous materials in less hazardous forms.[56] The flammability properties of such solid mixtures have been investigated by many other researchers[53–55,58,60], but limited information exists on the MIT of such mixtures, especially in the nano-sized range. In addition, uncertainties remain as to whether adding solid inertants to nano-sized metal particles may affect particle dispersion, resulting in additional effects on MIT.[24]

3.1.2 Flocculent Dusts

Research on explosions associated with fibers, which are widely present in the textile industries, is limited in the literature. In the review on dust explosions by Abbasi & Abbasi[25], several dust explosion incidents that occurred in the textile industry are reported. Frank[27] describes the importance of conducting research on the explosibility of flocculent materials in explaining the description of the 1995 Malden Mills explosion (an accident involving nylon fibers). The work presented by Amyotte et al.[61] that used bulk samples of fibrous wood and polyethylene demonstrated that particle shape, in addition to particle size, is an important material property affecting dust explosibility. Flocculent materials (fibrous wood and polyethylene) were observed in the study conducted by Amyotte et al.[55] to display the same general trend of increasing explosion likelihood and consequence severity with a decrease in fibre diameter as is displayed by materials having a more spherical shape.

Research on the minimum ignition energy of nylon fiber and a further case study have been illustrated by Marmo & Cavallero[62] and Marmo[63]. This case study revealed that the properties of flock need to be considered in the risk analysis of fibrous materials. Marmo & Cavallero[62] also mentioned the importance of further research on flocculent materials as there is a lack of assessable data to describe the actual explosion behaviour of fibrous materials. Pidoll[64] conducted research on the ignition sensitivity of various samples of cotton, polyamide 6.6, viscose, and polyester with various fine diameters and cut lengths. The ignition sensitivity and explosion severity data are influenced by larger geometric dimensions, compared to general dust as observed by Pidoll[64].

3.1.3 Hybrid Mixtures

Hybrid mixtures of a combustible dust and flammable gas are found in many industrial processes. Such fuel systems are often encountered in the pharmaceutical industry when excipient (non-active ingredient) powders undergo transfer in either a dry or solvent pre-wetted state into an environment possibly containing a flammable atmosphere. Perry et al.[18] stated that many industries handle dust that is wetted with an organic solvent, which corresponds to a similar instance of pre-wetting, as explained in this study.

It has been observed that a hybrid mixture elevates the hazard level.[18] Dufaud et al.[14,15] investigated the effect of solvents (ethanol, diisopropyl ether and toluene) on the maximum explosion pressure and the maximum rate of pressure rise of dust (magnesium stearate, niacin and antibiotic). In all cases, they found a significant increase of both maximum explosion pressure and maximum rate of pressure rise in the hybrid mixtures, compared to the individual magnitude of dust and solvent. The above findings indicate that the ignition of such hybrid mixtures could lead to explosions with a greater severity than each compound considered separately. In another study, Pilão et al.[19,20] conducted explosion tests on the hybrid mixture of methane and cork dust. They found a significant influence of methane on the explosion severity of cork dust. A substantial increase of the explosibility parameters was also observed by adding ethylene with respect to the polyethylene dust, as determined by Amyotte et al.[16]. From the aforementioned studies on hybrid mixtures, it has been identified that the mixtures can produce explosions more destructive than either of their components on their own.

The influence of the co-presence of a flammable gas on the explosibility parameters of a fuel dust alone is a well-established fact as described by Amyotte & Eckhoff[13]. However, due to the extent of the subject matter and its wide range of industrial

applications, continued research on hybrid mixtures is still needed, as seen in recent studies[14–21,28].

From the aforementioned reviews, it is found that there are significant influences of nano size, fibrous shape, and solvent admixture on the explosibility parameters of dust. Further research is needed to develop a comprehensive knowledge on nontraditional dust explosions and to address adequate safety measures to prevent and mitigate explosions associated with nontraditional dusts.

3.2 CFD Simulation of Dust Explosion

Simulations based on the principles of computational fluid dynamics (CFD) are useful for solving complex geometries. A number of articles on the application of CFD tools to dust explosions have already been published.[65–71] Among them, some researchers performed simulations using CFD tools in conjunction with input from laboratory scale experiments.[67–69] Satisfactory prediction in real geometries could be attained by using the same physics and estimated kinetic parameters obtained in the 20-L apparatus as mentioned by Bind et al.[65], which includes simulations with starch-air using the density-based solver of commercial CFD software Fluent 6.3.26.

Skjold et al.[68,69] described how the dust explosion simulation code (DESC) uses CFD coding for the transport equations for mass, momentum, enthalpy, fuel mixture fraction, turbulent kinetic energy, and the rate of dissipation turbulent kinetic energy on a 3-dimensional Cartesian grid. As stated earlier, FLACS-DustEx (FLame ACceleration Simulator—Dust Explosions) has been used in the current study, which was previously marketed as DESC (Dust Explosion Simulation Code). FLACS-DustEx is generally based on the Finite Volume (FV) method which uses an integral form of the conservation equations. In

FLACS-DustEx, the solution domain is divided into a number of control volumes (CV). The conservation equations are applied to each CV to explore the calculation for real geometries. Since FLACS-DustEx simulations are dependent on the flow characteristics and the dust concentration, the characterization of dust cloud properties in large volumes, together with experimental validation, would therefore be necessary for accurate simulations.[70] FLACS-DustEx has proven to be a useful tool for studying how to protect against dust explosions, and has been applied in the current work for dryers and flocculent storage tanks in order to improve our knowledge on dust explosions and their consequences.

3.3 ISD Based Control Measures in Dust Explosion Risk Reduction

There are several opportunities for reducing risk through inherent safety when the basic principles of inherent safety are applied early in the engineering design cycle.[54] As mentioned earlier, the difference between inherent safety and the other two categories in the hierarchy of controls (engineered and procedural) is that inherent safety seeks to eliminate the hazard at the source as a foundation as opposed to accepting the hazard and looking to prevent its occurrence or mitigate its effects.[13] Unlike the other controls for risk reduction, inherent safety is mainly applied for removing the hazard in the design of the process.

Amyotte et al.[16] have quantified the effects of particle size reduction and flammable gas admixture for the ethylene/polyethylene, hexane/polyethylene, and propane/polyethylene hybrid systems. They recommend that the inherent safety principle of moderation by avoidance of both fine dust sizes and hybrid mixtures is a beneficial approach in the process industries to reduce the risk arising from the hazards posed by combustible dusts and their mixtures with flammable gases. The effects of substituting petroleum coke for coal in fossil fuel-fired power plants were investigated by Amyotte et

al.[72] They found petroleum coke was to be an inherently safer fuel than either of the coals they tested.

Inherently safer design (ISD) can be applied at any stage in a plant's life cycle. But, it is most effectively addressed at the early stages of the process (e.g., research and development, and plant design). As a process continues to evolve through its life cycle, minor changes of preliminary design become more difficult and expensive, and the process may not be able to handle the difficulties and to afford the extra expenses needed for the development of an alternate manufacturing scheme.[73]

Inherent safety principles (minimization, substitution, moderation) were applied in the recommended sequence to control the expected main causes of the *Semabla* silo explosion and the Imperial Sugar refinery explosion as seen in Tables 3-2 and 3-3, respectively.

Table 3-2 Applying inherent safety principles to the factors that caused the Semabla explosion.[74]

Factors contributing to the explosion event	**Inherent safety principle**	**Recommendation**
Dust-air explosion occurred in the dust removal circuit	Minimization	- Good housekeeping (dust removal/cleaning). - Keeping dust concentration outside explosible range.[13]
Open interspaces between the two groups of cells		Minimize dust cloud volume by filling the open interspaces with grain or sealing them tightly.
Unloading of maize and dryers procedure	Substitution	Replace the hazardous unloading and drying procedures with others that are less hazardous.
Existence of combustible gases from fermentation	Moderation	Identify processing (storage) options that involve less severe processing conditions.

Table 3-3 Applying inherent safety principles to the factors that caused the Imperial Sugar refinery explosion.[74]

Factors contributing to the explosion event	Inherent safety principle	Recommendation
Spilled sugar around the working machines	Minimization	- Good housekeeping (dust removal/cleaning) to mitigate secondary dust explosion and/or prevent primary dust explosion. - Keeping dust concentrations outside explosible range.[13]
Stainless steel panels to cover the conveyor belts below the tall silos	Simplification	Eliminate opportunities for errors by eliminating excessive add-on safety features and protective devices by removing the new stainless steel panels that cover the conveyor belts below the tall silos.
Using compressed air to clean the packaging machines	Substitution	Replace the hazardous cleaning procedure (using compressed air to clean the packaging machines) with one that is less hazardous.

For prevention and mitigation of dust explosions, the control measures (inherent, passive, active, and procedural) need to be categorized along a spectrum of process safety approaches and should not be considered to be discrete categories with clear boundaries as mentioned by Hendershot[75] and as shown in Figure 3-4. In an example, Hendershot mentioned that some people might consider that reducing the potential severity of a release from downstream equipment by limiting pipe size or adding restricted orifices is an example of a "passive engineered" safety measure. Others would prefer the categorization of this strategy as "inherent safety design". But, the important thing is to limit pipe size or to restrict orifices, not what to call it. The ultimate target should be the ideal situation (a process which has a high degree of inherently safer design characteristics and for that process to be built from individual components which incorporate a high degree of inherently safer features)[75]. The safety measures of the process need to be designed with a high degree of inherently safer design characteristics and for that process to be built

from individual components which incorporate a high degree of inherently safer features (Figure 3-5).

Figure 3-4 A spectrum of options from inherent through procedural safety measure.[75]

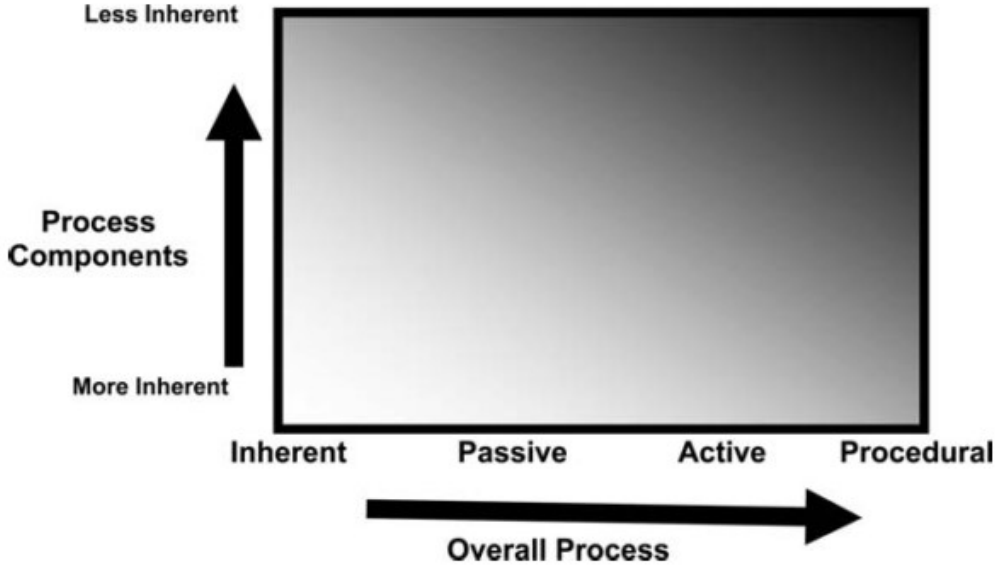

Figure 3-5 Inherently safer design in a process at the overall process level and also for all of the individual components.[75]

Chapter 4 Experimental Work

The experimental work of the current research is based on a comprehensive investigation of the explosibility parameters (both explosion severity and likelihood) for the following three categories of nontraditional particulate fuel systems: (i) nanomaterials having particles with dimensions between 1 and 100 nm [nano-titanium and titanium dioxide (to examine the inerting effect) powder]; (ii) flocculent materials characterized by a length-to-diameter ratio rather than a particle diameter (fibrous polyamide 6.6 and polyester); and (iii) hybrid mixtures consisting of a combustible dust and a flammable gas or flammable solvent (MCC and lactose admixed with flammable solvents). Among the three categories of nontraditional particulate fuel systems stated above, Ivan Iarossi (Research Assistant, Dalhousie University, 2012) and Simon Boilard (M.Sc. Student, Dalhousie University, 2013) conducted all experimentation with flocculent materials and Ti powders (except experimentation for investigating the inerting effect of TiO_2 powder on MIT and MIE of nano- and micron-sized Ti powders), respectively. The author conducted:

- All experimentation associated with hybrid mixtures consisting of a combustible dust and a flammable gas or flammable solvent (MCC and lactose admixed with flammable solvents).
- All experimentation to examine the inerting effect of nano-sized TiO_2 powder on the ignition sensitivity of nano- and micron-sized Ti powders.
- All experimentation to investigate the inerting effect of nano-sized TiO_2 powder on Minimum Ignition Temperature (MIT) of nano- and micron-sized Ti powders.

To determine the aforementioned inerting effects and to analyze the results through relevant comparisons, explosibility test results of three micron sizes: -100 mesh (<150 μm), -325 mesh (<45 μm), ≤20 μm, and three nano sizes: 150 nm, 60-80 nm, and 40-60 nm as

mentioned by Boilard et al.[7] have been presented in this Chapter in Tables 4-6, 4-7, and 4-8; and Figures 4-13 and 4-14. In addition, to investigate the influence of fibre length on the explosibility parameters of polyamide 6.6, computationally, and to analyze explosibility results for the polyamide 6.6 and polyester samples, Tables 4-11and 4-12 as described by Iarossi et al.[76] have been presented in this Chapter. Such analyses will help for further understanding of the explosion phenomena. Ultimately, the goal is to use the outcome of the analyses into the work of explosion risk management as explained in Chapter 5.

4.1 Materials, Apparatus and Procedures

Materials, apparatus and procedures of conduced explosibility tests for three categories of nontraditional particulate fuel systems are described in this section.

4.1.1 Materials

A brief description of the materials: (i) titanium and titanium dioxide powder; (ii) fibrous polyamide 6.6 and polyester; and (iii) hybrid mixtures consisting of a combustible dust and a flammable gas or flammable solvent (MCC and lactose admixed with flammable solvents) used for explosibility tests has been presented in this section.

4.1.1.1 Titanium powder

Titanium was selected as it is unique in its reactivity and available in both micron- and nano-size[7]. Three micron sizes: -100 mesh (<150 μm), -325 mesh (<45 μm), ≤20 μm, and three nano sizes: 150 nm, 60-80 nm, and 40-60 nm were selected to analyze the explosibility parameters. Additionally, 10-30 nm TiO_2 sample was used for experiments which involved in dust inerting. A Malvern particle size (PS) analyzer was used to determine

PS distribution of micron-sized Ti. A primary PS of the nano titanium samples was taken as documented by the manufacturer (Skyspring Nanomaterials Inc.), and no further size analysis was performed.

A scanning electron micrograph (SEM) of the micron-sized titanium sample (Figure 4-1) shows that individual particles of titanium are not spherical but have a granular shape. Figures 4-2 and 4-3 show the presence of agglomerates in the 60-80 nm Ti sample and the 10-30 nm TiO_2 sample, respectively.

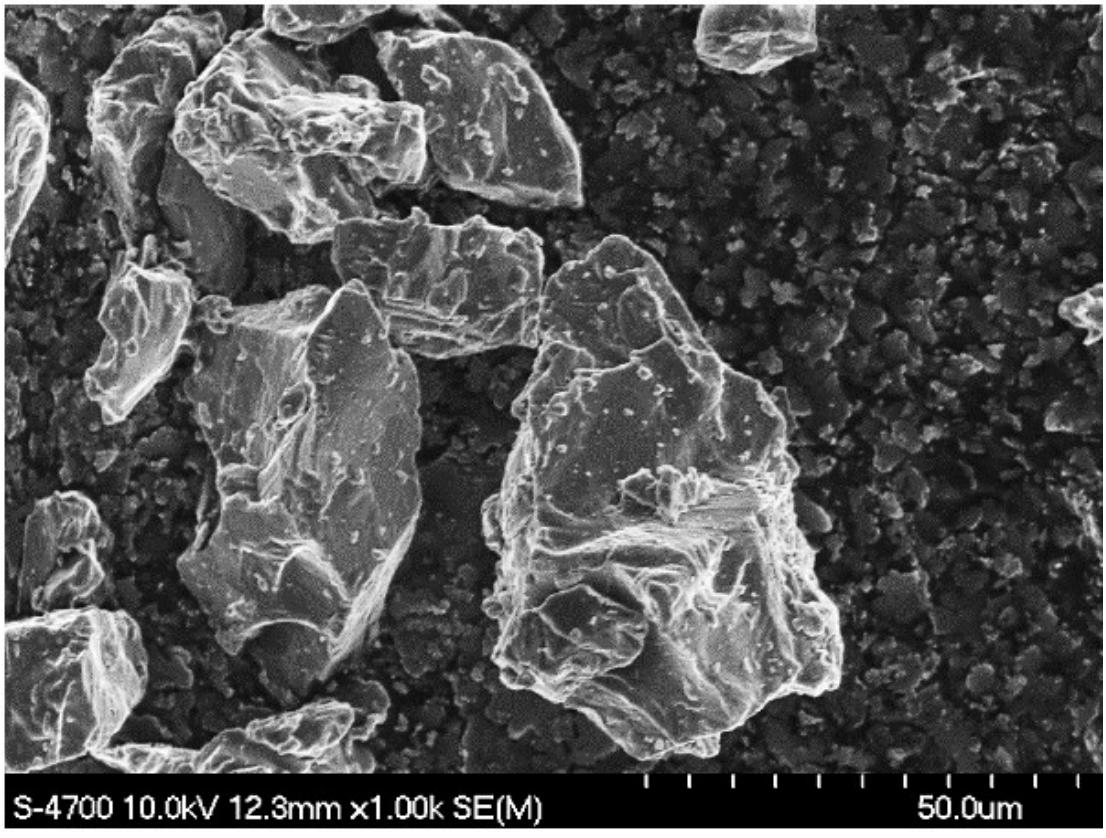

Figure 4-1 SEM of micron-sized Ti (≤20 µm) powder.[7,24]

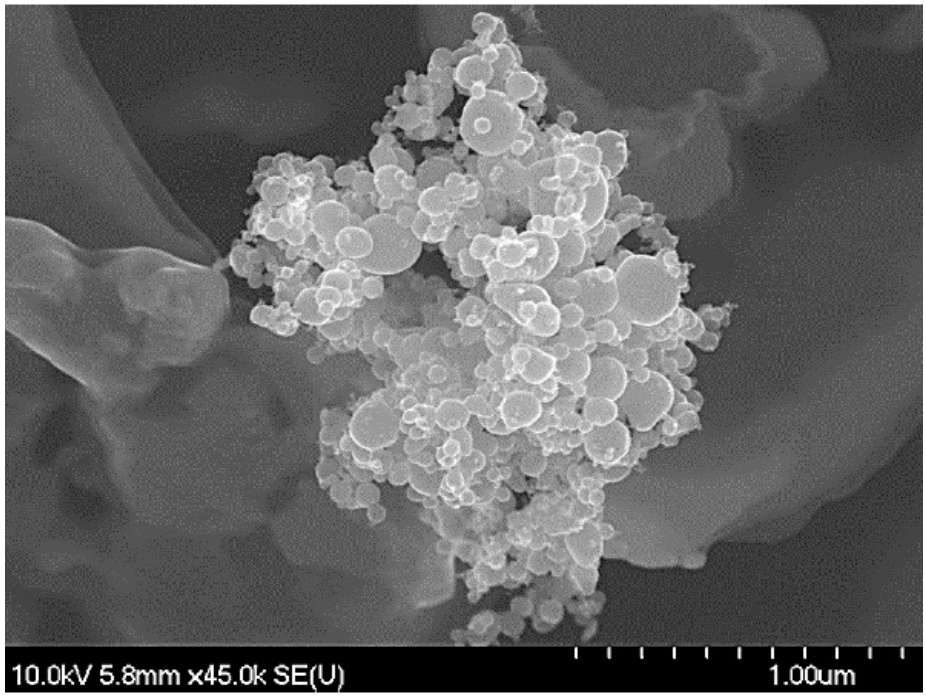

Figure 4-2 SEM of 60-80 nm Ti powder.[7,24]

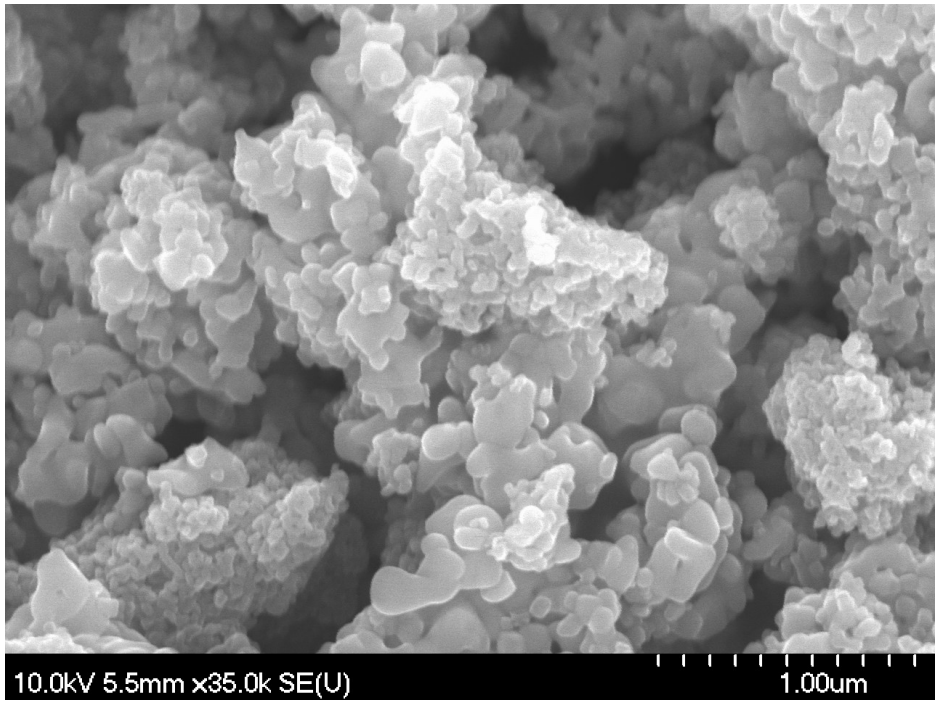

Figure 4-3 SEM of 10-30 nm TiO_2 powder.[77,78]

4.1.1.2 Fibrous Polyamide 6.6 and Polyester

Polyamide 6.6 and polyester were selected to be representative of common fibrous materials. The polyamide 6.6 used for the experiments is poly hexamethylene adipinamide which contains about 1.1 to 2 % of carbon black that increases stability while decreasing sensitivity to humidity.[76] The polyester tested is polyethylene terephthalate (PET) containing 2.5 % carbon black.[79] Carbon black is important for its melt strength during the polymer formation. Both polyamide 6.6 and polyester are strong and resistant to abrasion and damage from oil and many chemicals. As reported in the literature mentioned by Sanders & Seager[80], an important difference between these two fibers that can influence the explosibility parameters is the melting and burning process; polyamide first melts and then burns rapidly, while polyester melts and burns at the same time. The ranges of commercial fibers are generally found between 1 dtex (11 μm) and 22 dtex (50 μm), and their mean length is from 0.3 to 3 mm.[79] The parameter dtex is a unit of measure for the linear density of fibers. It is equivalent to the mass in g per 10,000 m of a single filament, and can be converted to a particle diameter. Tables 4-1 and 4-2 display the properties of polyamide 6.6 and polyester, respectively.

Table 4-1 Properties of Polyamide 6.6.[79]

POLYAMIDE 6.6	
Diameter [μm]	11-50
Length [mm]	0.3-3
Carbon black [%]	1.1-2
Melting range [°C]	250-260
Flash point [°C]	about 400
Thermal decomposition [°C]	start at about 350
Density [g/cm^3]	1.13-1.15
Apparent density [kg/m^3]	50-200
Moisture [%]	2.9-4.5

Table 4-2 Properties of Polyester (PET).[79]

POLYESTER (PET)	
Diameter [μm]	10-45
Length [mm]	0.3-3
Carbon black [%]	2.5
Melting range [°C]	250-260
Flash point [°C]	340-400
Thermal decomposition [°C]	start at about 350
Density [g/cm3]	1.38-1.42
Apparent density [kg/m3]	80-200
Moisture [%]	0.55-0.95

The experiments were conducted using the most common dtex 3.3 and 1.7 of 0.5-mm long fiber to investigate the influence of dtex on the explosibility parameters.[76] In addition, testing of polyamide 6.6 of dtex 1.7 with various lengths was conducted to investigate the influence of fiber length on the explosibility parameters.

4.1.1.3 Hybrid mixtures

The specific hybrid fuel systems were selected to be representative of common pharmaceutical mixtures of excipients (non-active ingredients) and solvents. The hybrid mixtures that were selected for testing in the current research involved lactose and microcrystalline cellulose (MCC) dusts admixed with methanol (methyl alcohol), ethanol (ethyl alcohol) and isopropanol (isopropyl alcohol) solvents.

All materials tested were pharmaceutical-grade in terms of composition and, in the case of the solids, particle size distribution (PSD) as received from the supplier. Tables 4-3 and 4-4 summarize the relevant material characteristics of the dust (excipients) and solvents, respectively. A sieve analysis was used for the lactose PSD determination because of initial concerns about lactose solubility with Malvern light scattering analysis (which was performed for the MCC). The PSD results are consistent with the trend of the nominal mean diameters of 50 and 75 μm provided by the suppliers of the MCC and lactose samples, respectively.

Table 4-3 Material characterization of MCC and lactose powder.

Characteristic	MCC	Lactose
Supplier	Sigma-Aldrich	Hilmar Ingredients
Particle Size [weight %]	Malvern Analysis: 90 % < 56 μm 50 % < 27 μm 10 % < 9 μm	Sieve Analysis: 98 % < 250 μm 84 % < 150 μm 62 % < 89 μm 18 % < 75 μm
Moisture Content [weight %]	4.5	5.1

Table 4-4 Material characterization of solvents.

Characteristic	Methanol	Ethanol	Isopropanol
Formula[81]	CH_3OH	C_2H_5OH	C_3H_7OH
Molecular weight[81]	32	46	60
Lower flammability limit [volume %][82]	6.7	3.3	2.2
Laminar burning velocity [cm/s] (Methanol,[83] Ethanol,[84] Isopropanol[83])	56	42	41
Vapour pressure at 25 °C [mm Hg][81]	127	59	43
Specific heat capacity (liquid) at 25 °C [J/mol·K][85]	81	112	155
Boiling point at 1 atm [°C] [81]	64.7	78.5	82.2
Heat of vapourization at boiling point and 1 atm [kJ/mol] (Methanol,[81] Ethanol,[81] Isopropanol[85])	35.2	38.5	39.9
Heat of combustion (liquid) at 25 °C and 1 atm with H_2O(l) product [kJ/mol][81]	–726.6	–1366.9	–1986.6
Specific gravity [20°C/4°C][81]	0.792	0.789	0.785

Figures 4-4 and 4-5 show scanning electron micrographs (SEMs) of the MCC and lactose samples, respectively. MCC is observed to be fibrous in nature, while lactose consists of irregularly-shaped, oblong particles.

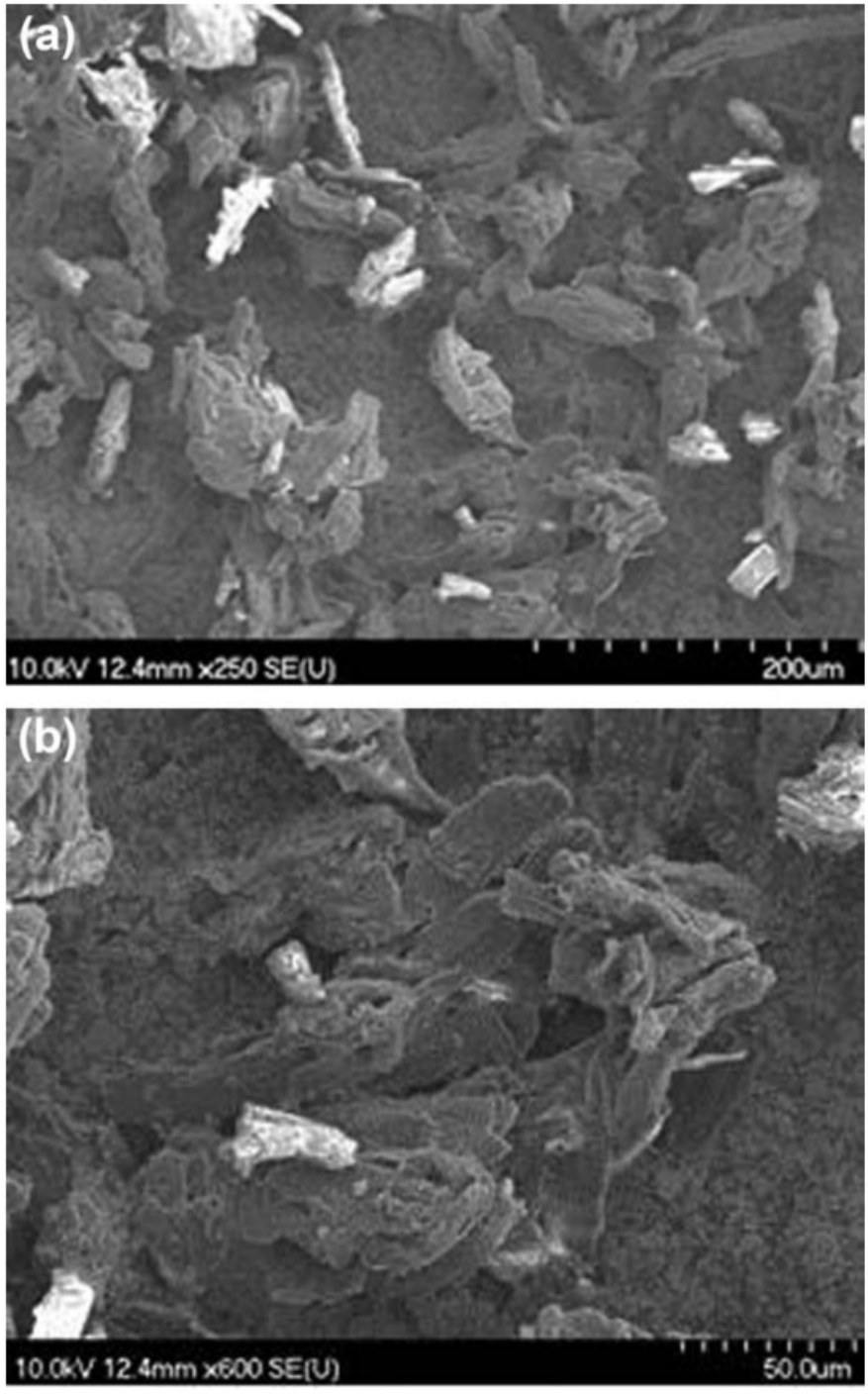

Figure 4-4 Scanning electron micrograph of MCC powder: (a) 250 magnification, (b) 600 magnification.

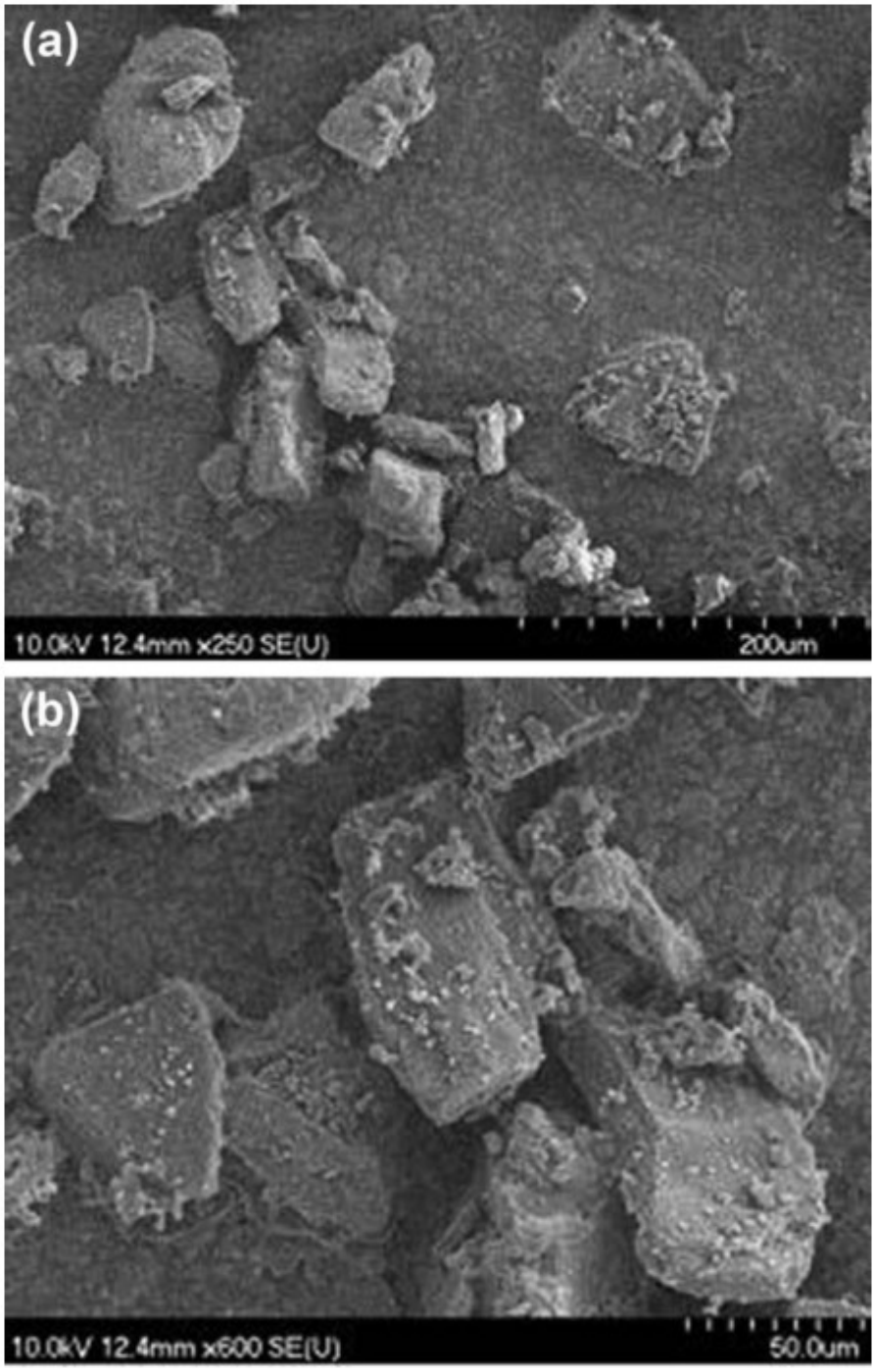

Figure 4-5 Scanning electron micrograph of lactose powder: (a) 250 magnification, (b) 600 magnification.

4.1.2 Apparatus and Procedures

Explosibility parameters investigated include maximum explosion pressure (P_{max}), size-normalized maximum rate of pressure rise (K_{St}), minimum explosible concentration (MEC), minimum ignition energy (MIE), and minimum ignition temperature (MIT). ASTM international standards mentioned in Table 4-5 were followed using standardized dust explosibility test equipment: (i) Siwek 20-L explosion chamber for P_{max}, K_{St} and MEC, (ii) MIKE 3 apparatus for MIE, and (iii) BAM oven for MIT. These are critical features of the current work that facilitate widespread application of the research findings, i.e., determination of a full suite of explosion parameters using standard test equipment and standard test protocols.

Table 4-5 Standards used for testing.

ASTM Designation	Title	Parameter
ASTM E1226-12(a)[41]	Standard Test Method for Explosibility of Dust Clouds	P_{max}, $(dP/dt)_{max}$ and K_{St}
ASTM E1515-14[39]	Standard Test Method for Minimum Explosible Concentration a Dust Cloud in Air	MEC
ASTM E2019-03(2013)[38]	Standard Test Method for Minimum Ignition Energy of a Dust Cloud in Air	MIE
ASTM E1491-06(2012)[40]	Standard Test Method for Minimum Auto Ignition Temperature of Dust Clouds	MIT

The following sections (4.1.2.1 to 4.1.2.3) describe the procedures used for testing the three categories of nontraditional fuel particulate systems. Details of the apparatus and

procedural descriptions can be found on the equipment manufacturer's web site (www.kuhner.com). Each sample was tested using the applicable ASTM standards ensuring that the tests were consistent, accurate and reliable.

4.1.2.1 Siwek 20-L chamber

The Siwek 20-L chamber, manufactured by Kühner A.G. of Switzerland, was used to determine various explosion parameters including: maximum pressure (P_{max}), maximum rate of pressure rise ($(dP/dt)_{max}$), size-normalized maximum rate of pressure rise (K_{St}) and minimum explosible concentration (MEC). A schematic of the Siwek 20-L chamber is shown in Figure 4-6.[86] The main part of this test facility is a spherical chamber combined with a dust storage container.

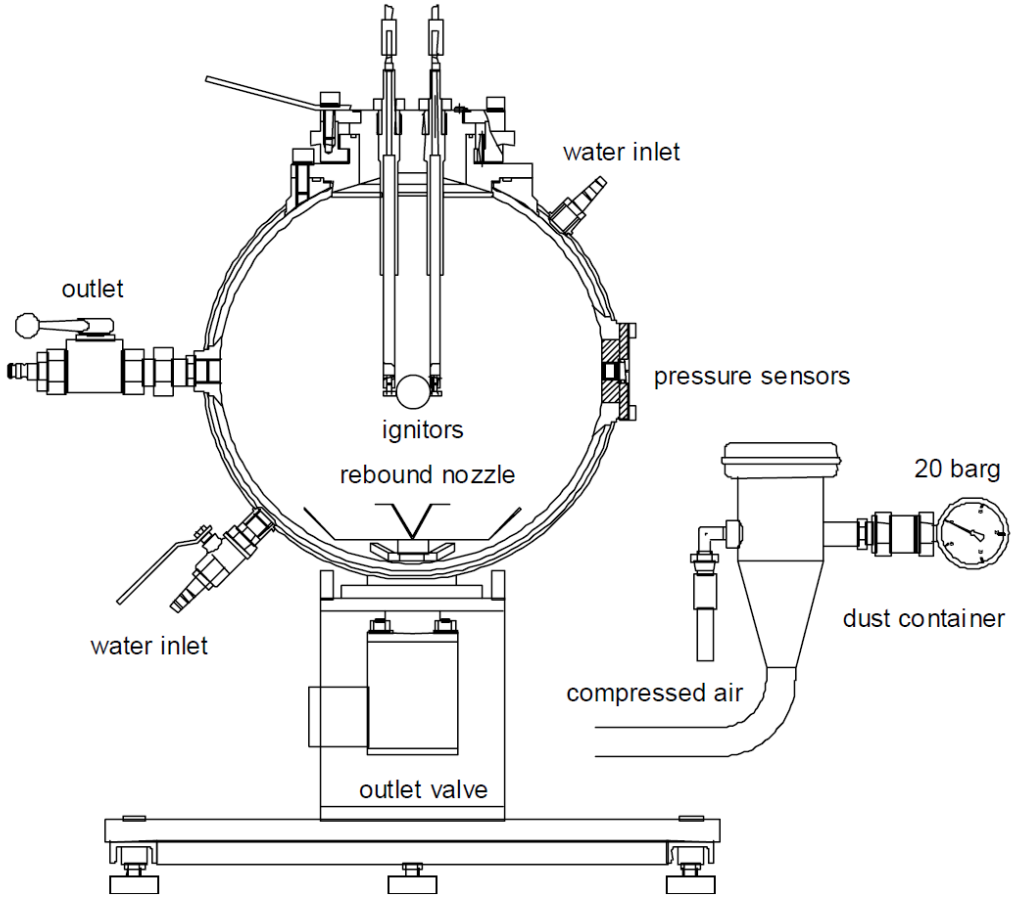

Figure 4-6 Schematic of a Siwek 20-L chamber.[86]

Measured dusts are placed in the dust storage chamber. After proper connection to the igniters, the chamber is closed and evacuated to 0.4 bar (absolute). As soon as the solenoid valve under the rebound nozzle opens, the pressure difference between the two reservoirs carries the dust into the 20-L chamber and disperses the dust/air mixture through the rebound nozzle. The computer controls the firing of igniters by igniting after 60 ms of dust mixture dispersion. The pressure transducers transmit the explosion information to the KSEP program. For example, Figure 4-7 shows a typical pressure-time curve that was generated by the KSEP software. Figure 4-7 indicates the maximum pressure reached P_m (bar(g)) and the maximum rate of pressure rise $(dP/dt)_m$ (bar/s) as recorded.

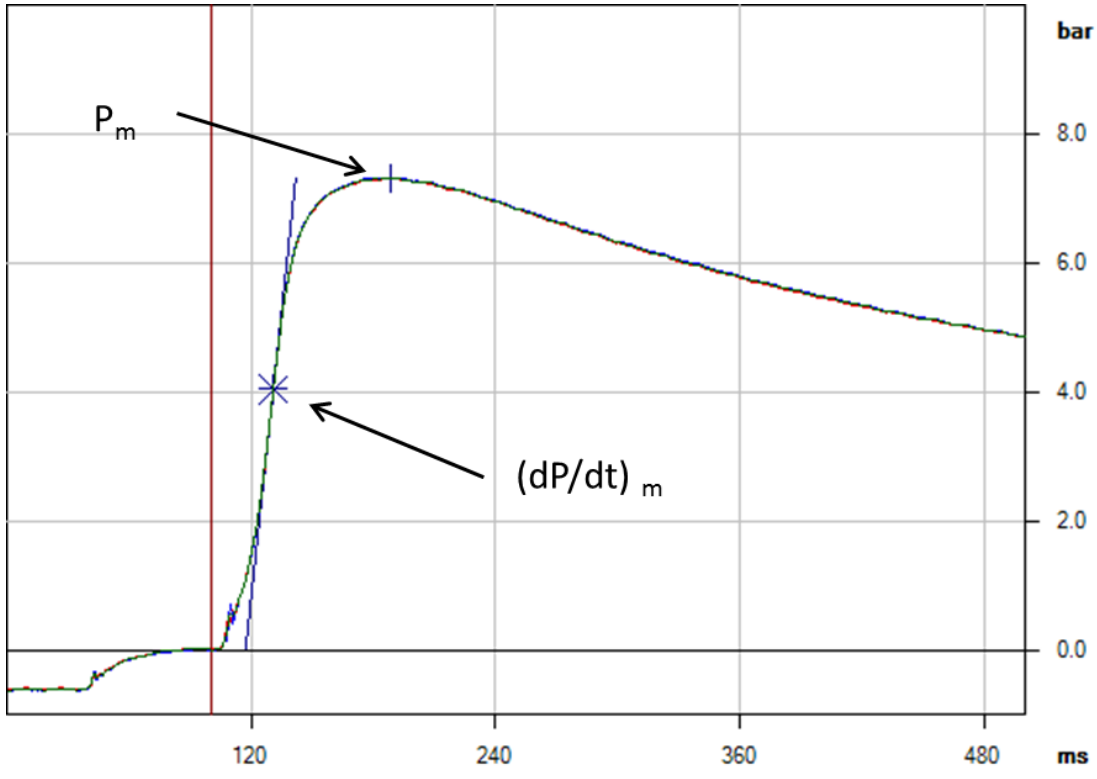

Figure 4-7 KSEP pressure-time curve during MCC (50-µm) dust explosion in 20-L chamber.

With a few exceptions (applied for testing with some samples of nano-sized titanium powder and hybrid mixtures), a standard test procedure ASTM E1226-12(a)[41] was followed for all samples in the Siwek 20-L chamber. The nano-titanium 20-L chamber explosion test procedure was similar to the standard procedure except for preparing samples in an inert environment and using nitrogen to disperse the nano-titanium into the 20-L chamber. The nano-titanium was placed in a glove bag which contains nitrogen gas. The complete process of sample preparation including opening the bag, handling and weighing were performed within the glove bag maintaining sufficient nitrogen inside the glove bag. The inert gas (nitrogen) helped to prevent any oxidation, as well as any unwanted hydrogen formation. No ignitors were used for any P_{max} and $(dP/dt)_{max}$ testing of nano-sized samples because of its ability to ignite with static or frictional sparking while dispersing into the 20-L chamber as stated by Boilard et al.[7].

In case of higher concentrations (> 750 g/m^3), due to the low bulk density of the flocculent samples, a method was followed for the 20-L chamber in which a maximum of 15 g dust was placed in the external dust storage container, the remainder of the sample was placed directly in the 20-L chamber.[76]

All hybrid mixture testing involved a fixed solvent concentration of 80% of the respective LFL (Table 4-4), calculated using the respective molecular weights and specific gravity data in Table 4-4 and the volume of the particular test apparatus (20, 1.2, and 0.34 L for the Siwek chamber, MIKE 3 apparatus, and BAM oven, respectively). For the pre-wetted (PW) tests, the required amount of liquid solvent—methanol (M), ethanol (E), or isopropanol (IPA)—was mixed with the amount of dust corresponding to the dust concentration being tested. The pre-wetted dust was then dispersed into the specific apparatus (Siwek 20-L chamber, MIKE 3 apparatus, or BAM oven) via the usual procedure.

For the atmospheric (ATM) tests (Siwek 20-L chamber only), the chamber was first evacuated to a pressure of 185 mm Hg (as low as could be attained in relation to the respective solvent vapor pressures given in Table 4-4). The required amount of liquid solvent was then injected through a septum into the 20-L chamber, with the majority of the solvent flashing to vapor. The chamber was subsequently backfilled with air to the standard pre-dispersion pressure (300 mm Hg) such that the chamber pressure at the time of dust ignition was approximately 1 bar. From a material balance perspective, any small amount of remaining liquid solvent would be vaporized by the shower of sparks originating from the chemical ignitors (1 × 5 kJ for MEC and 2 × 5 kJ for P_{max}/K_{St}) acting as the ignition source in the 20-L chamber.[16]

4.1.2.2 MIKE 3 apparatus

The MIKE 3 apparatus (manufactured by Kuhner AG of Switzerland), as shown in Figure 4-8 was used to determine MIE. The MIKE 3 apparatus consists of a vertical, cylindrical glass tube with an inner diameter, height, and volume of 68 mm, 300 mm, and 1.2 L, respectively. Space between the electrodes was 6 mm and was measured using an insulated glass rod. The apparatus induces dust cloud explosion by means of high voltage ignition sparking. Energy values for the MIKE 3 were: 1000, 300, 100, 30, 10, 3, and 1 mJ. The ignition time delay was adjustable with regular settings at 60, 90, 120, 150, and 180 ms. Inductance could be set at either 0 or 1 mH allowing changes in spark duration.

Experimental procedures were conducted in accordance with ASTM E2019-03(2013)[38]. According to standard test methods, a visual inspection of the glass tube was required to determine if an explosion had occurred. After three consecutive, non-igniting trials, the dust sample was changed. A total of 10 consecutive non-ignitions were required for a given test to be considered non-ignitable. The MIE lies between the lowest energy

value at which ignition occurred (IE) and the energy at which no ignition was observed (NIE). Test procedures were the same for nano Ti, flocculent materials and hybrid mixtures except for a few differences in sample preparation as mentioned in the previous section.

Nano-sized Ti samples of concentrations above 900 mg were not attempted due to the risk of damage to glass components of the MIKE 3 apparatus and operator's safety concerns. Even at such low dust loadings (e.g., 900 mg) with nano Ti powders, the explosion in the MIKE 3 glass tube (modified Hartmann tube) was violent and produced an audible 'boom'. MIE tests were done using both inductance settings and three time delays (90, 120, and 150 ms). The ignition delay time of 120 ms was employed preferentially with an attempt to make MIE results comparable with the ones reported by Boilard et al.[7]. Once tests were completed and MIEs determined with the time delay, only points of non-ignition near the MIE were tested with the two others (90 and 150 ms) in order to confirm test results and find possible exceptions.

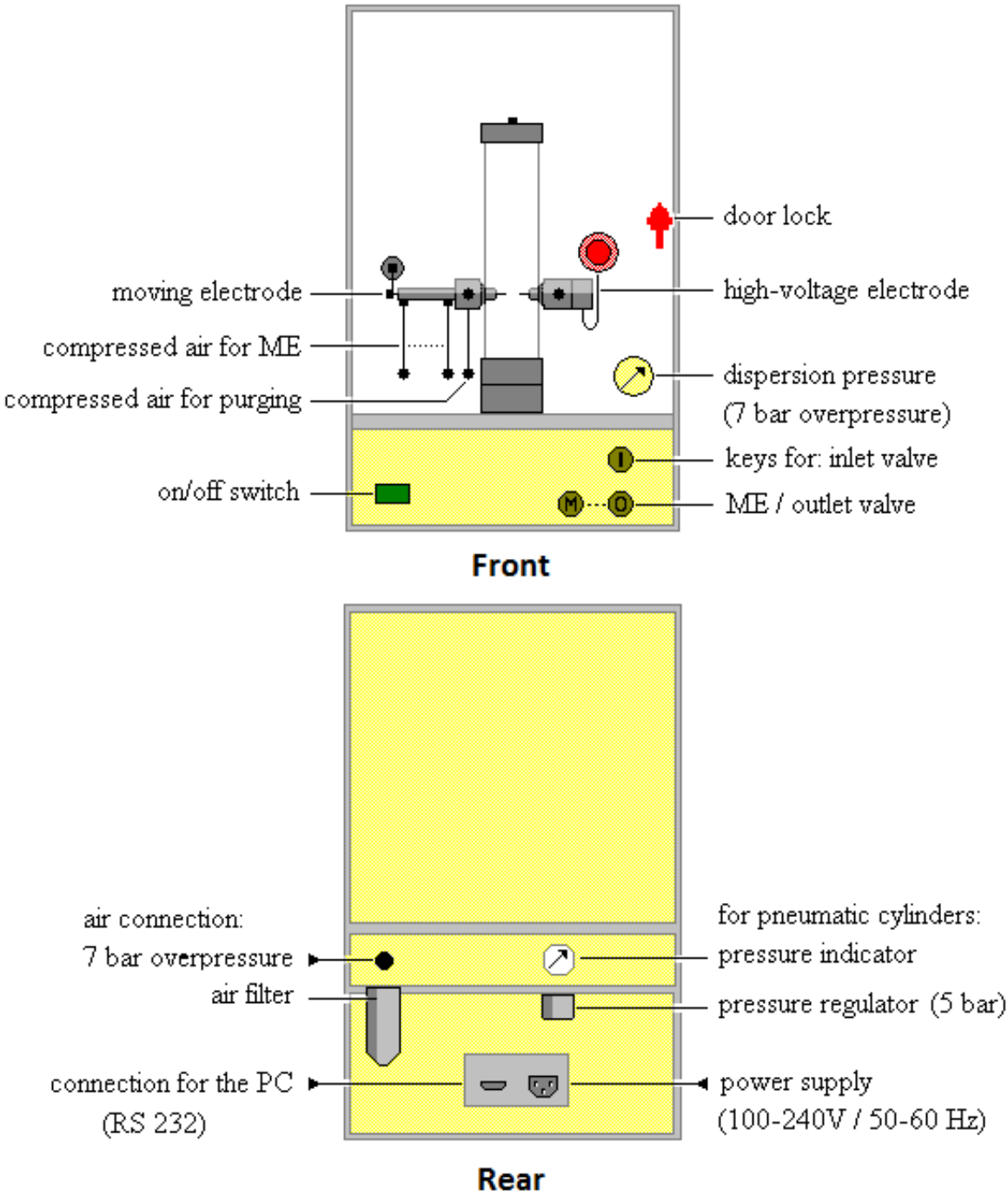

Figure 4-8 Schematic of the MIKE 3 apparatus.[87]

4.1.2.3 BAM oven

All MIT tests were conducted in a BAM oven (Figure 4-9) by following ASTM E1491-06(2012)[40]. The chamber volume of 0.34 L was approximated by a cylinder with a diameter (D) of 0.06 m and length (L) of 0.125 m. The test chamber was surrounded by a 1500 W heater enabling the BAM oven walls to reach temperatures up to 600 °C. Heater temperature was controlled externally and the temperature was monitored using two thermocouples with an accuracy of +/- 1°C.[88] Once the desired starting temperature was reached, 1 ml of dust was placed in the dispersion nozzle. A dust cloud was then generated by squeezing a rubber bulb which directed the dust against a circular concave metal disc of about 20 cm^2 area. Observation of a flame within 5 seconds of dust dispersion was considered an ignition event. If ignition occurred, the oven temperature was recorded and then reduced by 10 °C followed by re-testing at the lower temperature until no ignition was observed. The oven was then cooled and cleaned for a subsequent testing series. The non-ignition point was then determined similarly with 0.5 and 2 ml of dust in order to confirm test results. If both volumes resulted in a non-ignition point, the MIT was recorded as the last ignition temperature.[24,89]

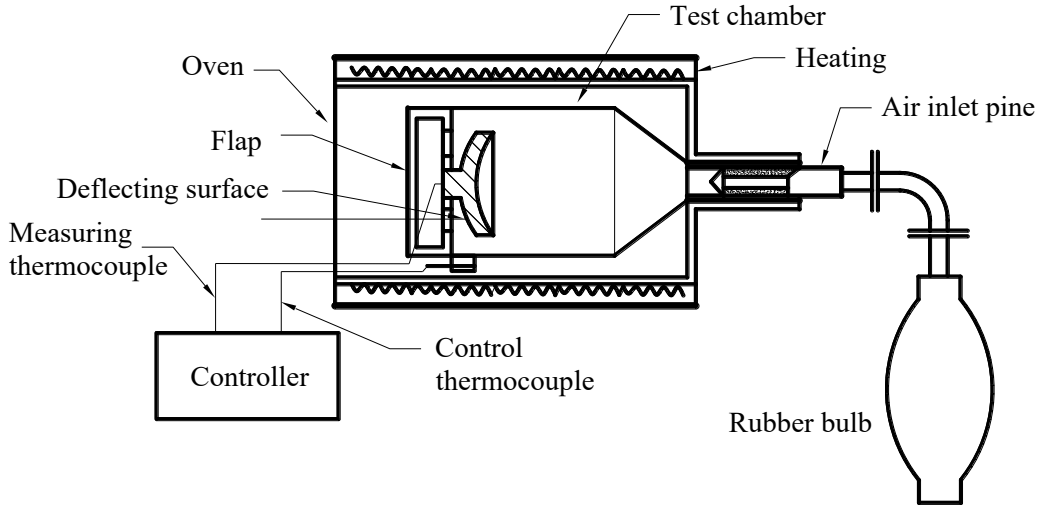

Figure 4-9 Schematic of the BAM oven.[78]

ASTM E1491-06(2012)[40] guidelines for samples measured by volume were followed for flocculent and hybrid mixtures. However, for nano Ti powder, micron Ti powder, and nano TiO_2 powder, target sample volumes of 0.5, 1, and 2 ml were weighed out using a bulk density calculation instead of by measuring volume, thereby assuring accuracy and repeatability in sample size. Average bulk density of each material (*i.e.*, nano-sized (60-80 nm) Ti powder, micron-sized (<45 μm) Ti powder, and nano-sized (10-30 nm) TiO_2 powder) was determined by weighing 10 samples of 1 ml each (Figure 4-10), with an accuracy of ±5 mg. These bulk densities were used in preparation for both single component samples as well as mixtures. Weighed samples were mixed well in a beaker and then transferred to a metering tank. Figures 4-11 shows that the volume of each mixture was 1 ml as required in ASTM E1491-06(2012). Nano Ti was handled and weighed in a glove bag under N_2 gas before testing (Figure 4-12).

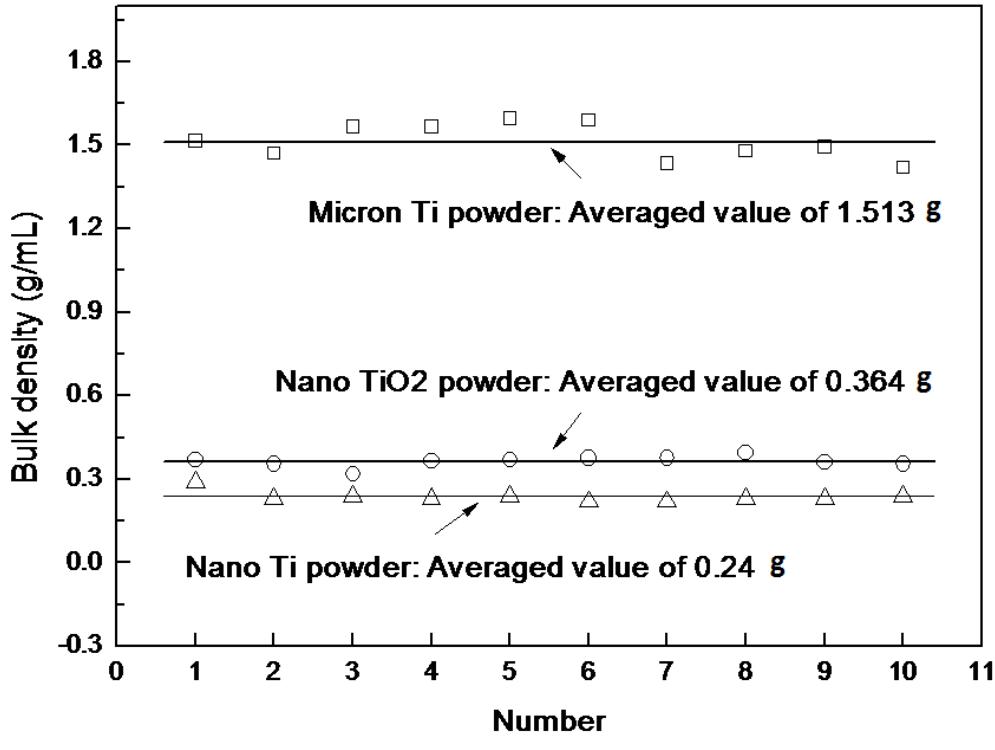

Figure 4-10 Determination of bulk density of each component.[78]

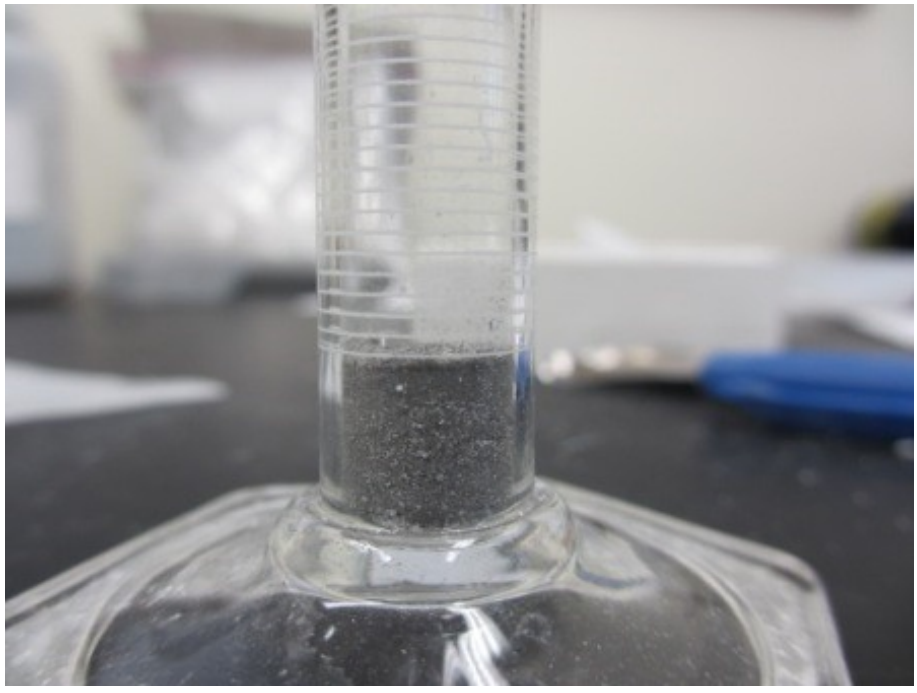

Figure 4-11 Volume of solid mixtures determined by weight.[78]

Figure 4-12 Glove bag for nano Ti sample preparation.[78]

4.2 Results and Discussion

Experimental Results are described in this section based on a comprehensive investigation of the explosibility parameters (both explosion severity and likelihood) for the following three categories of nontraditional particulate fuel systems: (i) nanomaterials having particles with dimensions between 1 and 100 nm [nano-titanium and titanium dioxide (to examine the inerting effect) powder]; (ii) flocculent (fibrous) materials characterized by a length-to-diameter ratio rather than a particle diameter (fibrous polyamide 6.6 and polyester); and (iii) hybrid mixtures consisting of a combustible dust and a flammable gas or flammable solvent (MCC and lactose admixed with flammable solvents).

4.2.1 Micron- and nano-sized Titanium Powder

In this section, experimental results for micron- and nano-sized titanium powder found by Boilard[24] have been analyzed first, and then results of the experimental work conducted by the author to examine the inerting effect of nano-sized TiO_2 powder on ignition sensitivity and Minimum Ignition Temperature (MIT) of nano- and micron-sized Ti powders are described.

4.2.1.1 Explosion severity

The explosion severity of the micron-sized titanium samples can be seen in Table 4-6 as found by Boilard et al.[7] Both P_{max} and K_{St} increase significantly with decreasing size from -100 mesh to -325 mesh. As the particle size is further decreased to $\leq$20 μm, P_{max} decreases by approximately 0.8 bar and K_{St} by 4 bar·m/s. The micron-sized data, therefore, show the expected increase in P_{max} and K_{St} with decreasing particle size, but to a limit that may be imposed by particle agglomeration effects. Formation of clouds of well-

dispersed primary particles is extremely difficult to achieve by dust dispersion in the 20-L chamber, due to the strong inter-particle cohesion forces. Dispersed smaller-sized particles eventually transformed into larger sized particles due to rapid coagulation; therefore, results in Table 4-6 have shown that titanium samples of ≤20 μm have a lower K_{St} value than -325 Mesh (<45 μm)-sized titanium powder.

Table 4-6 Explosion severity of micron-sized titanium powders.[7]

Sample	P_{max} [bar(g)]	$(dP/dt)_{max}$ [bar/s]	K_{St} [bar·m/s]
-100 Mesh (<150 μm)	5.5	84	23
-325 Mesh (<45 μm)	7.7	436	118
≤20 μm	6.9	420	114

To attempt to counteract pre-ignition, Boilard et al.[7] used nitrogen to disperse the dust into the chamber during 20-L testing of nano-sized titanium powder, but still explosions occurred prior to the activation of the chemical ignitor. Either frictional or static sparking ignited the dust before the chemical ignitors were fired; therefore, it is difficult to provide a direct comparison of explosion severity between the micron-sized and nano-sized titanium powder. Supplementary evidence of similar ignition sensitivity exhibited by some nano-particle metal powders was presented by Wu et al.[90]. At the same time, surface area clearly plays a major role in the combustion of the different sizes of titanium samples. Perhaps due to increased specific surface area of the particles, the tendency to produce oxide layers also increased. Therefore, the surface area plays a great influence on both kinetic and thermodynamic aspects of the combustion reaction.

4.2.1.2 Explosion likelihood

Very low MIE values (less than 1 to 3 mJ) for micron- and nano-sized titanium powders were measured by Boilard et al.[7] as shown in Table 4-7 (1 mJ being the lowest spark energy attainable with the MIKE 3 apparatus).

MIE of micron-sized Ti (e.g., ≤20 μm) was determined very low and it was observed at very high dust loadings (3000 or 3600 mg). However, for nano Ti powder, ignition at 1 mJ occurred even at low dust loadings (as low as 50 mg) as shown in Figures 4-13 and 4-14.

Adding inductance causes the ignition energy to be released over a longer period of time. Two possible reasons why ignition with fast sparks is more difficult than with slow ones are: (a) violent expansion which consumes thermal energy by doing work against the surrounding atmosphere and (b) enhanced demand for ignition energy due to the enlarged surface area, which may not be met easily by the expanded kennel.[91] Beside the above-mentioned reasons, the shock waves induced by the rapid expansion may contribute to this phenomenon. In the case of nano-sized Ti powders, inductance had no effect on ignition energies at almost all concentrations investigated except for 50 mg (Figure 4-13). However, for micron-sized Ti powders, the effect of inductance on ignition energy has been observed in dust loadings (600 to 1500 mg range) as shown in Figure 4-15.

As mentioned by Boilard[24], nano-titanium does not require an ignitor for an explosion to occur, therefore, no ignitors were used for any P_{max} and $(dP/dt)_{max}$ testing. MEC was determined within a range of 40-60 g/m^3 as the particle size decreased as shown in Table 4-7. As mentioned earlier, the reason could be rapid coagulation as smaller-sized particles eventually transformed into larger-sized particles.

Table 4-7 Explosion likelihood of micron- and nano-sized titanium powders.[7]

Sample	MIE [mJ] (Without Inductance)	MEC [g/m³]	Comment
-100 Mesh (<150 µm)	1 – 3	60	Standard procedure
-325 Mesh (<45 µm)	1 – 3	60	Standard procedure
≤20 µm	<1	50	Standard procedure
150 nm	<1	40	*MEC performed without any chemical ignitor
60-80 nm	<1	50	*MEC performed without any chemical ignitor
40-60 nm	<1	50	*MEC performed without any chemical ignitor

*Nano-titanium does not require an ignitor for an explosion to occur, therefore, no ignitors were used for any P_{max} and $(dP/dt)_{max}$ testing.

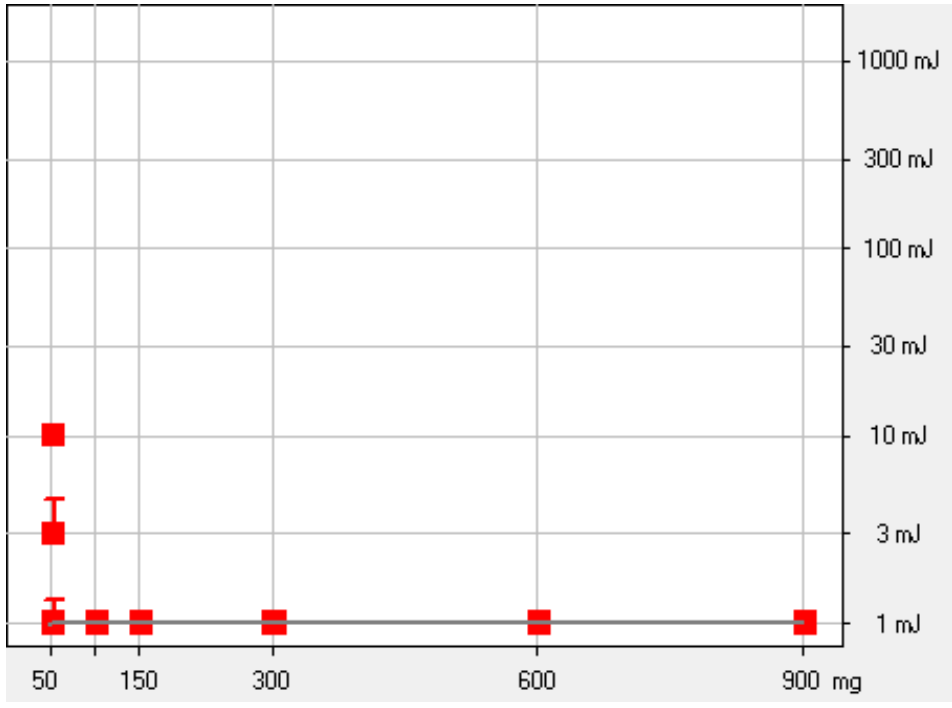

(a)

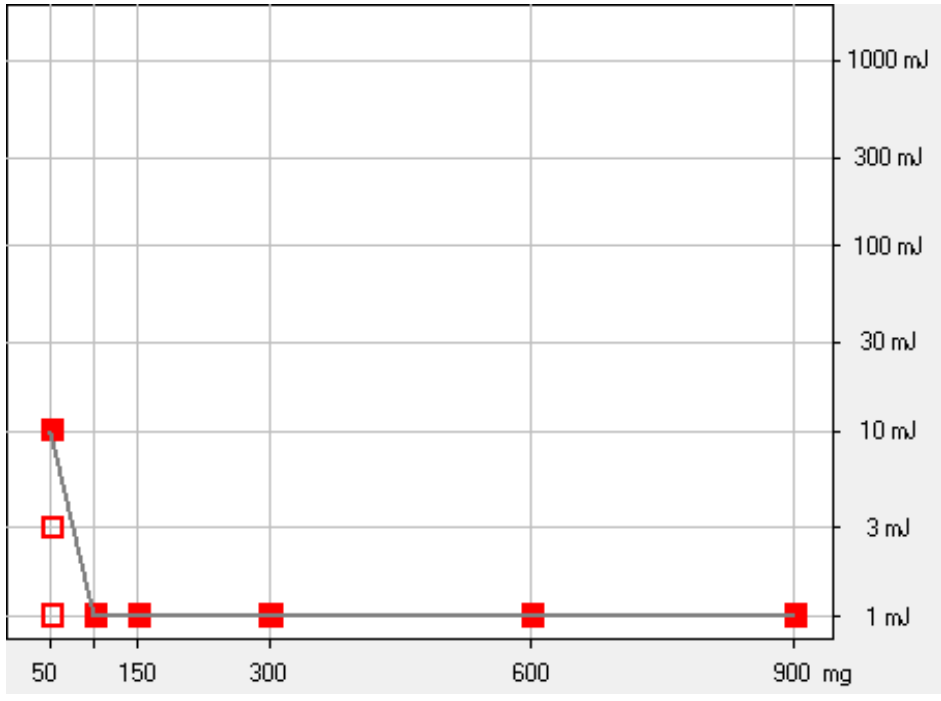

(b)

Figure 4-13 Effect of concentration on ignition energy of 60-80 nm Ti powder: (a) with inductance, and (b) without inductance.

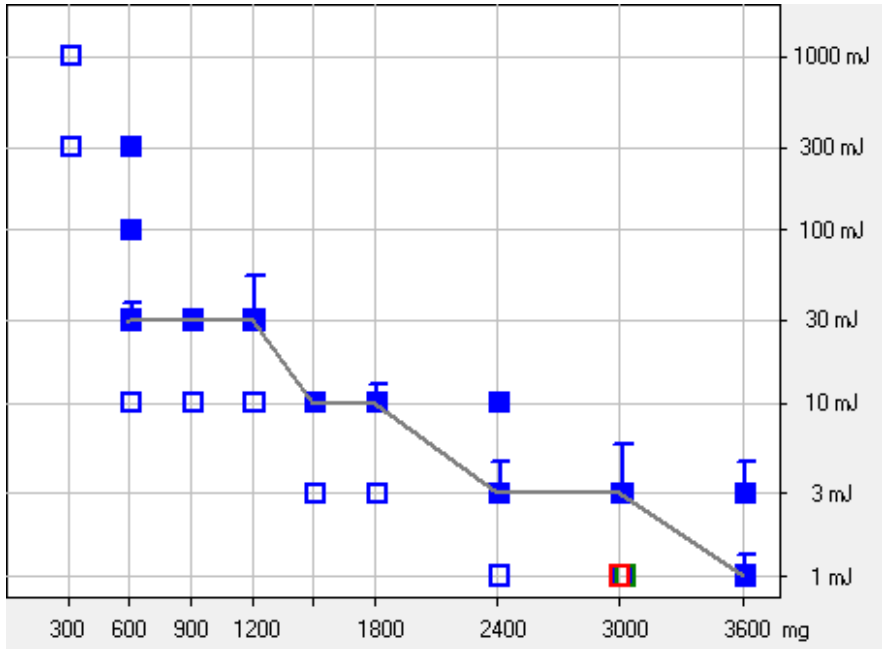

(a)

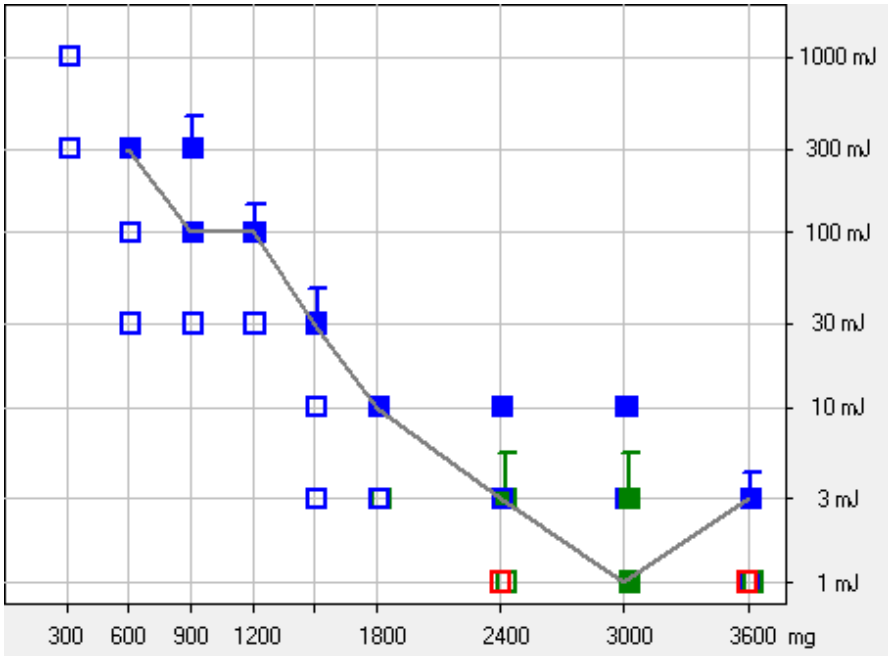

(b)

Figure 4-14 Effect of concentration on ignition energy of micron-sized Ti (≤20 μm) powder: (a) with inductance, and (b) without inductance.

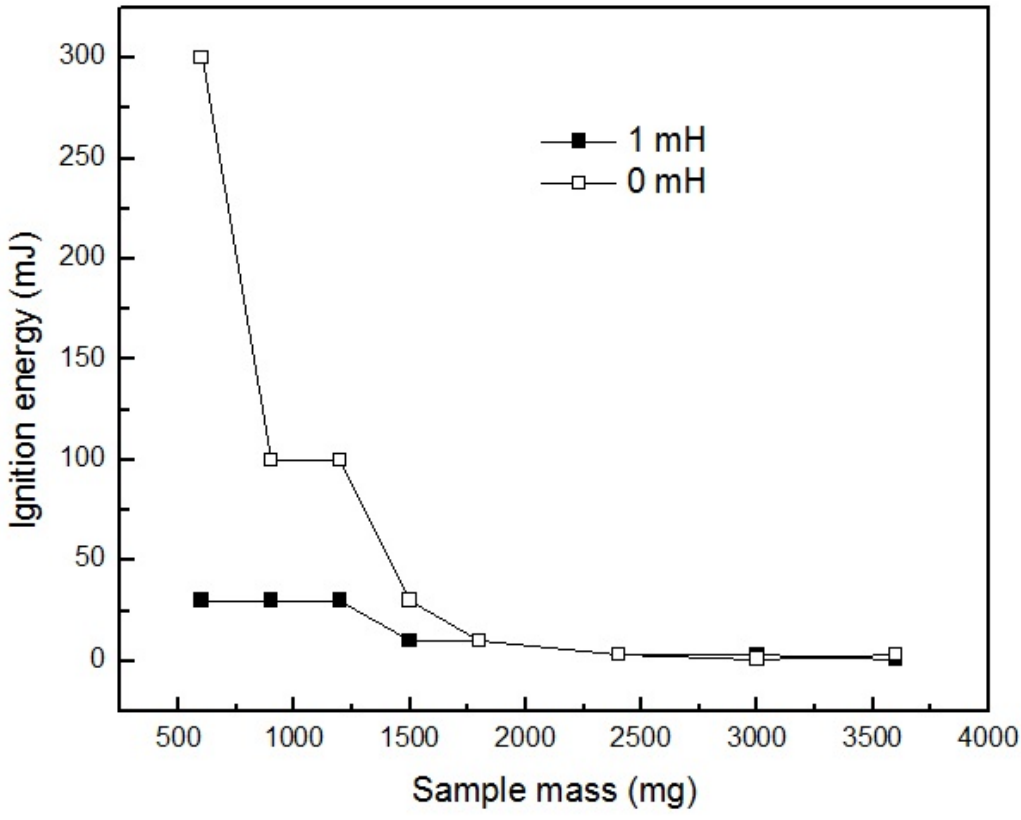

Figure 4-15 Effect of inductance on ignition energy of micron-sized Ti (≤20 µm) powders.

A significant increase occurs with MIT as the particle size of titanium powder decreases. These results have been displayed in Table 4-8. The -100 mesh (<150 µm) particles (largest size among six sizes) could not be ignited in the BAM oven at 590 °C which is the highest temperature attainable with the BAM oven as designed. Titanium samples of -325 mesh (<45 µm) and ≤20 µm ignited at 460 °C. The MIT of all three nano-titanium samples was in the range of 240-250 °C. These MIT values are very low, indicating the enhanced potential for nano-titanium ignition by hot surfaces.

For the same volume of titanium samples dispersed within the BAM oven, there are more nano-sized titanium particles than micron-sized particles. Therefore, particle interaction has less influence on heat transfer for micron-sized titanium powder than nano-sized. This causes a higher temperature required for micron-sized titanium to be ignited by hot surfaces.

At the same time, surface area clearly plays a major role in the combustion process. Therefore, the heat transfer process may be faster for nano-sized titanium powder as compared to micron-sized due to increased specific surface area and particle interaction.

Table 4-8 Minimum ignition temperature of micron- and nano-sized titanium powder.[7]

Sample of nano titanium	**MIT [°C]**
-100 Mesh (<150 μm)	>590
-325 Mesh (<45 μm)	460
≤20 μm	460
150 nm	250
60-80 nm	240
40-60 nm	250

4.2.1.3 Dust inerting

MIE of micron (≤20 μm) Ti and nano (10-30 nm) TiO_2 powder mixtures

MIE results of micron (≤20 μm) Ti mixed with 10, 30, and 50% nano (10-30 nm) TiO_2 by mass are shown in Figures 4-16, 4-17 and 4-18, respectively. For the mixture with

70% TiO_2, ignition at 1000 mJ (the highest spark energy attainable with the MIKE 3) occurred only at the dust quantity of 3600 mg (Figure 4-19), while no ignition occurred for dust loadings from 300 to 3600 mg with 80% TiO_2 (Figure 4-20). For a given TiO_2 percentage, a higher amount of dust loading has a greater probability to ignite at lower ignition energy (Figure 4-21) due to higher amount of combustible material (*i*.e., titanium powder) in the mixture. For the purpose of an inerting effect comparison between different TiO_2 percentages, the statistical MIEs of the mixtures were calculated by using Equation (4) as follows.[92]

$$\log MIE = \log IE - N_I \times \frac{\log IE - \log NIE}{N+1} \qquad (4)$$

Here, N and N_I represent the number of trials conducted and the number of explosions successfully induced, respectively, at energy level IE. At least 5 trials of N are required at energy level IE. The 5-mJ statistic MIE of a mixture with 30% TiO_2 was very close to that for 10% TiO_2 (4 mJ), indicating that less than 30% solid TiO_2 inertants had almost no effect on MIE of mixtures. These data support the conclusion by Amyotte[12] that "a little is not good enough", even with nano-sized solid inertants. When the TiO_2 percentage was higher than 50%, the statistic MIE of mixtures increased sharply with an increased TiO_2 percentage. Mixtures with 70% TiO_2 were ignited by 1000-mJ electric spark. Mixtures were not ignited by a 1000-mJ spark when the TiO_2 percentage reached 80% (Figure 4-22). The complete numerical data can be found in Appendix C.

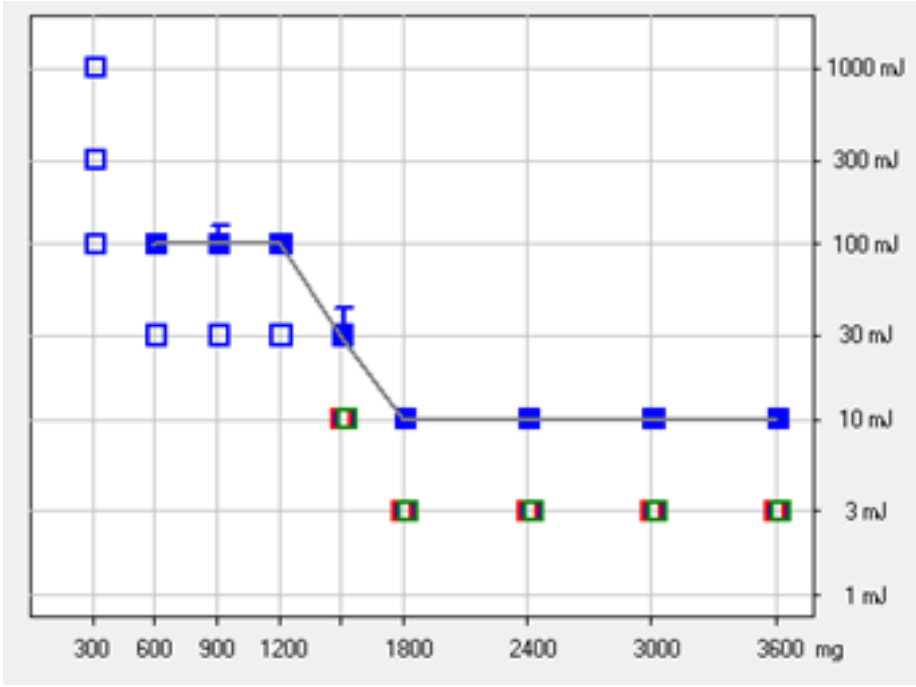

Figure 4-16 Effect of 10% TiO_2 on ignition energy of micron-sized titanium.

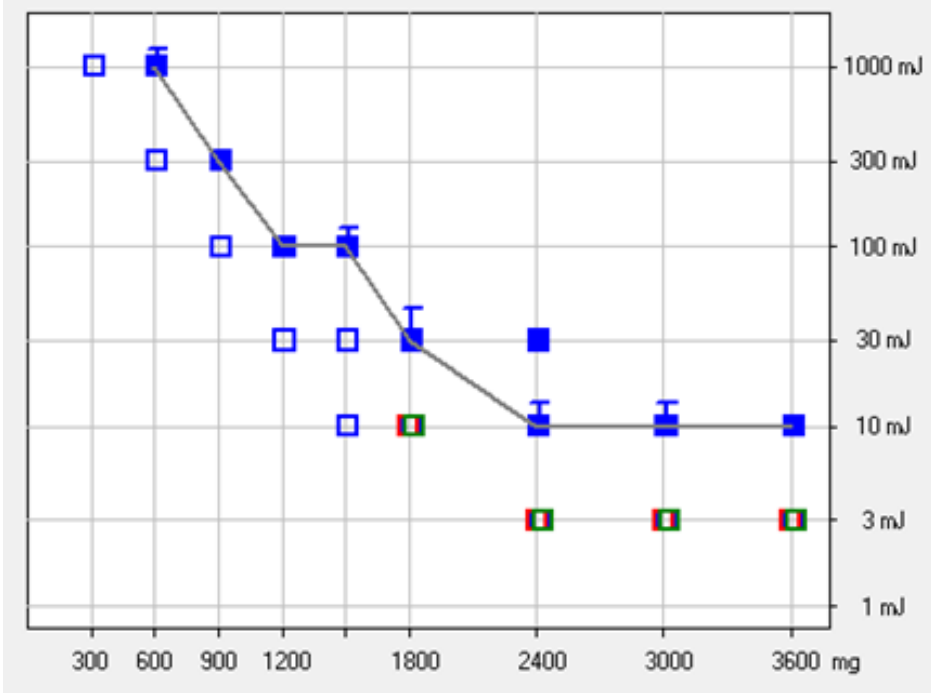

Figure 4-17 Effect of 30% TiO_2 on ignition energy of micron-sized titanium.

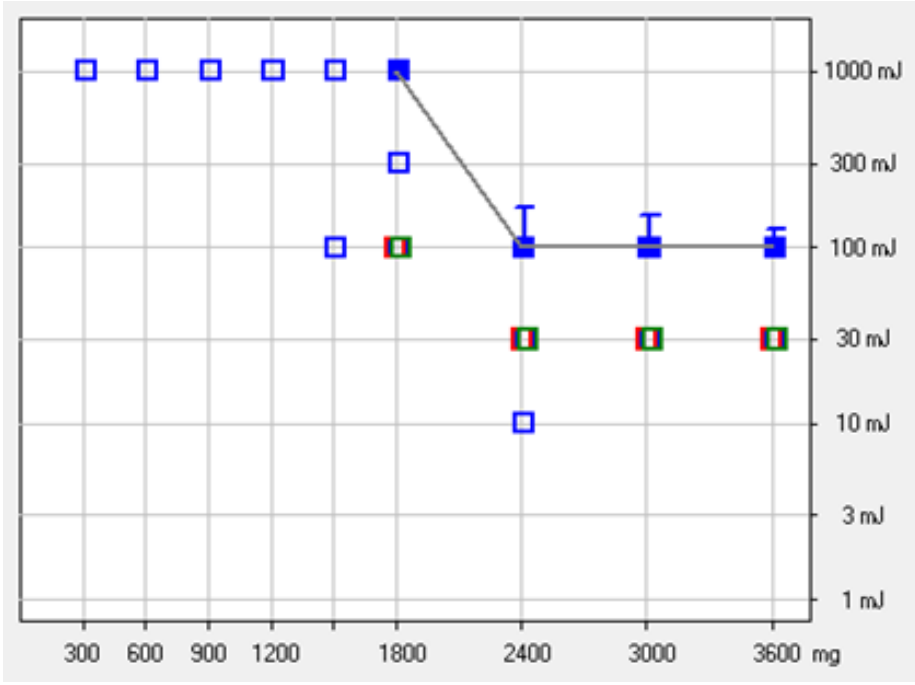

Figure 4-18 Effect of 50% TiO_2 on ignition energy of micron-sized titanium.

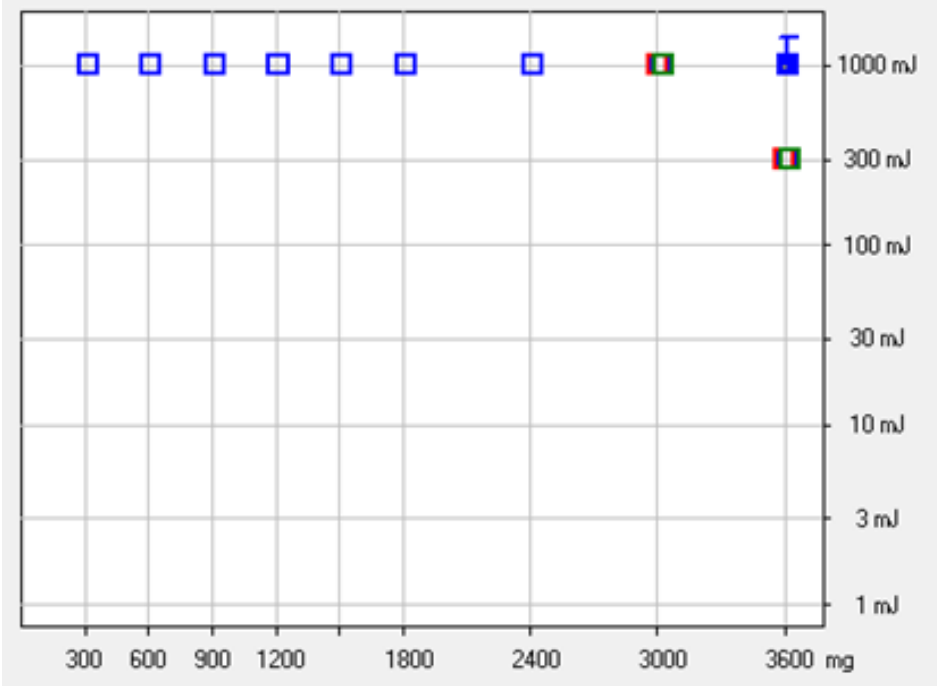

Figure 4-19 Effect of 70% TiO_2 on ignition energy of micron-sized titanium.

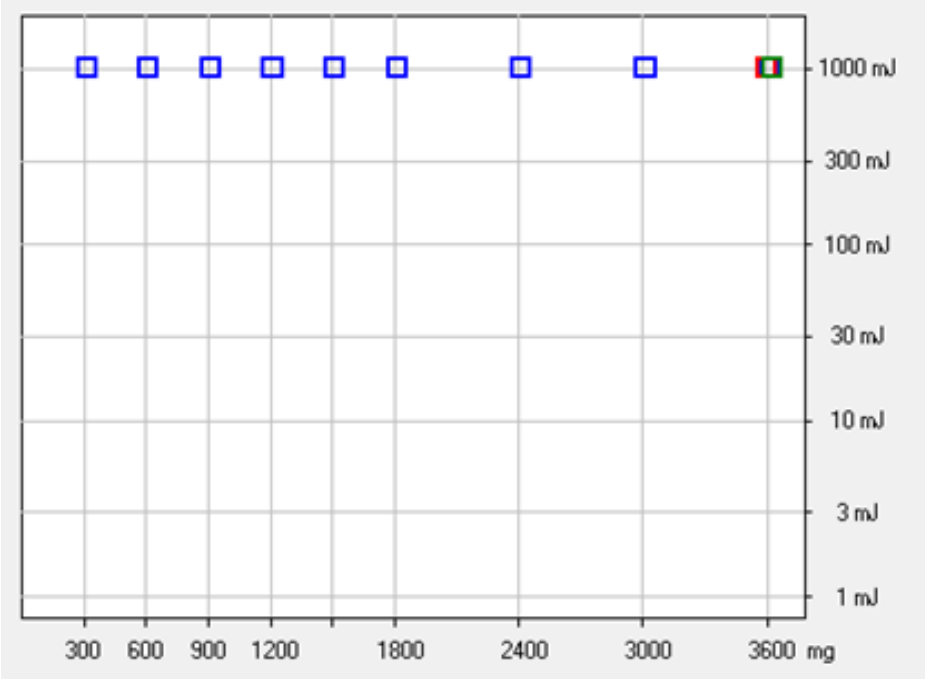

Figure 4-20 Effect of 80% TiO_2 on ignition energy of micron-sized titanium.

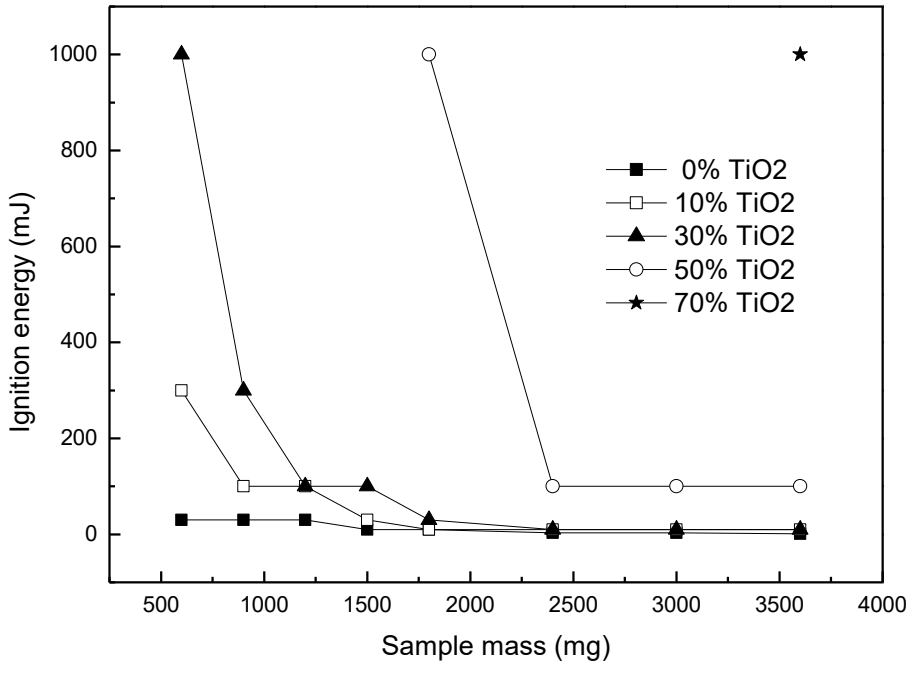

Figure 4-21 Effect of solid inertants on ignition energy of micron-sized titanium powder.

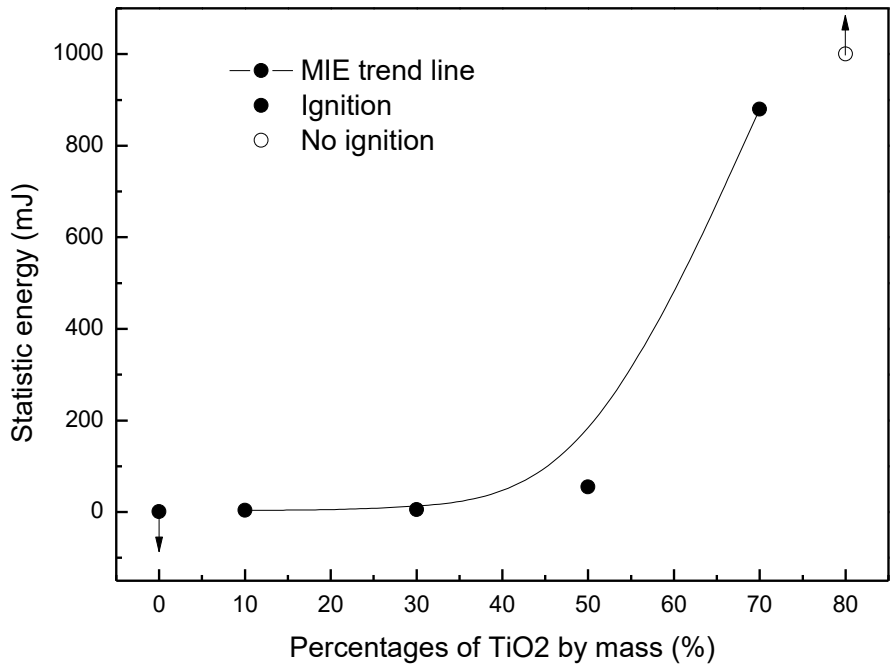

Figure 4-22 Statistic energy of micron-sized Ti powders with various percentages of TiO_2 by mass.

MIE of nano (60-80 nm) Ti and nano (10-30 nm) TiO_2 powder mixtures

The MIE results of nano (60-80 nm) Ti admixed with 50, 70, and 90% nano (10-30 nm) TiO_2 by mass have been described in Figures 4-23, 4-24 and 4-25, respectively. The complete numerical data can be found in Appendix C. The statistic energy is observed to be as low as 2.1 mJ for the mixture even with 90% TiO_2, demonstrating that solid inertants had almost no effect on the MIE of nano Ti powder, especially at higher dust loadings. Mixtures with 90% TiO_2 were not ignited by a 1000-mJ spark energy at dust loadings from 50 to 300 mg due to the inclusion of much less nano Ti powder in the mixture. The explosion inerting tests performed by Boilard[24] in the Siwek 20-L sphere indicated that Ti powders of 60-80 nm still have pre-ignition activity at 60% TiO_2, which converges with the results of current MIE tests.

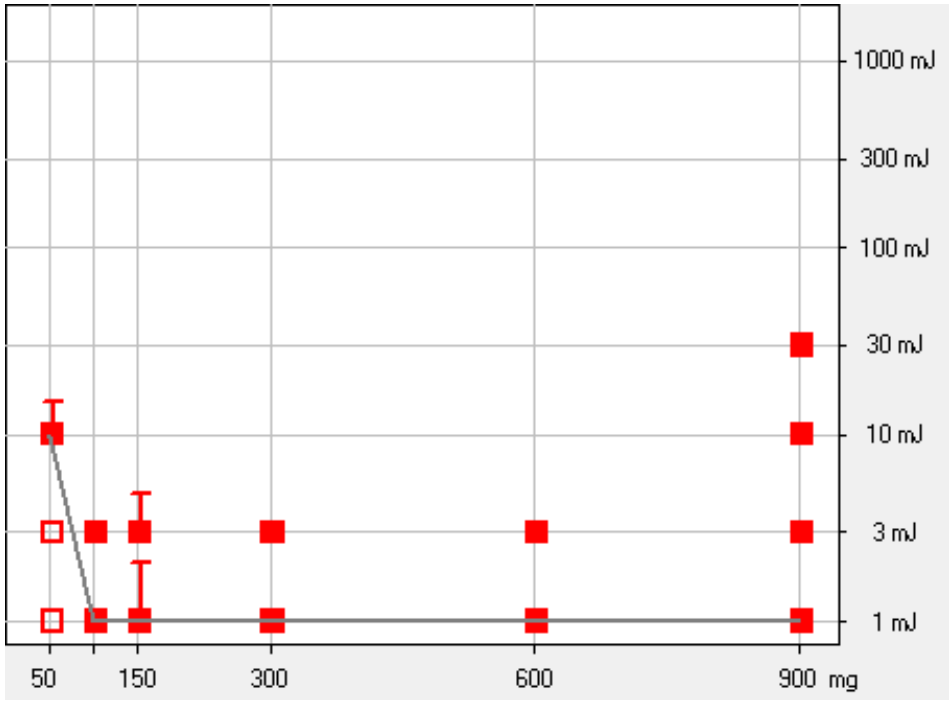

Figure 4-23 MIE results of nano (60-80 nm) Ti admixed with 50% nano TiO_2.

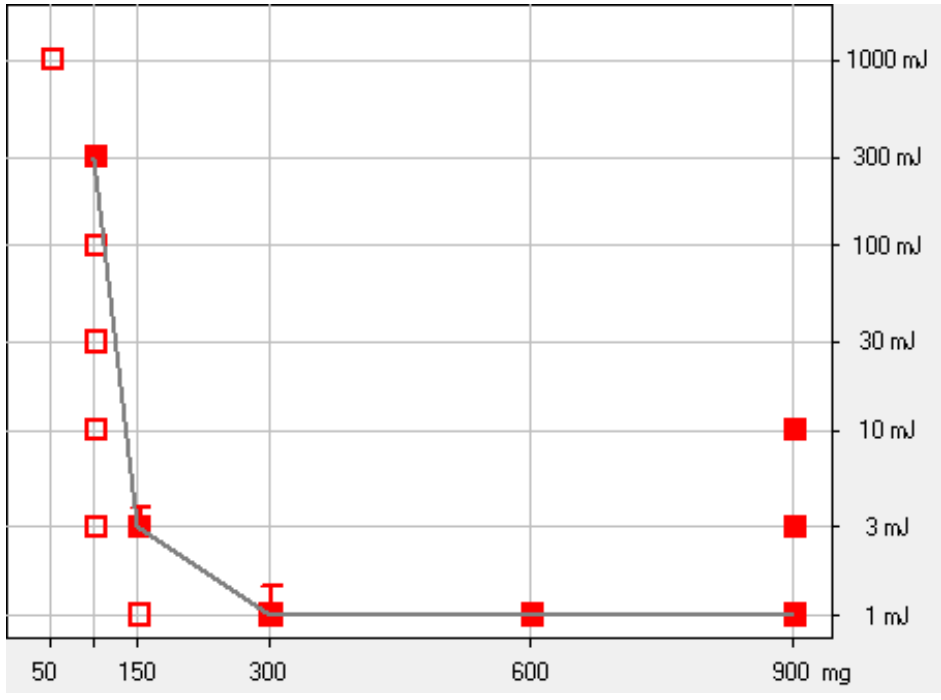

Figure 4-24 MIE results of nano (60-80 nm) Ti admixed with 70% nano TiO_2.

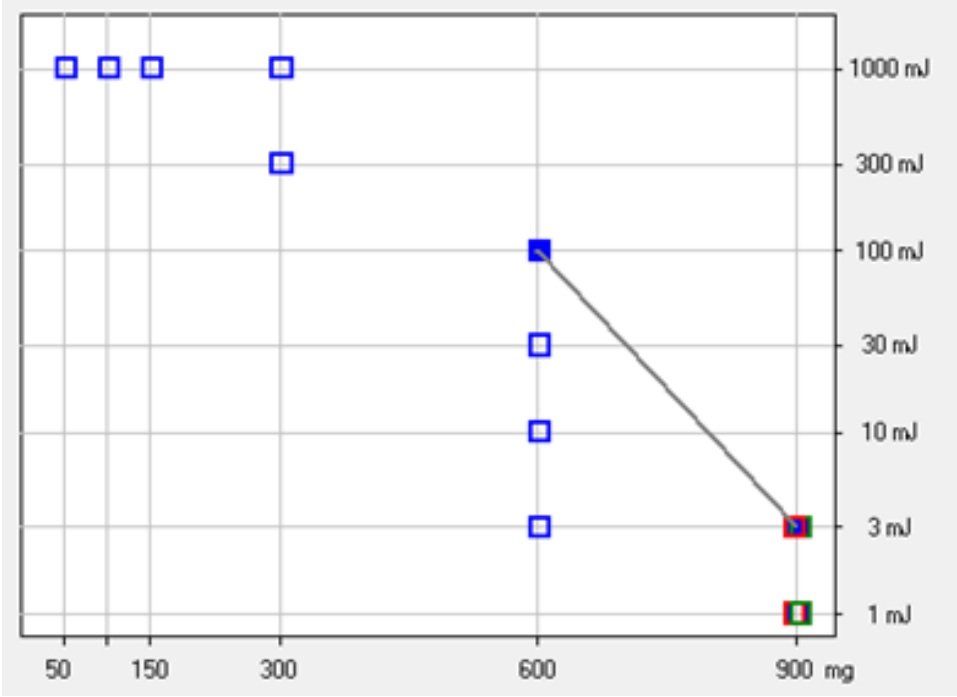

Figure 4-25 MIE results of nano (60-80 nm) Ti admixed with 90% nano TiO_2.

Layer fires induced by electrical spark

For pure micron-sized Ti powder and its mixtures with TiO_2, the more the ignition energy exceeded the MIE, the more titanium powder was ignited with a concurrent violent explosion. Subsequently, metal powder settled into the bottom of the glass tube before burning out, resulting in a layer fire. The layer fire is a non-stationary self-propagating process after local ignition by burning metal powder, and is similar to that described elsewhere.[93] For example, with the 30% TiO_2 mixture ignited by a 30-mJ ignition energy (Figure 4-26), metal sparks were observed falling to the bottom of the glass tube from 1000 to 1125 ms after the dust explosion and before burning out, resulting in a layer fire that was sustained for a comparatively long time (about 20 s from 1125 to 20833 ms). When the mass of titanium powder was changed to 1500 mg and also mixed with 30% TiO_2, a flamelet was produced around the electric spark with 30-mJ ignition energy, after

which ignited powder settled into the bottom of the glass tube. This ignition process was short and constituted an incomplete dust explosion (Figure 4-27). After that, a layer fire similar to that in Figure 4-26 occurred. If the ignited layer (for example, at the time of 2167 ms in Figure 4-27) was dispersed, a dust explosion similar to that at 833 ms in Figure 4-26 could be observed. The complete numerical data can be found in Appendix C.

The aforementioned finding suggests that such an explosion was induced by the layer fire in the dust container instead of by electric spark. One of the reasons for the above-mentioned explosion process could be a comparatively high burn temperature of micron-sized Ti powder which is sufficient to initiate a sustainable self-propagating layer fire of pure Ti powder.[93] One other reason could be a comparatively long burning time which is more than that required for sedimentation. An increased TiO_2 percentage led to decreased reaction kinetics (*i*.e., $(dp/dt)_{max}$). One possible factor is that more combustible material may have been left after spark ignition, due to the lower combustion rate in the presence of a higher percentage of solid inertants. Thus, additional precautions should be implemented to prevent metallic layer fires in addition to dust explosions, especially in the case of high dust loadings. Such dust fires may cause primary damage or initiate dust explosions by supplying an ignition source. No such layer fires were observed during MIE tests of nano Ti powders. The reason is due to faster flame propagation (or burning speed) in nanoparticle cloud with respect to the case of micron particles.

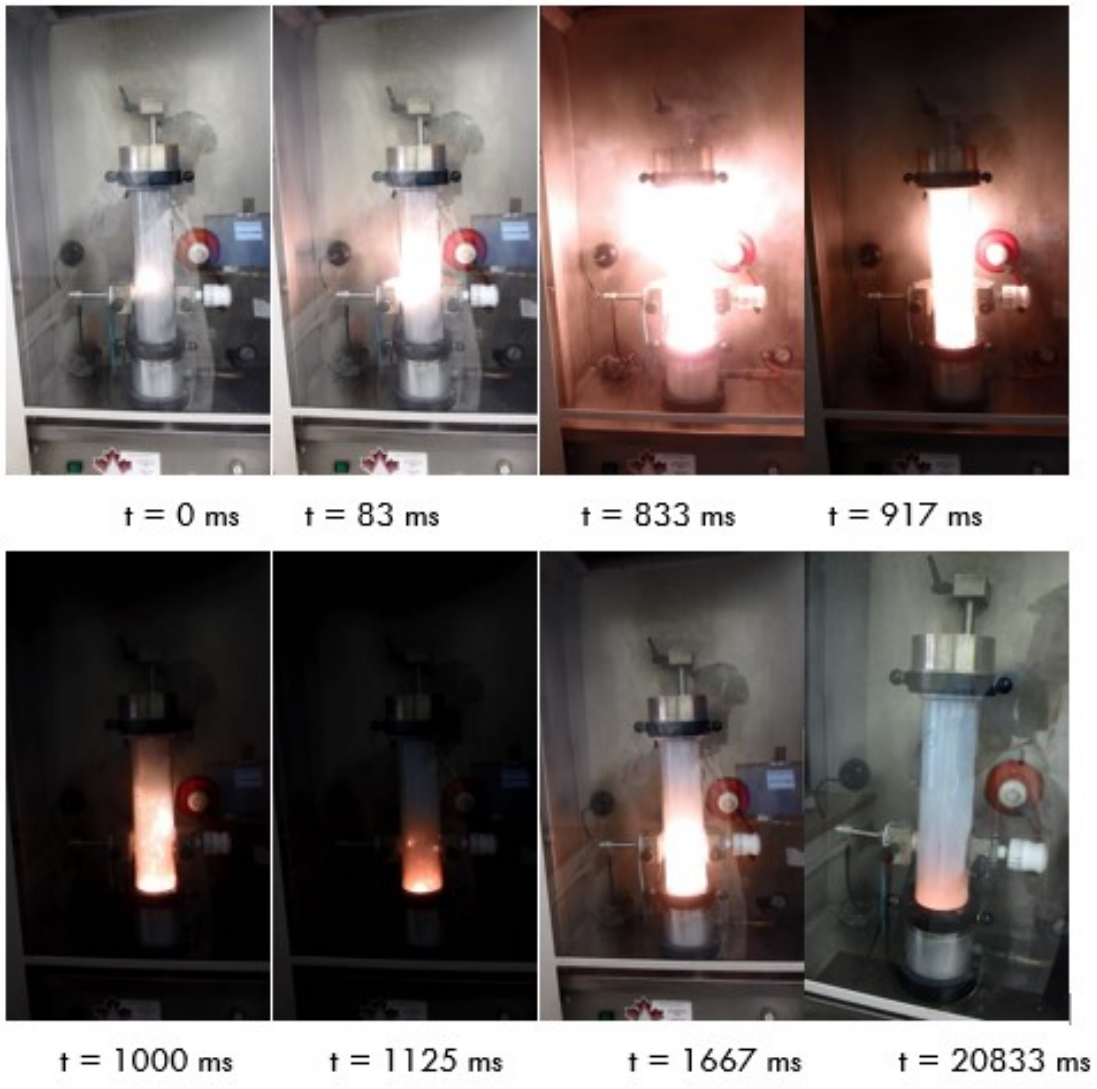

Figure 4-26 Ignition process of a complete dust explosion of Ti mixed with 30% TiO_2 (ignition energy: 30 mJ; mass of micron-sized Ti: 1680 mg; mass of TiO_2: 720 mg; time delay: 120 ms; inductance: 1 mH).

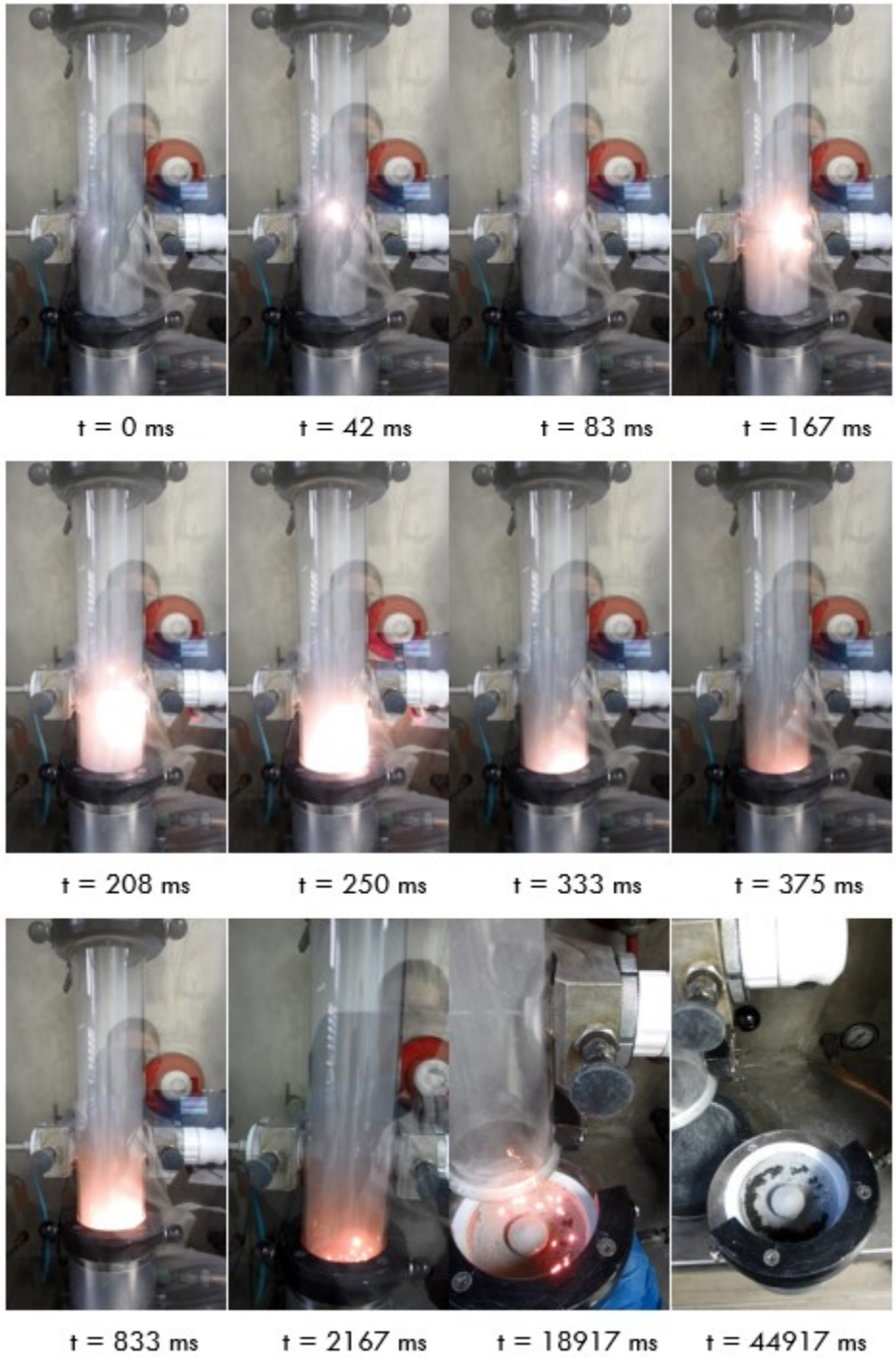

Figure 4-27 Ignition process of an incomplete dust explosion of Ti mixed with 30% TiO_2 (ignition energy: 30 mJ; mass of micron-sized Ti: 1500 mg; mass of TiO_2: 640 mg; time delay: 120 ms; inductance: 1 mH).

Effect of nano (10 to 30 nm) TiO_2 powder on MIT of micron (≤20 μm) Ti powder

The minimum ignition temperature of micron Ti powder (≤20 μm) increased gradually with increased nano (10-30 nm) TiO_2 percentage (Table 4-9). The complete numerical data can be found in Appendix C. The solid mixtures (when TiO_2 percentage reached 70%) were observed as not ignited by 590 °C (highest temperature attainable with the BAM oven). Thus, nano-sized inertants were effective in decreasing ignition sensitivity of micron-sized metal powders in contact with hot surfaces. When micron-sized Ti particles and nano-sized TiO_2 particles were mixed, the large individual micron-sized particles would possibly be coated to some extent with small nanoparticles due to physical adsorption, by forming a packed powder resulting in somewhat lower reaction kinetics of solid mixtures compared to pure micron Ti powder.

Table 4-9 MIT of the solid mixtures of nano TiO_2 and micron (≤20 μm) Ti powder.

Nano-TiO_2 %, by Vol.	0	30	40	50	60	70
Micron-Ti powder % by Vol.	100	70	60	50	40	30
MIT [°C]	460	480	540	570	590	> 600

Effect of nano (10-30 nm) TiO_2 powder on MIT of nano (60-80 nm) Ti powder

The minimum ignition temperature of nano (60-80 nm) Ti powder admixed with various percentages of nano (10-30 nm) TiO_2 powder is shown in Table 4-10. The complete numerical data can be found in Appendix C. MIT of the mixtures was still as low as 310 °C even with 90% TiO_2, indicating that solid inertant (nano TiO_2 powder) had little effect on the MIT of nano Ti powder. Thus, in this case, solid inertant technology does not appear to offer promise in significantly reducing the ignition hazard for nano Ti powder subjected to hot surfaces.

Table 4-10 MIT of the solid mixtures of nano TiO_2 and nano (60-80 nm) Ti powder.

Nano-TiO_2 %, by Vol.	0	30	50	70	90
Nano-Ti powder % by Vol.	100	70	50	30	10
MIT [°C]	240	260	280	300	310

4.2.2 Fibrous Polyamide 6.6 and Polyester

In this section, experimental results for polyamide 6.6 and polyester samples found by Iarossi et al.[76] have been analyzed. Results of the experimental work used by the author in simulating explosion scenarios are described later in Chapter 5.

4.2.2.1 Explosion severity

Explosion severity data for the polyamide 6.6 and polyester samples are given in Tables 4-11 and 4-12 as described by Iarossi et al.[76] Different chemical structures of polyamide 6.6 and polyester are most likely one of the key factors for the difference in their explosibility results. For example, the presence of phenyl groups in the polyester structure may impose a greater influence of dtex on P_{max} and K_{St} than for polyamide 6.6. As mentioned earlier, an important difference between these two fibres that can influence the explosibility parameters is the melting and burning process; polyamide first melts and then burns rapidly, while polyester melts and burns at the same time.[80]

Table 4-11 Explosion severity parameters for polyamide 6.6 with changing length.[76]

dtex	Length [mm]	P_{max} [bar(g)]	$(dP/dt)_{max}$ [bar/s]	K_{St} [bar.m/s]
3.3	0.3	7.1	178	48
3.3	0.5	6.6	135	37
3.3	0.75	6.4	102	28
3.3	0.9	6.3	102	28
3.3	1	6.4	94	26

Table 4-12 Explosion severity parameters for polyamide 6.6 and polyester with changing diameter.[76]

Material	dtex	Length [mm]	P_{max} [bar(g)]	$(dP/dt)_{max}$ [bar/s]	K_{St} [bar.m/s]
Polyamide 6.6	1.7	0.5	6.6	183	50
Polyamide 6.6	3.3	0.5	6.6	135	37
Polyester	1.7	0.5	6.9	247	67
Polyester	3.3	0.5	5.5	104	28

A decreasing trend was observed for polyamide 6.6 in both P_{max} and K_{St} values as length increased (Table 4-11). One possible reason for this decreasing trend could be due to more time was required for heat to propagate along the covalent fiber bonds as length increased.[76] Such evidence was noticed in the pressure-time tresses as shown in Figure 4-28. The values for t_1 (which is the time difference between the activation of the ignition and the

culmination point) were observed higher for explosions associated with 1.0-mm long fiber as compared to 0.3-mm long fiber.

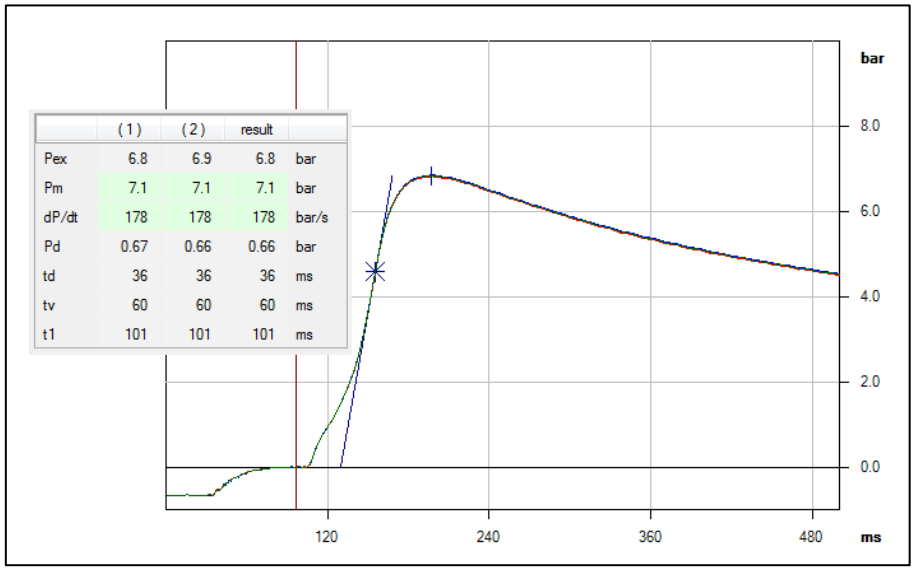

(a)

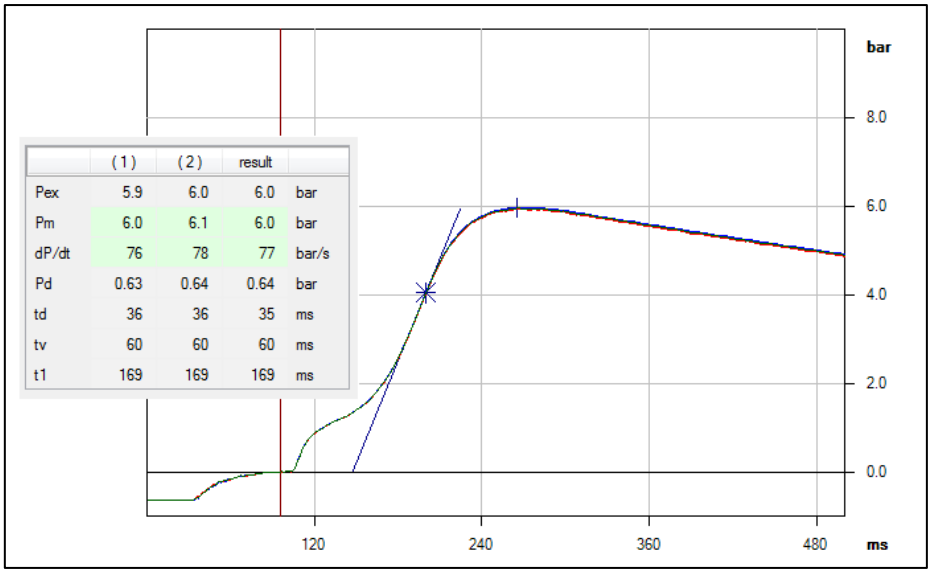

(b)

Figure 4-28 KSEP pressure-time curves in the 20-L chamber for polyamide (a) 0.3-mm long and (b) 1-mm long fibers of 500 g/m^3 concentration.

Lower values of P_{max} and K_{St} were noticed for polyester as dtex increased. However, the same value of P_{max} and a lower K_{St} value were observed as dtex increased for polyamide 6.6 (Table 4-12). Different chemical structures of polyamide 6.6 and polyester are most likely the reason for this difference as stated earlier. Thermodynamic properties, such as thermal conductivity and change of enthalpy could play an important role for such variation.

4.2.2.2 Explosion likelihood

The MIE for polyester (Table D.1, Appendix D) is observed to undergo a far less significant change than for polyamide 6.6 with an increase in dtex. Moreover, Iarossi et al.[76] found the structure of polyester could lead to a reduced tendency to coagulate which would be expected to affect dispersion and thus undergoes a far less significant change than for polyamide 6.6 with an increase in dtex. An increase in dtex from 1.7 to 3.3 had no effect on minimum explosible concentration for the polyester samples as shown in Table D.1 (Appendix D). However, for the polyamide 6.6, a noticeable increase was observed as described by Iarossi et al.[76] The minimum ignition temperatures were observed to be similar for all four samples as shown in Tables D.1 (Appendix D).

The MIE results in Table D.2 (Appendix D) indicate that only the finest fibers (0.3-mm long) of polyamide 6.6 (dtex 3.3) ignited in the MIKE 3 apparatus with a spark energy of 580 mJ. Other fibers (0.5, 0.75, 0.9 and 1-mm long) were observed to be not ignited at even 1000 mJ (the maximum attainable with this equipment).

4.2.3 Hybrid Mixtures

This section presents the experimental results for hybrid mixtures according to the severity of explosion consequences (overpressure and rate of pressure rise) and the likelihood of explosion occurrence (minimum explosible concentration, minimum ignition energy and minimum ignition temperature).

Because the MIKE 3 apparatus and BAM oven are not closed systems, only baseline excipient-alone testing and excipient pre-wetted with solvent testing were possible for MIE and MIT determination. With the Siwek 20-L chamber (a closed system), it was feasible to conduct P_{max}, K_{St} and MEC testing for all three cases of the dust alone, pre-wetted with solvent, and with solvent admixed to the combustion atmosphere at 80 % of the lower flammability limit for each solvent prior to dust dispersal.

4.2.3.1 Explosion severity

Figures 4-29 and 4-30 show the influence of dust concentration on explosion overpressure, P_m, and rate of pressure rise, $(dP/dt)_m$, for the excipient dust (MCC and lactose). (All figures in this section give average values of P_m and $(dP/dt)_m$ at dust concentrations for which replicate testing was performed according to ASTM E-1226-12(a)[41])

The data in Figures 4-29 and 4-30 display the expected trend of an increase in the measured explosibility parameter as dust concentration increases. Eventually, peak values of P_m and $(dP/dt)_m$ are attained, followed by a parameter decrease or leveling-off with further increases in dust concentration. For MCC, the maximum explosion pressure of 8.5 bar (g) was observed at a concentration of 1250 g/m^3 however, the peak value of 7.1 bar (g) for lactose was noticed at 1750 g/m^3. The higher peak values at lower concentrations for MCC over lactose are indicative of both compositional differences

between the two materials and the smaller particle size of the MCC (Table 4-3). The complete numerical data can be found in Appendix E.

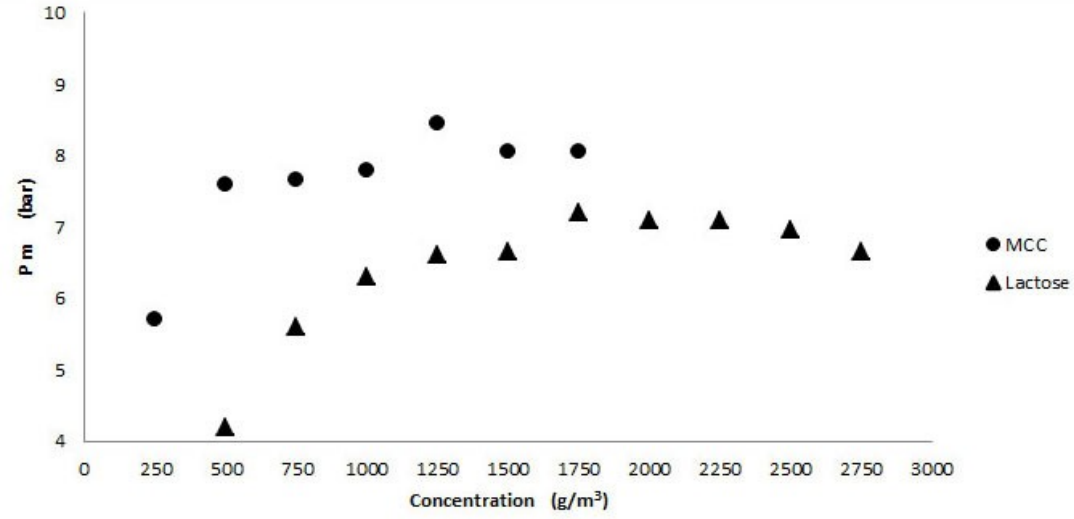

Figure 4-29 Influence of dust concentration on explosion overpressure of MCC and lactose (baseline excipient alone).

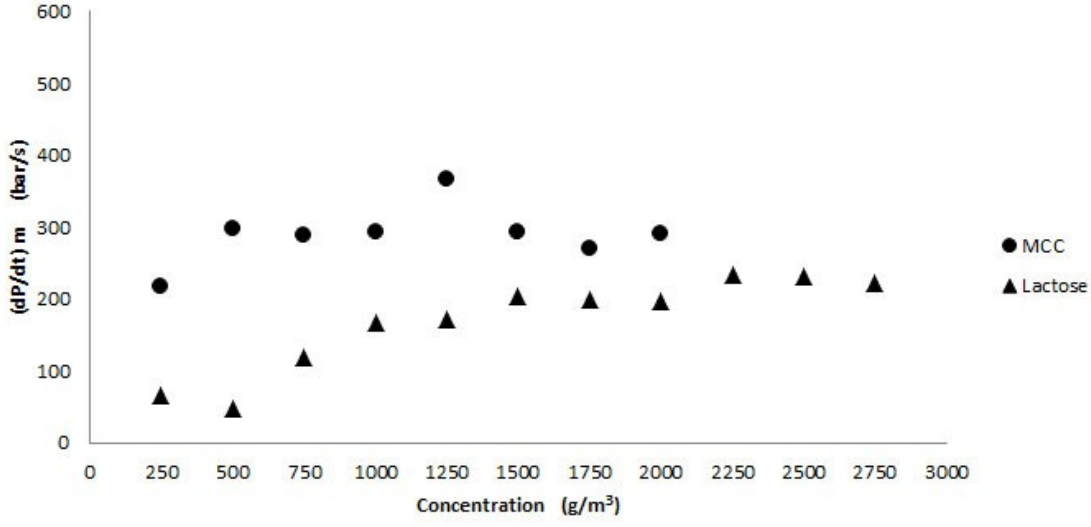

Figure 4-30 Influence of dust concentration on rate of pressure rise of MCC and lactose (baseline excipient alone).

Tables 4-13 and 4-14 give the complete P_{max} and K_{St} data sets for all test conditions. The complete numerical data can be found in Appendix E.

Table 4-13 P_{max} and K_{St} data for MCC.[94]

Material	**P_{max} [bar(g)]**	**K_{St} [bar·m/s]**
MCC	8.5	103
MCC + M (PW)	7.9	144
MCC + E (PW)	7.8	117
MCC + IPA (PW)	7.7	116
MCC + M (ATM)	7.9	168
MCC + E (ATM)	8.3	149
MCC + IPA (ATM)	8.4	172

Table 4-14 P_{max} and K_{St} data for lactose.[94]

Material	**P_{max} [bar(g)]**	**K_{St} [bar·m/s]**
Lactose	7.1	65
Lactose + M (PW)	8.1	149
Lactose + E (PW)	8.4	148
Lactose + IPA (PW)	8.6	144
Lactose + M (ATM)	8.0	155
Lactose + E (ATM)	7.4	94
Lactose + IPA (ATM)	7.8	102

In all cases, pre-wetting (PW) of MCC and lactose with solvent had a measurable impact on both P_{max} and K_{St}. As expected, the influence was generally an enhancement of each explosibility parameter; the lone exception was P_{max} for MCC which displayed a decrease of 0.6 to 0.8 bar (g) with solvent admixture by pre-wetting. These results depict how common pharmaceutical solvents such as methanol, ethanol, and isopropanol can significantly increase the explosion severity of common pharmaceutical excipients such as MCC and lactose.

In both PW and ATM conditions, solvents influence significantly the rate of combustion. The values for t_1 (which is the time difference between the activation of the ignition and the culmination point) were observed lower for explosions associated with solvents as compared to the base-line excipient. MCC powder and MCC admixed with methanol in both PW and ATM conditions have been considered here as presented in Figures 4-31, 4-32 and 4-33 (KSEP pressure-time curves in the 20-L chamber). The minimum t_1 has been recorded as 62, 46 and 32 ms for MCC, MCC admixed with methanol in PW, and MCC admixed with methanol in ATM condition, respectively.

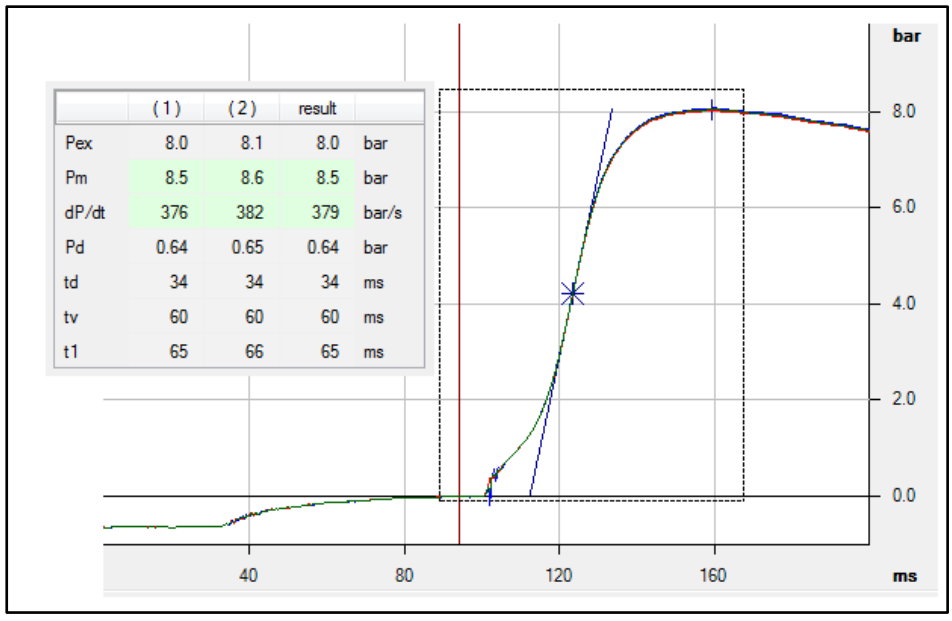

Figure 4-31 KSEP pressure-time curve in 20-L chamber for a single test of MCC which exhibited maximum explosion pressure.

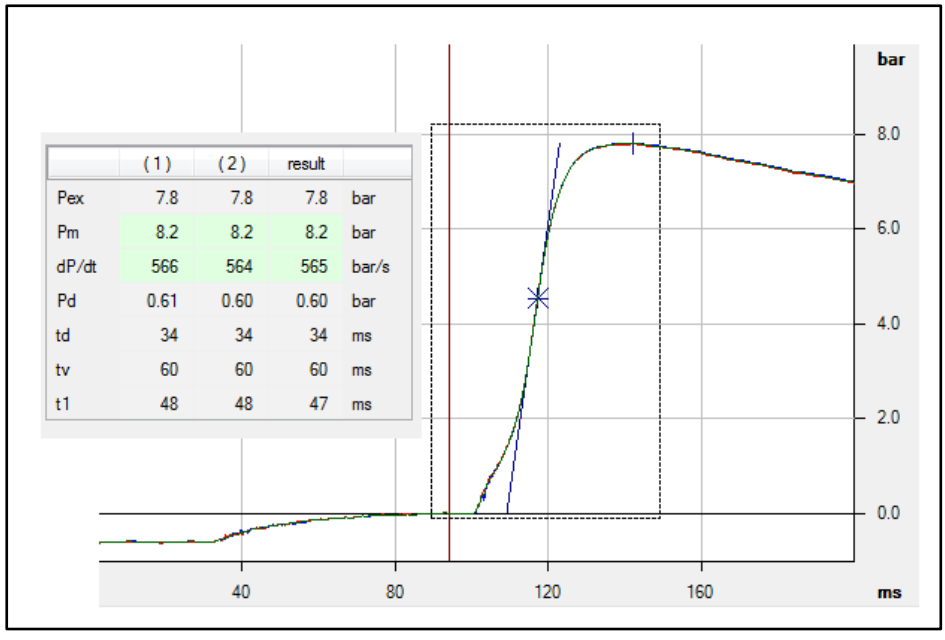

Figure 4-32 KSEP pressure-time curve in 20-L chamber for a single test of MCC admixed with methanol in PW condition which exhibited maximum explosion pressure.

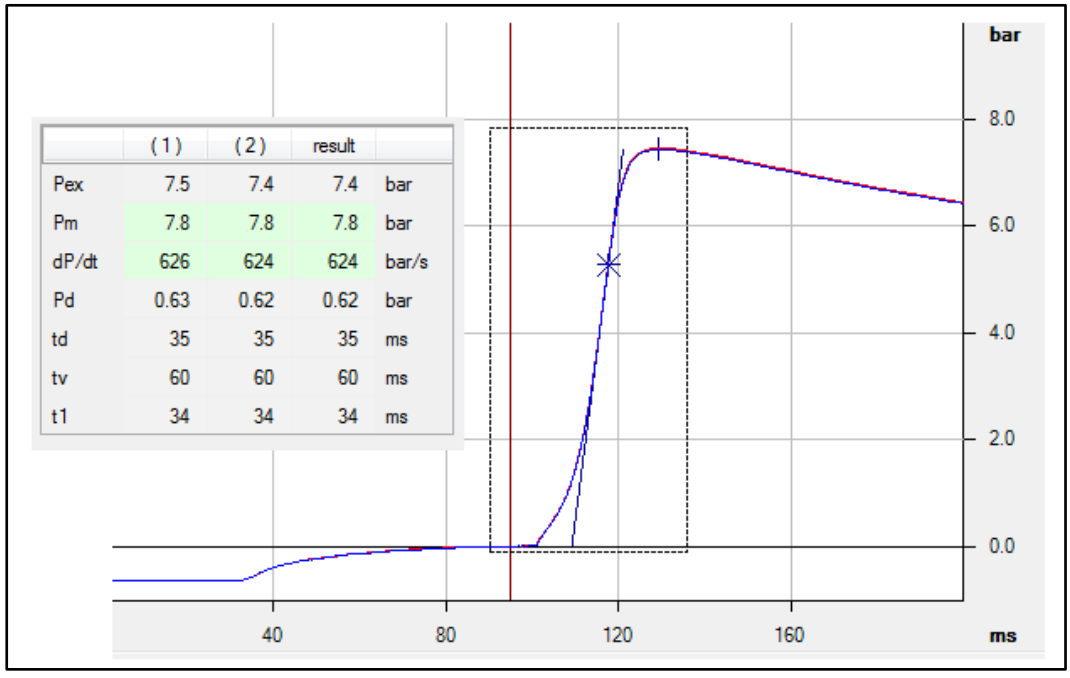

Figure 4-33 KSEP pressure-time curve in 20-L chamber for a single test of MCC admixed with methanol in ATM condition which exhibited maximum explosion pressure.

While the magnitude of the effect on K_{St} of solvent pre-wetting for MCC was generally distinguishable for the different solvents, this was not the case for lactose. Pre-wetting of lactose with each of the three solvents resulted in similar K_{St} values. This trend suggests an approximate correlation of K_{St} with burning velocity (Table 4-4) for pre-wetted MCC but not for pre-wetted lactose. Such a correlation was previously shown to hold in the atmospheric-type tests conducted by Amyotte et al.[16] for polyethylene admixed with various hydrocarbons.

The atmospheric (ATM) test data in Tables 4-13 and 4-14 show a reversal of the above trend for the two excipients. Here, the admixed solvent has generally the same effect on K_{St} of MCC regardless of the nature of the solvent. On the other hand, the lactose K_{St} values can be approximately ranked according to solvent burning velocity.

It is likely that some of the other solvent physical properties shown in Table 4-4, and additional excipient considerations such as solubility, will be required to advance the phenomenological modeling of these data. For example, Flory–Huggins[95] theory could be helpful in examining the influence of solubility on enthalpy of mixing; lactose is slightly soluble in alcohol whereas MCC is not, meaning that prewetting of lactose with each of the three solvents resulted in more homogeneous mixtures than the prewetting of MCC. What seems clear at present is that the influence of each solvent is specific to the particular excipient and the method of admixture (prewetting or atmospheric). This is clearly demonstrated by Figures 4-34 and 4-35 which display overpressure data for the lactose/ethanol and MCC/methanol systems, respectively.

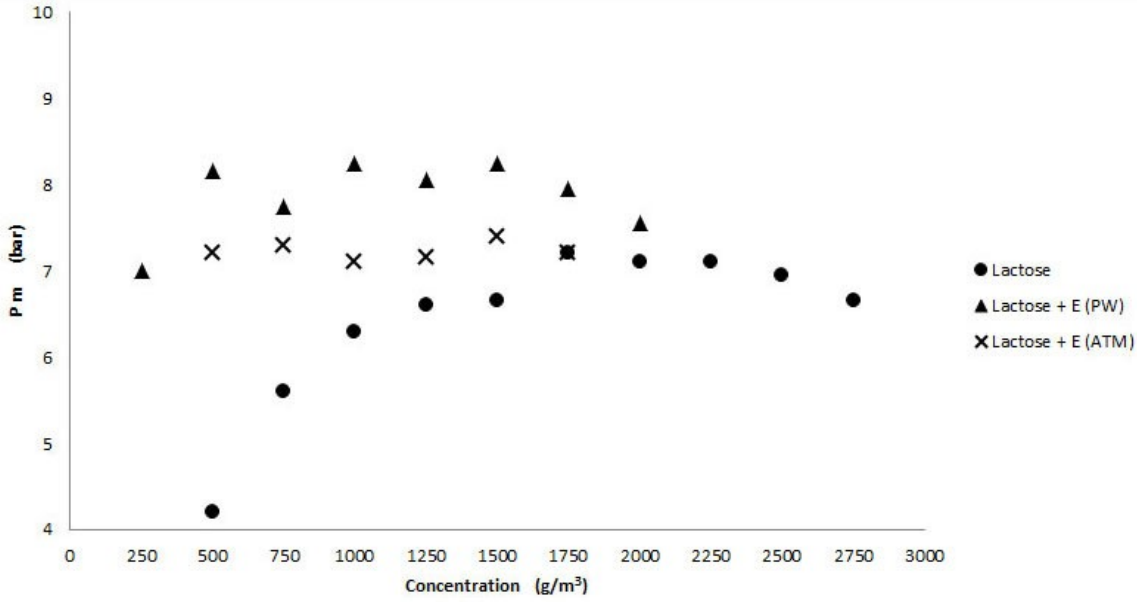

Figure 4-34 Influence of ethanol admixture on explosion overpressure of lactose.

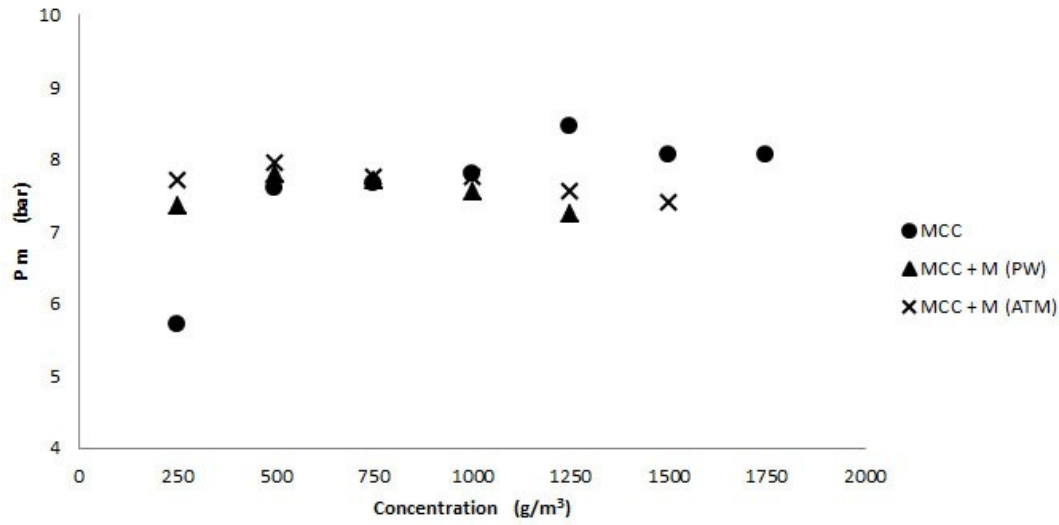

Figure 4-35 Influence of methanol admixture on explosion overpressure of MCC.

Similarly, Figures 4-36, 4-37, 4-38, 4-39 and 4-40 provide the rate of pressure rise data that further demonstrate the excipient- and admixture-specific nature of the influence of a given solvent. The systems shown are lactose and isopropanol; lactose and methanol; MCC and methanol; MCC and ethanol; and MCC and isopropanol, respectively.

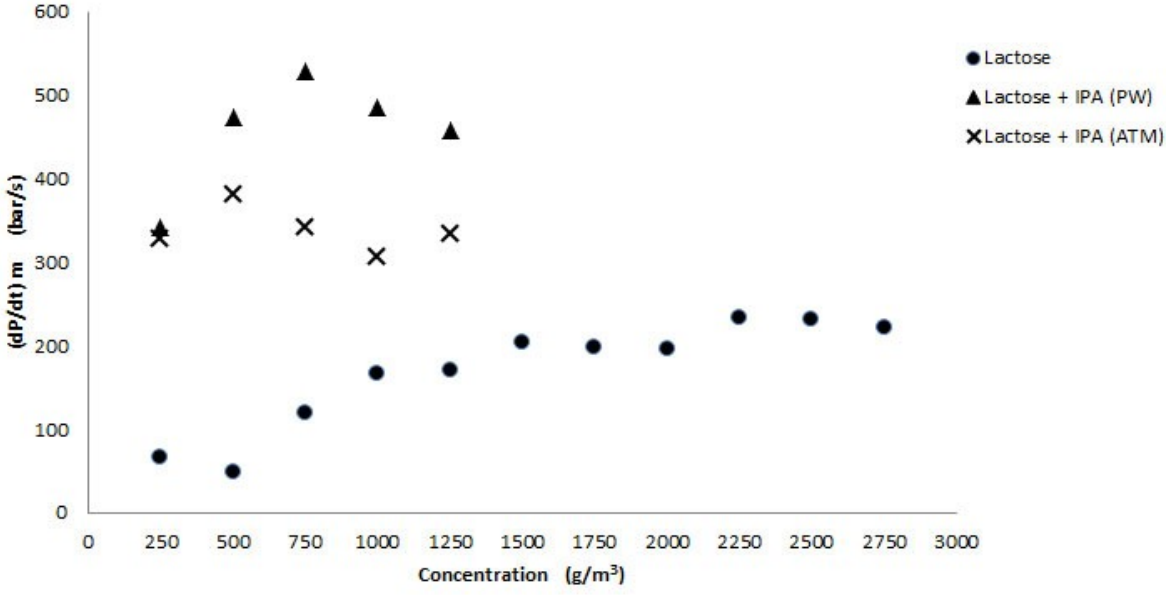

Figure 4-36 Influence of isopropanol admixture on rate of pressure rise of lactose.

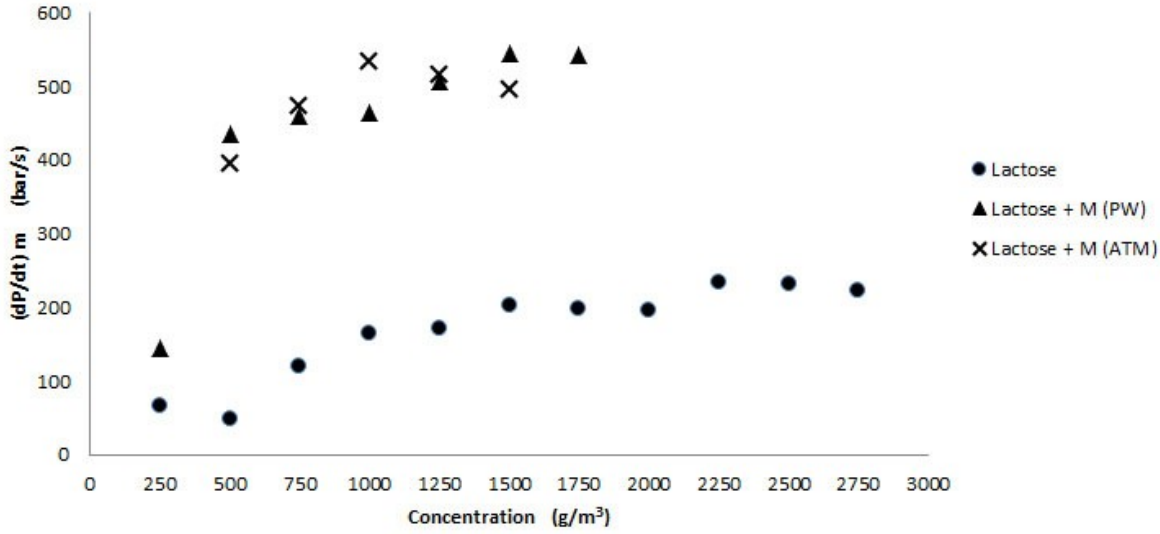

Figure 4-37 Influence of methanol admixture on rate of pressure rise of lactose.

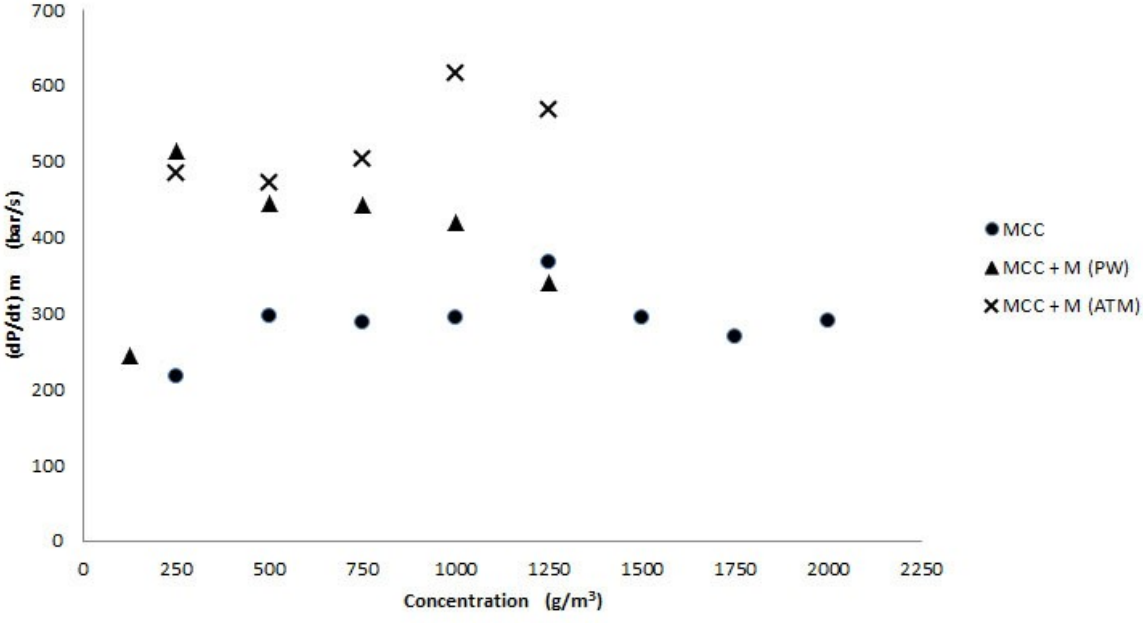

Figure 4-38 Influence of methanol admixture on rate of pressure rise of MCC.

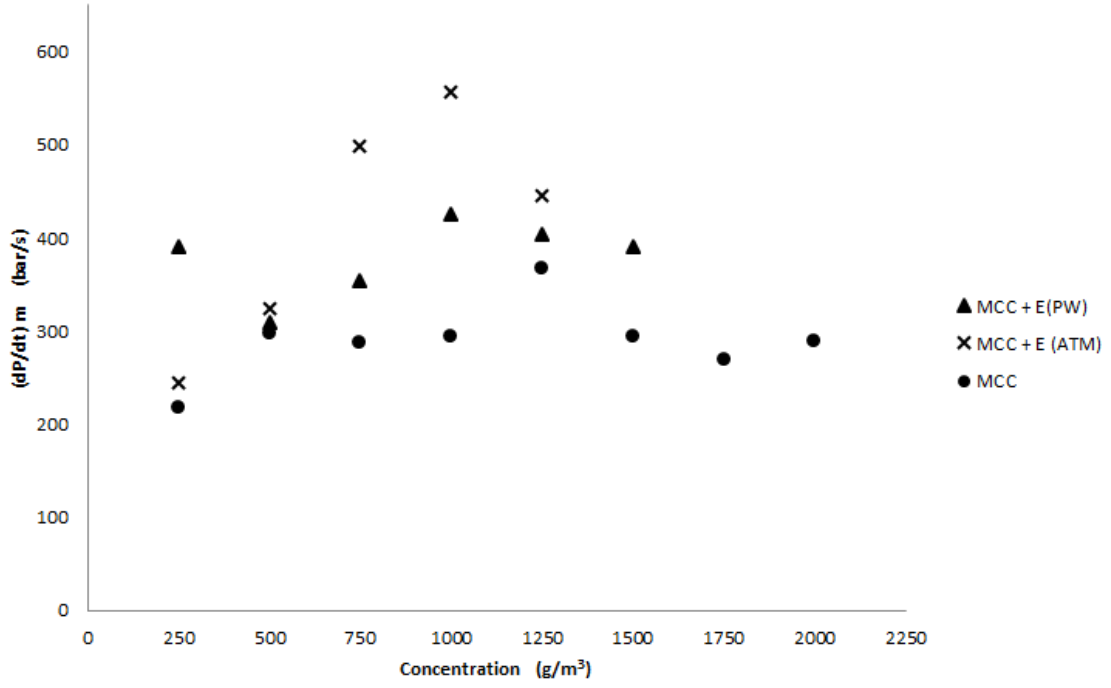

Figure 4-39 Influence of ethanol admixture on rate of pressure rise of MCC powder.

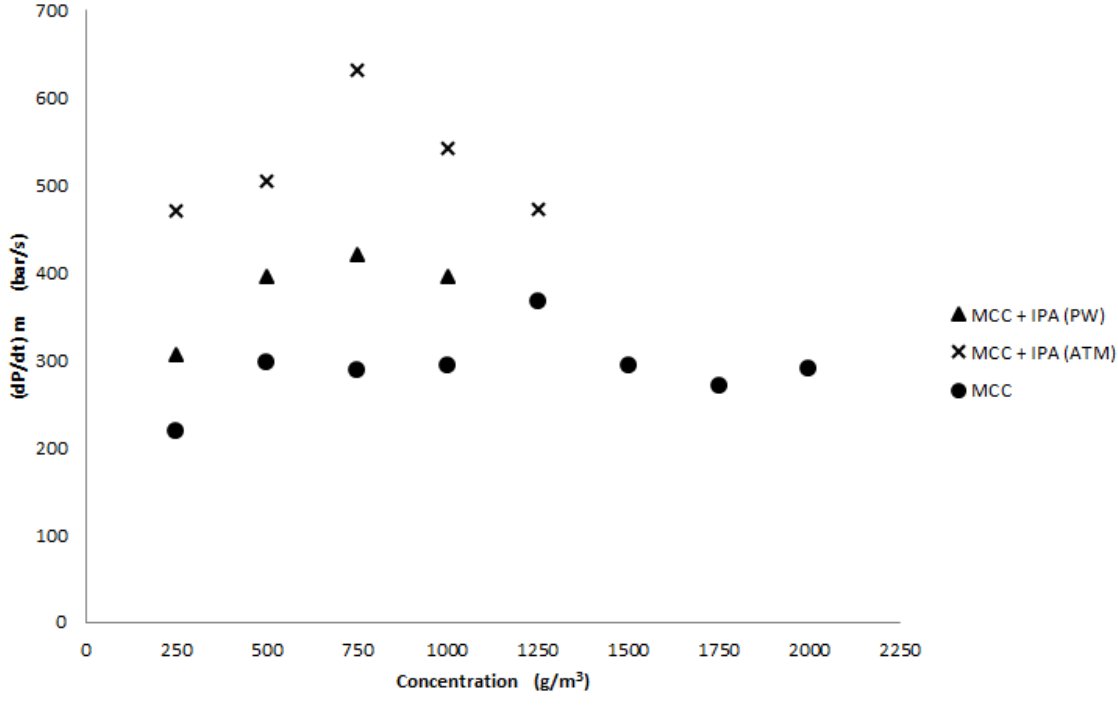

Figure 4-40 Influence of isopropanol admixture on rate of pressure rise of MCC powder.

4.2.3.2 Explosion likelihood

Tables 4-15 and 4-16 give the complete MEC, MIE and MIT data sets for all test conditions. The complete numerical data can be found in Appendix E. As with P_{max} and K_{St}, the influence of solvent admixture was generally an enhancement of these explosion likelihood (or ignition sensitivity) parameters – i.e., a reduction in MEC, MIE and MIT. Consistent with the pre-wetted lactose K_{St} values in Table 4.16, the pre-wetted lactose MIE values are all similar. The effect of inductance via the production of a protracted spark leading to lower MIEs is also seen in Tables 4-15 and 4-16.[94]

Table 4-15 MEC, MIE and MIT data for MCC.[94]

Material	**MEC [g/m³]**	**MIE [mJ] (Inductance)**	**MIE [mJ] (No Inductance)**	**MIT [°C]**
MCC	50	30–100[c] (74)[d]	300–1000 (540)	430
MCC + M (PW)	DL[a]	30–100 (55)	30–100 (67)	380
MCC + E (PW)	DL	10–30 (27)	300–1000 (380)	410
MCC + IPA (PW)	40	30–100 (42)	100–300 (180)	400
MCC + M (ATM)	< 10 (2.6 bar(g))[b]	ND[e]	ND	ND
MCC + E (ATM)	< 10 (1.5 bar(g))	ND	ND	ND
MCC + IPA (ATM)	< 10 (3.6 bar(g))	ND	ND	ND

[a]DL = Dispersion Limitation. The excipient dissolved in the admixed solvent to the extent that dust dispersion was not possible.

[b]Explosion overpressure at dust concentration of 10 g/m^3. The explosion criterion is an overpressure of 1 bar(g).

[c]Range of ignition energies from lower value at which no ignition occurred to higher value at which ignition did occur.

[d]E_s (statistic energy) determined by manufacturer (Kuhner)-supplied software.

[e]ND = Not Determined. The MIKE 3 apparatus used for MIE measurement and the BAM oven used for MIT measurement are not closed systems (unlike the Siwek 20-L chamber used for determination of MEC).

Table 4-16 MEC, MIE and MIT data for lactose (Same footnotes as Table 4-15).

Material	MEC [g/m³]	MIE [mJ] (Inductance)	MIE [mJ] (No Inductance)	MIT [°C]
Lactose	70	30–100 (55)	100–300 (250)	420
Lactose + M (PW)	DL	10–30 (17)	100–300 (140)	350
Lactose + E (PW)	DL	10–30 (19)	100–300 (200)	380
Lactose + IPA (PW)	DL	10–30 (14)	100–300 (170)	400
Lactose + M (ATM)	< 10 (4.3 bar(g))	ND	ND	ND
Lactose + E (ATM)	< 10 (2.6 bar(g))	ND	ND	ND
Lactose + IPA (ATM)	< 10 (3.4 bar(g))	ND	ND	ND

Chapter 5 Explosion Risk Management

In the current study, the generalized framework described in Figure 2-5 (Chapter 2) has been adapted for managing risk associated with nontraditional categories of particulate fuel/air systems. Use of the QRMF for the three nontraditional fuel/air systems has been followed, with each system being considered from the key perspectives of hazard characterization, risk (consequence and likelihood) assessment, and risk control (along with other aspects of the quantitative risk management sequence) as discussed below.

5.1 Hazard Characterization

Hazard characterization has been undertaken as a first step to identify and evaluate the nature, magnitude and probability of risks associated with the nontraditional dusts. Various explosibility parameters, including maximum explosion pressure (P_{max}), size-normalized maximum rate of pressure rise (K_{St}), minimum explosible concentration (MEC), minimum ignition energy (MIE), and minimum ignition temperature (MIT), have been determined using standardized equipment and standardized test methods. The first two of these parameters (P_{max} and K_{St}) are related to explosion severity while the latter three (MEC, MIE and MIT) provide information on explosion likelihood. Some features related to hazard characterization of the aforementioned three nontraditional fuel/air systems are discussed below.

5.1.1 Nanomaterials

A large specific surface area, the possibility of particle agglomeration, and enhanced surface reactivity are some distinct properties of nanomaterials that need to be considered in hazard characterization. It is well- known for micron-size dusts that as particle size decreases, both explosion severity and explosion likelihood increase; the situation is

not as straightforward for nanomaterials. Findings from the analysis of the experimental results revealed that micron-size explosion severity results could not be directly compared with those for nano-titanium due to pre-ignition of the nano-dust in the explosion chamber.[7,24] The likelihood of explosion occurrence was observed to increase significantly with a particle size decrease from the micron- to the nano-range as evidenced during MIE and MIT testing by Boilard et al.[7,24]. Potential exposure of workers and the environment, and potential release during production, handling and processing of nanomaterials, must therefore be emphasized in conducting risk studies. Pre- or self-ignition and lack of explosion inerting are experimental findings that must be accounted for in hazard/risk characterization of titanium nano-dust explosions.

5.1.2 Flocculent Materials

Flocculent materials are non-spherical and cannot be easily characterized by a single measure such as particle diameter; these materials are better described in terms of their length-to-diameter ratio.[1] Explosibility results described in Chapter 4 revealed that fine flock (smaller dtex and shorter length) generally yields higher explosion pressures and rates of pressure rise, and are more easily ignitable by the electric spark, than larger flock sizes. The relevance here is that industrial flocking processes often involve size reduction and further manipulation as well as the presence of energetic ignition sources.

5.1.3 Hybrid Mixtures

The effects of flammable solvent admixture to a combustible dust (thus forming a hybrid mixture) depend on several factors, including the burning velocity of the solvent and the proximity of the solvent concentration to its lower flammability limit. Pre-wetting of microcrystalline cellulose (MCC) and lactose with solvent (methanol, ethanol and isopropanol) had a measurable effect on each explosibility parameter (P_{max}, K_{St}, MEC, MIE

and MIT). The influence was generally an enhancement of the particular parameter (e.g., increase in K_{St}, decrease in MIE, etc.) as anticipated. Additionally, while the effect of solvent admixture to MCC was generally distinguishable for the different solvents, that was not the case for lactose. Pre-wetting of lactose with each of the three solvents resulted in similar values of P_{max}, K_{St} and MIE. In the case of hybrid mixtures, explosion prevention and mitigation measures based on the dust component alone are inadequate.

5.2 Risk Assessment

Risk has two components: likelihood of occurrence and severity of consequences. For assessing risks of explosions associated with nontraditional dusts, these two components are described in this section.

5.2.1 Severity of Consequences

One of the available methodologies to evaluate the severity of different dust explosion scenarios is computational fluid dynamics (CFD). A CFD tool named FLACS-DustEx (FLame ACceleration Simulator—Dust Explosions) has been used in assessing the severity of consequences of explosions associated with aforementioned three categories of nontraditional dusts. Dust explosion simulation can be effective to estimate explosibility parameters and predict possible explosion scenarios in industrial facilities. The functionality of dust explosion simulations can be realized through the steps outlined in Figure 5-1, which have been applied in the current research for explosions associated with the nontraditional dusts (except the nano-sized titanium powder). As FLACS-DustEx is not capable of simulating metal dust due to some uncertainties with respect to thermodynamics and the effect of radiation on flame propagation, no simulation work has been attempted for explosions associated with titanium powder.

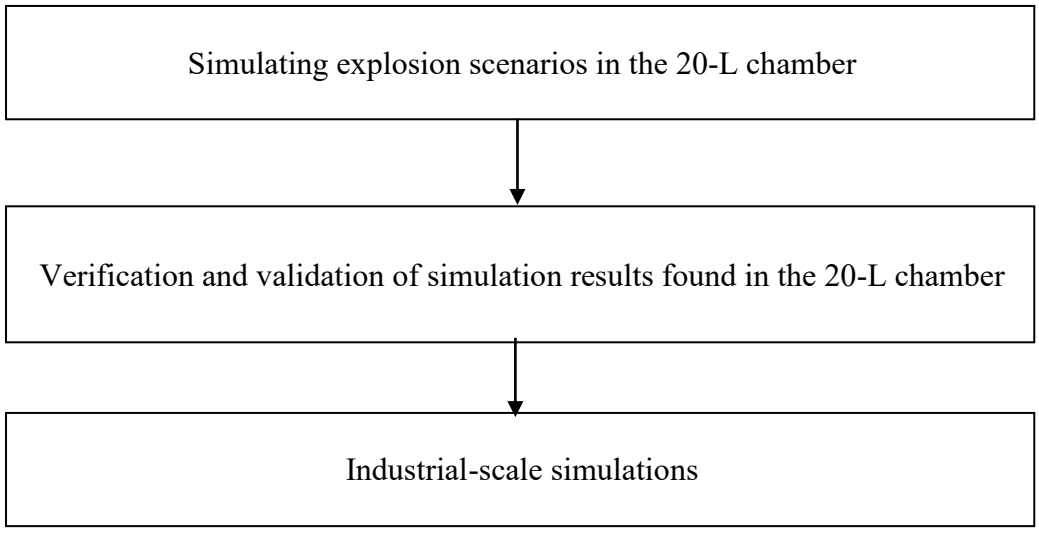

Figure 5-1 Steps used in simulating explosion scenarios.

5.2.1.1 Dust explosion simulation code

Both laboratory- and industrial-scale simulations were performed using the commercial CFD tool known as FLACS-DustEx (FLame ACceleration Simulator—Dust Explosions), provided by GexCon which was previously marketed as DESC (Dust Explosion Simulation Code). In the present study, version 10.3 was run under the Windows 7 operating system. FLACS-DustEx is based on FLACS (a CFD program for gas explosions). As FLACS-DustEx was used to estimate the consequences of the dust explosions in the given scenarios, the primary step for the FLACS-DustEx simulation was to prepare the fuel files. FLACS-DustEx requires physical and thermodynamic properties along with standardized (20-L) explosion test results presented in this thesis as input data to the combustion model. The fuel files were produced by Excel (Microsoft) spreadsheets using explosibility data as presented in this thesis, along with other properties (e.g., particle density, moisture content, particle size, enthalpy of formation and heat capacity). The fuel file was added to a predefined working directory to be read by the FLACS-DustEx simulator (FLACS Run Manager). Then,

the explosion geometry was built for each case study followed by setting of the scenarios. The simulations were run using the Run Manager program of the FLACS-DustEx simulator. Finally, results from the simulations were observed by using the post-processor Flowvis program. Skjold et al.[68,69] describe how FLACS-DustEx uses CFD code for the transport equations of mass, momentum, enthalpy, fuel mixture fraction, turbulent kinetic energy, and the rate of dissipation of turbulent kinetic energy on a three-dimensional Cartesian grid. The progress of the simulation work was monitored while the programs were running.

5.2.1.2 Laboratory-scale simulation

This section describes simulation results of dust explosions in the 20-L chamber. In simulations, the 'dust cloud' is assumed as a homogeneous mixture of solid dust particles and air. The ignition point was located at the central position of the chamber similar to that used in experimental tests. A 10-kJ Ignition energy was considered in simulations, as this is the energy used in the 20-L tests. Laboratory-scale simulation results of explosions associated with hybrid mixtures and flocculent materials are described below.

Hybrid Mixtures

CFD simulations of dust explosions at laboratory-scale were carried out for both MCC, and a hybrid mixture of MCC and methanol (MCC admixed with methanol in atmospheric condition was considered as an example of hybrid mixture in pharmaceutical applications). As verification and validation of simulation results, the maximum explosion pressure and the maximum rate of pressure rise produced through simulations were compared with the relevant experimental results. A dust concentration of 1250 g/m^3 was used (in the experimental results, both the maximum explosion pressure and maximum rate of pressure rise for MCC were observed at this concentration as shown in Figures 4-29 and 4-30) for simulations corresponding to MCC powder and the hybrid mixture. The error percentages between experimental and predicted data were found to be less than 4%, as

shown in Table 5-1. Simulation results displayed a good agreement with experimental results as predicted. Such agreement was expected because of using the 20-L data as input for simulations.

Table 5-1 Experimental and simulation results of MCC dust (baseline excipient and hybrid mixture) explosions in the 20-L chamber.

Dust	Explosibility Parameter	Experimental Results	Simulation Results	Error Percentage
MCC	P_{max} (bar(g))	8.5	8.5	0
	$(dP/dt)_{max}$ (bar/s)	379	386	1.8
MCC + methanol (ATM)	P_{max} (bar(g))	7.9	8.2	3.8
	$(dP/dt)_{max}$ (bar/s)	619	604	2.4

In addition to the 20-L chamber, FLACS-DustEx simulations were run for a large-scale geometry of 1-m^3 spherical vessel. The maximum explosion pressures for the simulations in the 1-m^3 spherical vessel were observed to be the same as the results found in the 20-L chamber for both MCC and MCC admixed with methanol, but they were reached at different times (see values of total explosion time (t_{exp}) in Table 5-2). These simulation results help to validate the CFD approach and support its application to industrial-scale geometries.

Table 5-2 Simulation results of MCC (baseline excipient and hybrid mixture) explosions in the 20-L chamber and 1-m³ vessel.

20-L Chamber			1-m³ Vessel	
Material	P_{max} (bar(g))	t_{exp} (s)	P_{max} (bar(g))	t_{exp} (s)
MCC	8.5	0.26	8.5	0.81
MCC + M (ATM)	8.2	0.14	8.2	0.54

Fibrous Polyamide 6.6 and Polyester

CFD simulations of dust explosions at laboratory-scale were carried out for both polyamide 6.6 and polyester fibres (0.5-mm long fiber of dtex 1.7 was considered as an example of one of the commonly used sizes). Simulations of fibrous materials were performed considering an equivalent characteristic size of the flock, D_{eq} as detemined by Equation (5).[96]

$$D_{eq} = 2\sqrt{\frac{d_f L}{\pi}} \qquad (5)$$

where

d_f and L are the diameter and length of a flock, respectively

The equivalent diameter, D_{eq} is the diameter of a sphere having the cross-sectional area equal to that of the fiber (cylinder).

The error percentages between experimental and predicted data (simulation results) in the 20-L chamber were found to be less than 2%, as shown in Table 5-3. In addition to the 20-L chamber, FLACS-DustEx simulations were run in a large-scale geometry of 1-m³ spherical vessel. The results showed the same maximum explosion pressure (P_{max})

for both polyamide 6.6 and polyester, but they were reached at different times, as can be seen in Table 5-4.

Table 5-3 Experimental and simulation results of polyamide 6.6 and polyester explosions in the 20-L chamber. (A concentration of 500 g/m^3 was used for both polyamide 6.6 and polyester.)

Dust	Explosibility Parameter	Experimental Results	Simulation Results	Error Percentage
Polyamide 6.6	P_{max} (bar(g))	6.6	6.6	0
Polyester	P_{max} (bar(g))	6.9	6.8	1.5

Table 5-4 Simulation results of polyamide 6.6 and polyester explosions in the 20-L chamber and 1-m^3 vessel. (A concentration of 500 g/m^3 was used for both polyamide 6.6 and polyester.)

20-L Chamber				1-m^3 Vessel	
Material	P_{max} (bar(g))	t_{exp} (s)		P_{max} (bar(g))	t_{exp} (s)
Polyamide 6.6	6.6	0.88		6.6	2.65
Polyester	6.8	0.68		6.8	2.03

5.2.1.3 Industrial-scale simulation

A dryer and a flock storage tank were considered in industrial-scale simulations for explosions associated with hybrid mixtures and fibrous materials, respectively. In FLACS-DustEx, it is not possible to simulate the filling of materials into a vessel and the consequent

dust cloud; therefore, the method adopted was to consider a homogenous dust cloud which completely filled the dryer and the flock storage tank prior to the ignition occurring.

Explosions Associated with Hybrid Mixtures:

In industrial facilities, drying operations for many combustible materials produce explosion risks. An explosion that could occur during drying operation in equipment, such as a dryer, can lead to a catastrophic failure of the complete industrial facility.

A spray dryer was considered for simulating explosions associated with hybrid mixtures according to the physical dimensions given by Wawrzyniak et al.[97], as a representative of widely used industrial-scale pharmaceutical dryers. The dryer of height 25 m was fixed with a diameter of 5.3 m throughout the tower. The bottom part of the tower was considered as cone-shaped with the diameter increasing from 0.5 to 5.3 m in the upper part as shown qualitatively in Figure 5-2. A 10-kJ ignition energy was used on the central axis of the dryer at a height of 5.1 m from the dryer's bottom due to the strong possibility of explosive atmospheres in that region.[97]

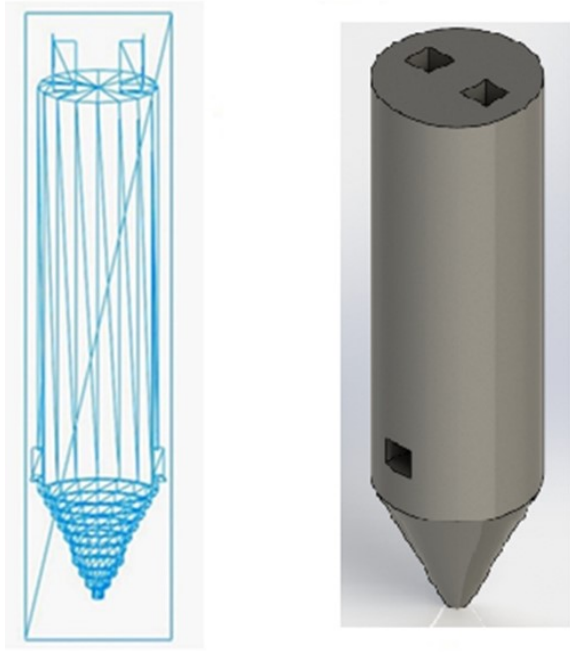

Figure 5-2 FLACS-DustEx geometry of an industrial spray dryer: (a) 2D view and (b) 3D view.

The results of the simulations of the dryer for MCC and MCC admixed with methanol (atmospheric condition) are given in Figures 5-3 and 5-4. The maximum explosion pressure in the dryer was similar for MCC and MCC admixed with methanol. However, the total explosion time (t_{exp}) was found to be almost 1 second shorter in the case of hybrid mixture (Figure 5-4) as compared to the excipient alone (Figure 5-3). The reason for such a difference is the occurrence of more rapid combustion of the hybrid mixture.

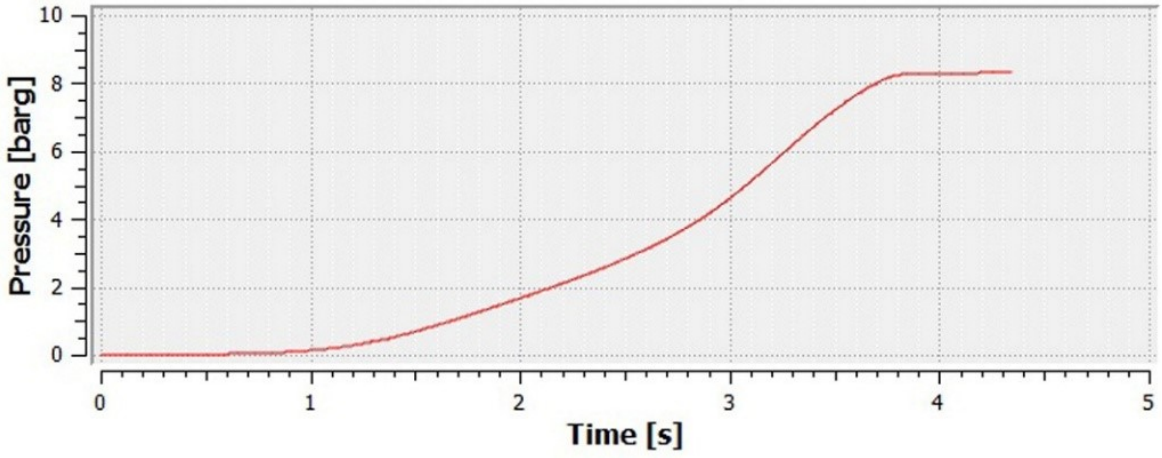

Figure 5-3 FLACS-DustEx pressure-time traces of an explosion associated with a dust cloud of MCC of concentration 1250 g/m^3 in the spray dryer.

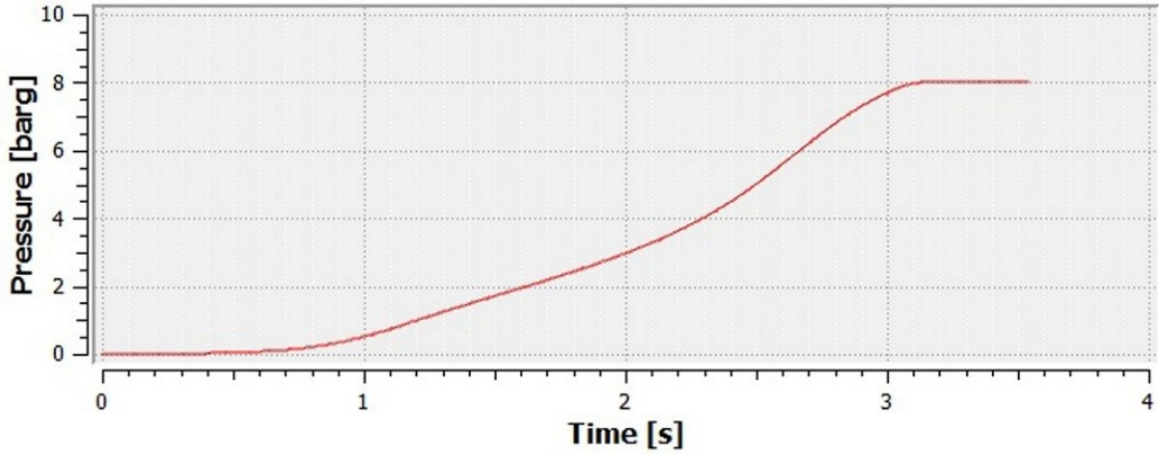

Figure 5-4 FLACS-DustEx pressure-time traces of an explosion associated with a dust cloud (concentration 1250 g/m^3) of MCC admixed with methanol (concentration of 80% of its LFL) in the spray dryer.

Explosions Associated with Fibrous Polyamide 6.6 and Polyester

A flock storage tank manufactured by Poly Processing Company[98] was considered for simulating explosions associated with fibrous materials on an industrial-scale. The height of the flock storage tank was 6 m with a diameter of 3 m throughout the tank as shown

qualitatively in Figure 5-5. A 10-kJ ignition energy was used on the central axis of the tank at a height of 3 m from the tank bottom.

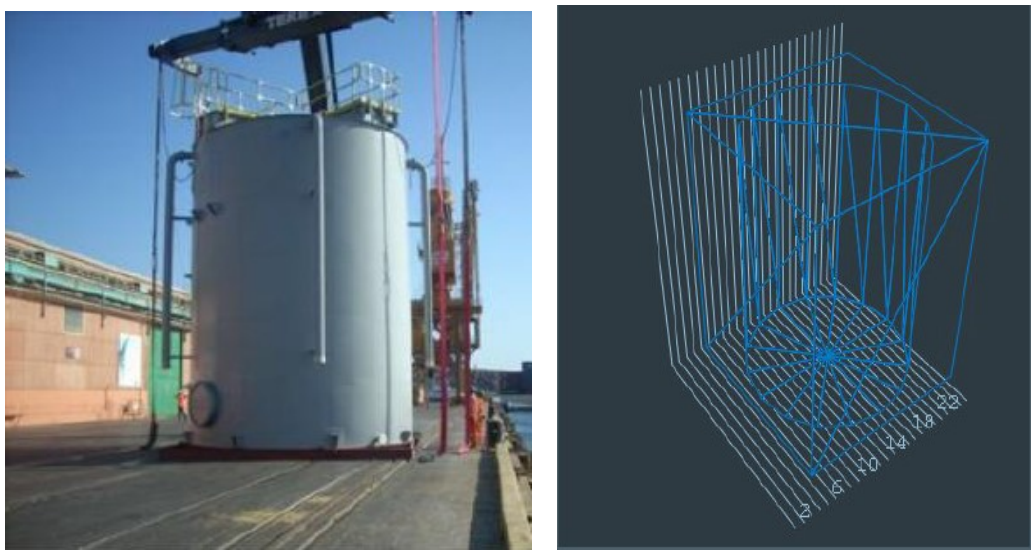

(a) (b)

Figure 5-5 A flock storage tank: (a) image taken from manufacturer's website[98], and (b) geometry drawn by FLACS-DustEx.

The simulation results for polyamide 6.6 and polyester fibers (0.5-mm long fiber of dtex 1.7) are given in Figures 5-6 and 5-7. The trends of the pressure-time traces for both polyamide 6.6 and polyester (maximum explosion pressures of 6.7 and 6.9 bar (g) for polyamide 6.6 and polyester, respectively) were found to be similar to the experimental results described in Table 4-12 (as illustrated in the previous chapter). Different chemical structures of polyamide 6.6 and polyester are one of the key factors for the difference in their explosibility results.

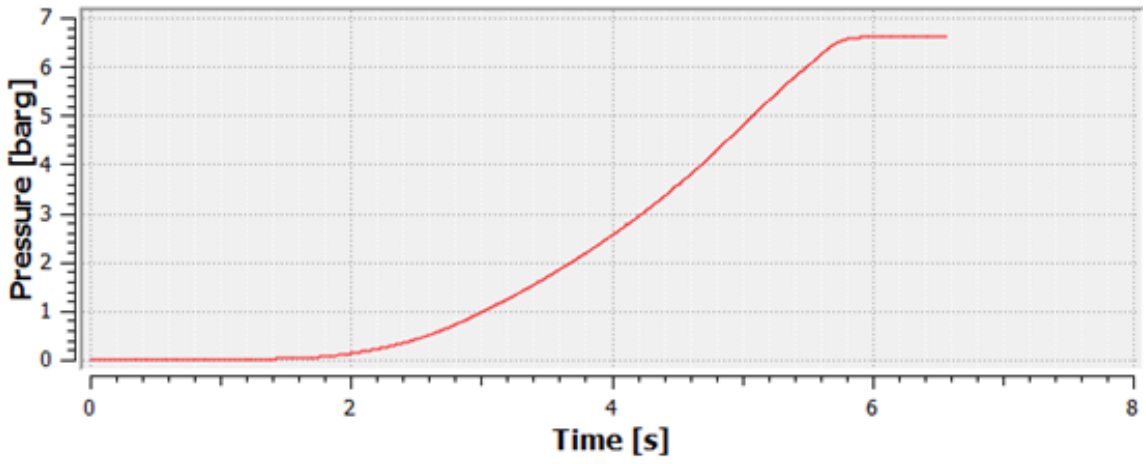

Figure 5-6 **FLACS-DustEx pressure-time traces of an explosion associated with a dust cloud of polyamide 6.6 (0.5-mm long fiber of dtex 1.7 and a concentration of 500 g/m³) in the flock storage tank.**

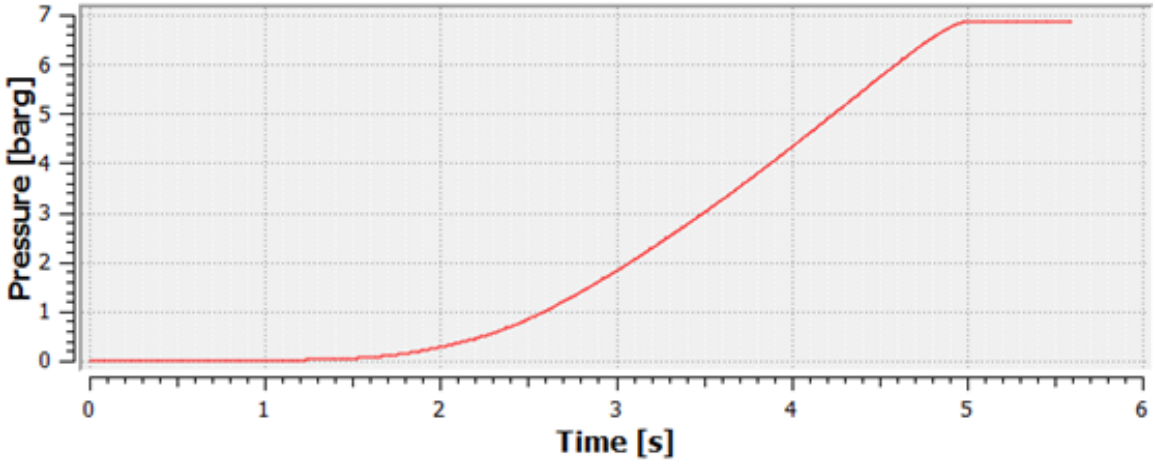

Figure 5-7 **FLACS-DustEx pressure-time traces of an explosion associated with a dust cloud of polyester (0.5-mm long fiber of dtex 1.7 and a concentration of 500 g/m³) in the flock storage tank.**

5.2.2 Likelihood of Occurrence

Relex (Reliability Excellence) software was used as the Fault Tree Analysis (FTA) tool to determine the occurrence of probable events by means of a series of logic gates. An example of a qualitative fault-tree diagram for an explosion associated with a nano-dust (e.g., nano-sized titanium powder) is given In Figure 5-8. This FTA diagram was established by modifying the generalized dust explosion fault tree developed by Abuswer[74]. Key features of Figure 5-8 include the possibilities of self-ignition, particle agglomeration and inerting inadequacies.

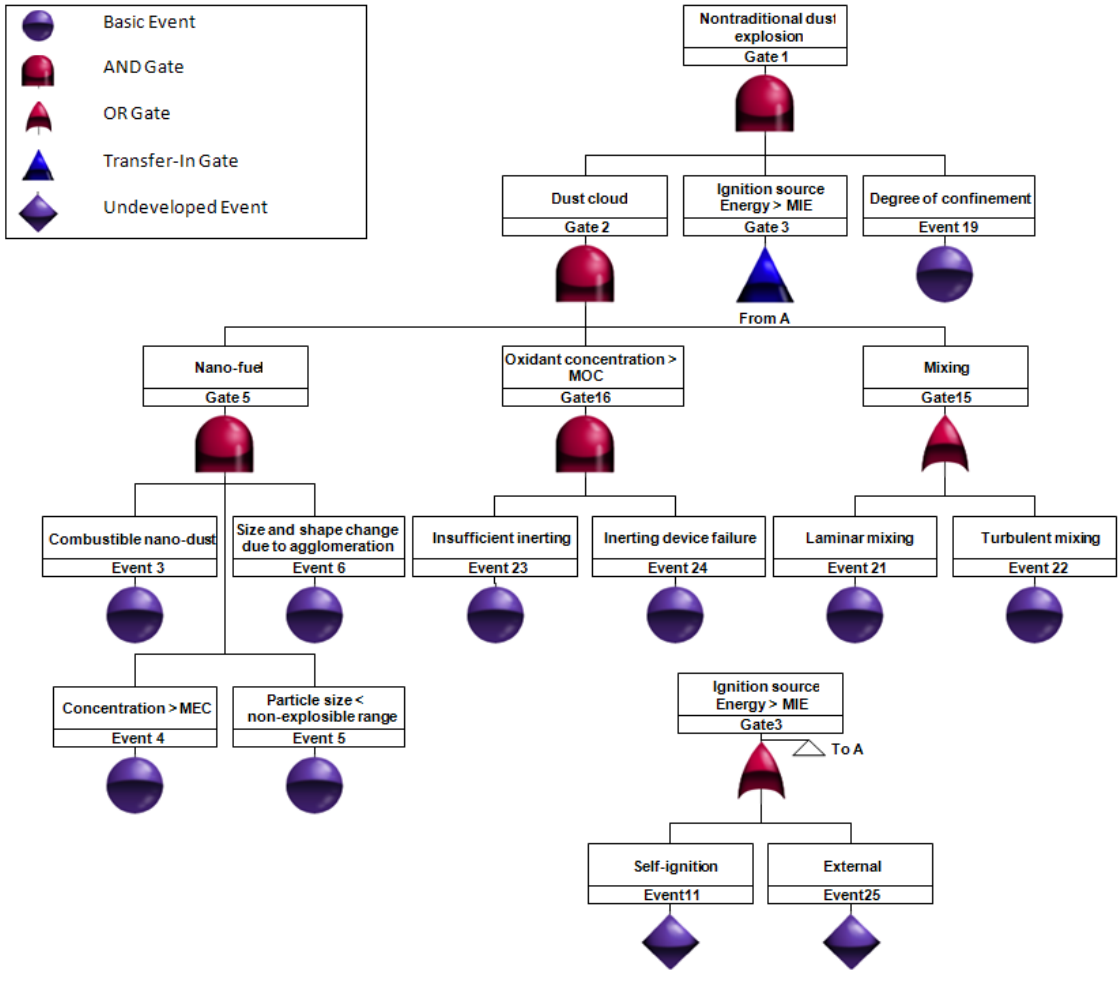

Figure 5-8 FTA diagram for nano-dust explosions

5.3 Risk Control

Risk reduction strategies for nontraditional dusts have been structured according to three categories of control measures (inherent, engineered and procedural safety) as described in section 2.5.3 of Chapter 2.

5.3.1 Safety Measures in Simulated Explosion Scenarios

The use of inherent safety and passive engineered safety measures to prevent and mitigate nontraditional dust explosions is explained in this section as examples. The following discussion is based on the results of simulations that were conducted for flocculent and hybrid mixtures.

Inherently Safer Design (ISD)

As mentioned earlier, four basic principles are required to construct an inherently safer design: minimization, substitution, moderation, and simplification. The provision of considering ISD principles to prevent or mitigate nontraditional dust explosions is explained below by simulating some hypothetical explosion scenarios.

Minimization principle of ISD

An example of an incident during drying operation in a facility is considered here as a hypothetical scenario. The operation is taking place in a facility designed for pharmaceutical applications; the dryer (shown in Figure 5-2) contains MCC powder. As the work progresses, the MCC dust cloud is ignited by an unknown ignition source (e.g., electrical discharge or spark).

Maximum explosion pressures that could be produced in real cases were simulated for high, medium and low loadings of MCC powder as demonstrated in Table 5-5. In each case, a 10-kJ ignition energy was used in the central axis of the dryer at a height of 12.5 m. For a high loading in the dryer (e.g., a loading of MCC powder that can produce a

MCC dust cloud with a concentration of 1250 g/m^3), the maximum explosion pressure could reach up to 8.4 bar (g) as observed in simulation results. If the size of the loading can be minimized so that the dust cloud concentration drops to a lower value, for example 80% lower than the concentration of high loading scenario, the maximum explosion pressure will be decreased by 30% as found in simulation results.

Table 5-5 Maximum explosion overpressures at different MCC dust loadings.

MCC dust loadings in drying operation	MCC dust cloud concentration (g/m^3)	P_{max} (bar(g))
High	1250	8.4
Medium	500	7.9
Low	250	6.0

From the aforementioned results, it is clear that minimizing dust loading into the dryer will produce a lower concentration of dust cloud; therefore, this will reduce the explosion overpressure.

Substitution principle of ISD

The substitution principle of ISD can be applied in pharmaceutical applications which deal with solvents and MCC powder in various processes. For example, in case of pre-wetting MCC with solvents, methanol can be substituted with ethanol and isopropanol. This is a safer selection as favorable experimental data were observed for such substitutions. A significant reduction (about 20%) in K_{St} values has been achieved when methanol were substituted by isopropanol (Table 5-6).

Table 5-6 P_{max} and K_{St} data for explosions associated with MCC pre-wetted with solvents in the 20-L chamber

Material	P_{max} [bar(g)]	K_{St} [bar·m/s]
MCC + methanol (PW)	*7.9*	144
MCC + ethanol (PW)	*7.8*	117
MCC + isopropanol (PW)	*7.7*	116

CFD simulations by using FLACS-DustEx can predict the explosion scenarios associated with the aforementioned substitution in the industrial-scale applications. For example, suppose a drying operation is taking place in a facility designed for pharmaceutical applications. The dryer (as mentioned in the previous scenario) contains a hybrid mixture (MCC admixed with solvent as pre-wetted). As the work progresses, the hybrid mixture is ignited from an unknown ignition source (e.g., electrical discharge or spark).

The scenario mentioned in the previous paragraph was simulated for two solvents: (a) MCC admixed with methanol, and (b) MCC admixed with ethanol, both in pre-wetted condition. The concentrations of solvents were 80% of their respective lower flammability limit. In both cases, a 10-kJ ignition energy was used in the central axis of the dryer at a height of 12.5 m and the concentration of the dust cloud was 1250 g/m^3. A similar maximum explosion pressure and total explosion time (t_{exp}). However, at a point after 3 second, MCC admixed with methanol displayed almost 1 bar (g) higher explosion pressure than ethanol. This indicates a higher rate of pressure rise for methanol as compared to ethanol. Similar results were also observed in the 20-L experimental tests.

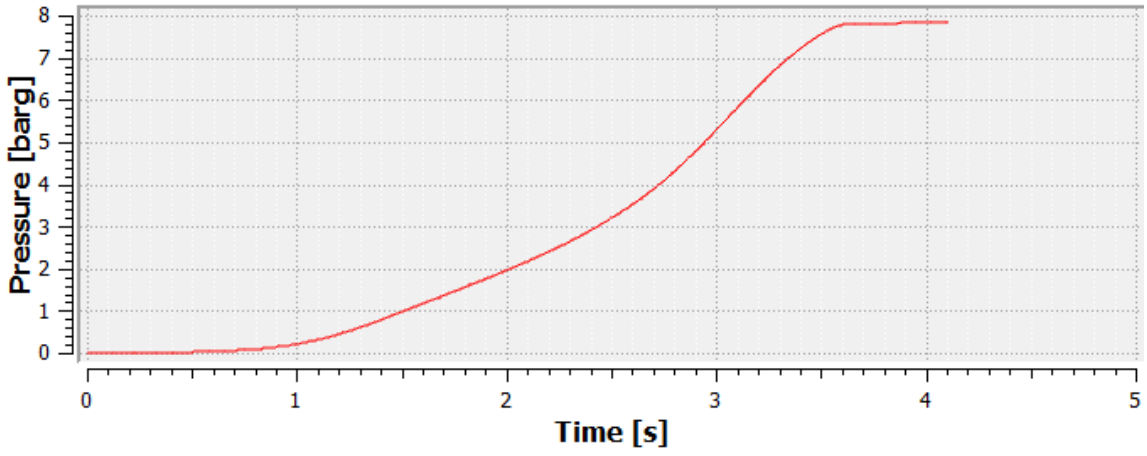

(a)

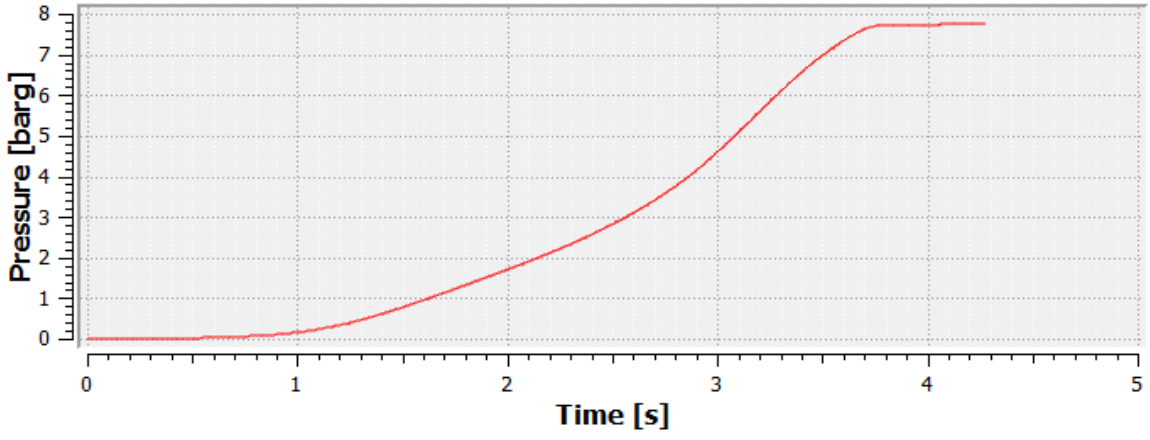

(b)

Figure 5-9 FLACS-DustEx pressure-time traces of explosions associated with dust clouds of (a) MCC + methanol (PW), and (b) MCC + ethanol (PW) in the spray dryer.

Moderation principle of ISD

If the length of the fiber of flocculent materials has been increased, dust explosion risk reduction can be achieved. This has been demonstrated through CFD simulations as seen in Figure 5-10. The maximum explosion pressure in simulation results was observed to decrease in the case of moderated fiber (e.g., by increasing the length of the polyamide

6.6 fiber from 0.3 to 1.0 mm) in the storage tank (the same tank as described in Figure 5-5). Similar results were observed in the 20-L tests conducted by Iarossi et al.[76]. For example, at $t = 4$ *s*, as seen in Figure 5-10, a higher explosion pressure (3.2 bar (g)) was observed for 1.0-mm long fiber than 0.3-mm long fiber (2.5 bar (g)).

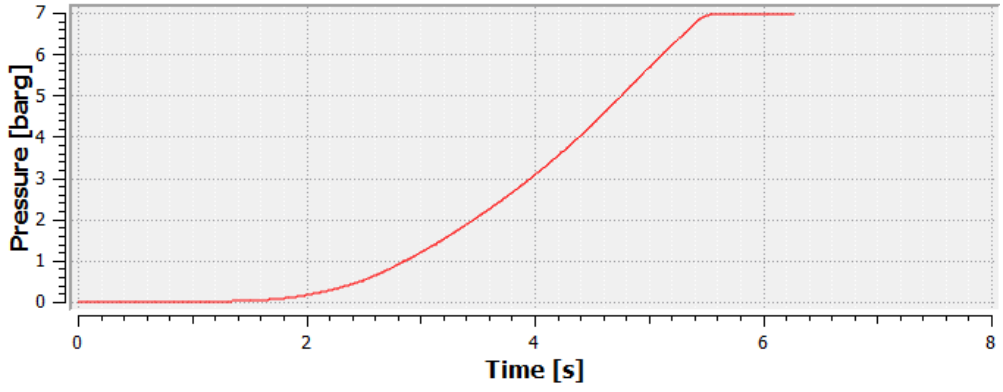

(a)

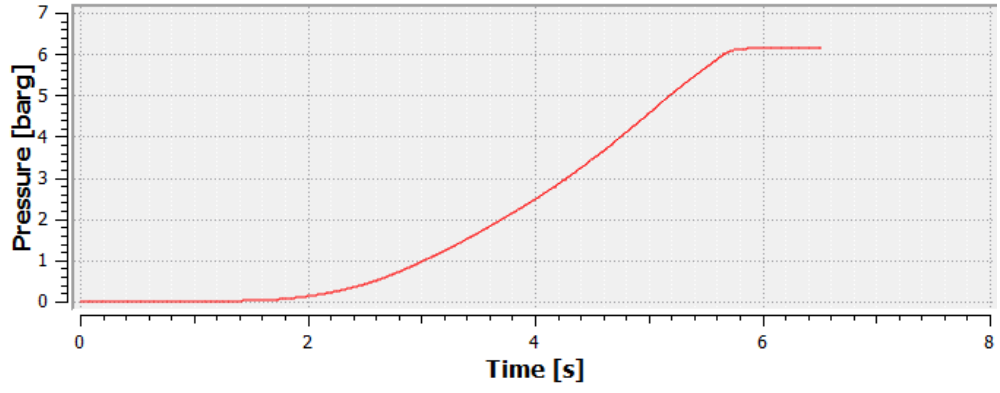

(b)

Figure 5-10 FLACS-DustEx pressure-time traces of explosions associated with polyamide 6.6 of dtex 3.3 for (a) 0.3-mm long, and (b) 1.0-mm long, fibre [explosions occurred on the central axis of the storage tank at a height of 3 m from the tank bottom; and concentration of dust cloud was 500 g/m^3].

Simplification principle of ISD

If adding solvents into the dust through an integrated mixing system attached internally within the equipment (e.g., a spray dryer) served satisfactory results, then pre-mixing of solvent in an additional mixing room can be eliminated. This will minimize the cost as well as make the process simpler. Such simplification was tested through CFD simulations. In simulation results for lactose admixed with ethanol, higher P_{max} value was observed in the pre-wetting mode than atmospheric as shown in Figure 5-11.

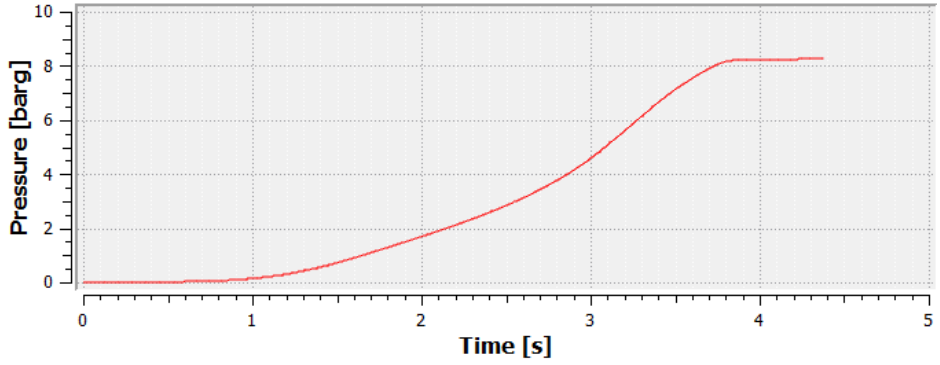

(a)

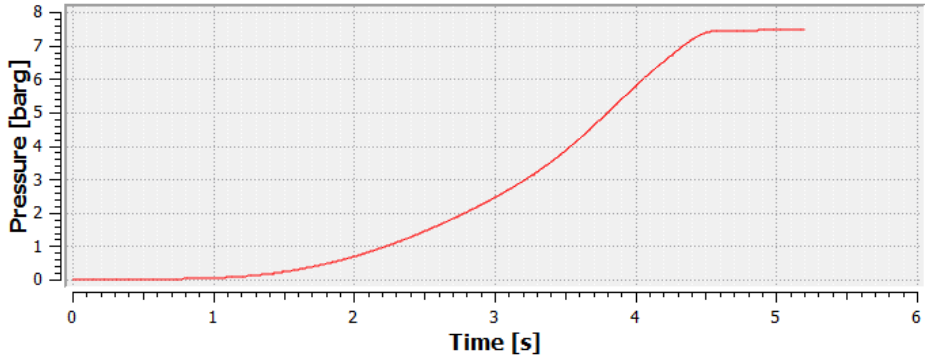

(b)

Figure 5-11 FLACS-DustEx pressure-time traces of explosions occurred on the central axis of the dryer at a height of 12.5 m from the dryer bottom during drying operation of lactose powder admixed with ethanol: (a) pre-wetted and (b) atmospheric, mode.

In both modes the concentrations of solvents were 80% of their respective lower flammability limit. A similar trend was observed in explosibility data found in 20-L tests as shown in Table 5-7. For example, at $t = 3$ *s,* as seen in Figure 5-11, a higher explosion pressure (4.4 bar (g)) was observed for pre-wetted condition than atmospheric one (2.6 bar (g)).

There are similarities between the simplification principle of ISD as observed in the aforementioned scenario and the explosion that occurred in East Rutherford, New Jersey at the US Ink/Sun Chemical Corporation on October 9, 2012 as found in a completed investigation report by the US Chemical Safety and Hazard Investigation Board (CSB).[35] The explosion and flash fires occurred in the ink mixing room after a loud 'thump' was heard from the newly installed dust collection system.[35] The explosion could possibly have been prevented if an alternative mixing system (similar to the mixing system integrated internally as described in the aforementioned scenario) had been used.

Table 5-7 P_{max} and K_{St} data for explosions associated with MCC admixed with ethanol in the 20-L chamber and spray dryer.

Material	**P_{max} [bar(g)] (20 L chamber)**	**P_{max} [bar(g)] (Industrial-scale simulation in a spray dryer)**
Lactose + ethanol (PW)	8.4	8.3
Lactose + ethanol (ATM)	7.4	7.5

Passive Engineering Safety Measure

Explosion venting is the most widely used dust explosion protection measure. CFD simulations were carried out to demonstrate that safety measures designed for dust explosions alone do not afford adequate protection in the case of hybrid mixture explosions.

To calculate the area of pressure panels, Equation (6) was used according to NFPA 68[83]:

$$A_{V0} = 1.10^{-4} \cdot \left(1 + 1.54 \cdot {P_{stat}}^{4/3}\right) \cdot K_{St} \cdot V^{3/4} \cdot \sqrt{\frac{P_{max}}{P_{red}} - 1} \qquad (6)$$

Where

A_{V0} = total calculated area of pressure panels (m^2)

P_{stat} = nominal static burst pressure of pressure panels (bar(g))

K_{St} = size-normalized maximum rate of pressure rise ($bar \cdot m/s$)

V = enclosure volume (m^3)

P_{max} = maximum explosion pressure (bar(g))

P_{red} = reduced pressure after explosion venting (bar(g))

Using Equation (6), the total calculated area of the pressure panels was determined as 4.6 m^2 for MCC and 7.2 m^2 for MCC admixed with methanol. The pressure panels were distributed among two side walls and the top wall of the spray dryer as described in Table 5-8.

Table 5-8 Size and orientation of pressure panels in the spray dryer.

Dust	Top Wall			Side Walls			Total area of pressure panels (m^2)
	Number	Area of pressure panel (m^2)	Total area of pressure panels (m^2)	Number	Area of pressure panel (m^2)	Total area of pressure panels (m^2)	
Dryer filled with MCC	2	1.0	2.0	2	1.3	2.6	4.6
Dryer filled with MCC and methanol (ATM)	2	1.5	3.0	2	2.1	4.2	7.2

Simulations in the spray dryer for MCC powder and MCC admixed with methanol in atmospheric condition were performed: (a) without using pressure panels (as a closed chamber), and (b) with pressure panels located at the top and side walls (as previously mentioned). For all pressure panels, 10 kPa (0.1 bar) was chosen as the opening pressure, which is within the acceptable range according to NFPA 68[83].

Considering the worst-case scenario of explosions for both baseline excipient and hybrid mixture, a full spray dryer (i.e., 100 % volume) was used in calculating the size of the pressure panels. Pressure panels used in the simulations are identical in their properties (e.g., type, opening pressure, weight, etc.); the only exception is the size of the pressure panels as calculated by NFPA 68[83] using the explosibility data determined for MCC and MCC admixed with methanol in atmospheric condition. The reduced pressure after explosion venting was set at 50 kPa (0.5 bar) as the maximum allowable pressure for spray dryers according to NFPA 68[83] is $\leq$ 1.0 bar. The point of ignition was fixed on the central

axis of the dryer at a height of 5.1 m from the dryer's bottom due to the strong possibility of explosive atmospheres in that region.[97]

When the chamber of the spray dryer was configured as closed, the maximum explosion pressure was determined to be similar for both MCC and MCC admixed with methanol. As expected, the total explosion time (t_{exp}) was found to be shorter in the case of the hybrid mixture as compared to the excipient alone; see Figures 5-3 and 5-4 which demonstrate the occurrence of more rapid combustion for the hybrid mixture as described earlier. Reduced pressures according to NFPA 68[83] and the CFD simulations are similar for both MCC and MCC admixed with methanol as shown in Table 5-9, and Figures 5-12 and 5-13. It has been clearly observed that the reduced pressure was higher than the acceptable value when the pressure panels designed for MCC were used in the case of the dryer filled with a hybrid mixture of MCC and methanol (see Figure 5-14). These simulations explicitly illustrate that safety measures designed for dust explosions alone cannot provide adequate protection in the case of hybrid mixture explosions.

Table 5-9 Comparison between NFPA standard and FLACS-DustEx results for MCC explosions in the spray dryer with pressure panels.

	Dryer filled with MCC	**Dryer filled with MCC +M(ATM)**
Method	Reduced pressure in bar(g)	Reduced pressure in bar(g)
NFPA 68	0.50	0.50
FLACS-DustEx Results	0.57	0.52

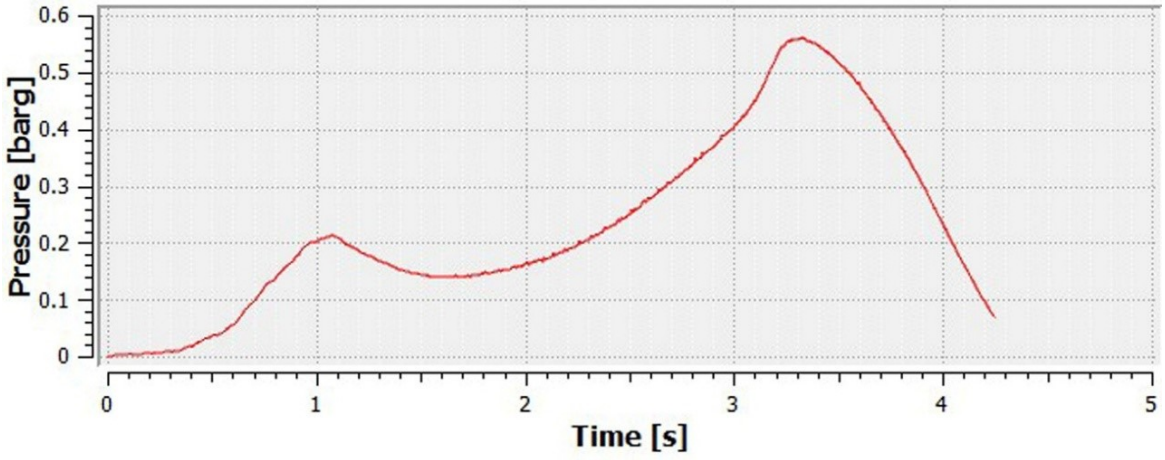

Figure 5-12 FLACS-DustEx pressure-time traces of an explosion in the spray dryer when the chamber of the dryer was filled with MCC and the pressure panels were used as designed for MCC.

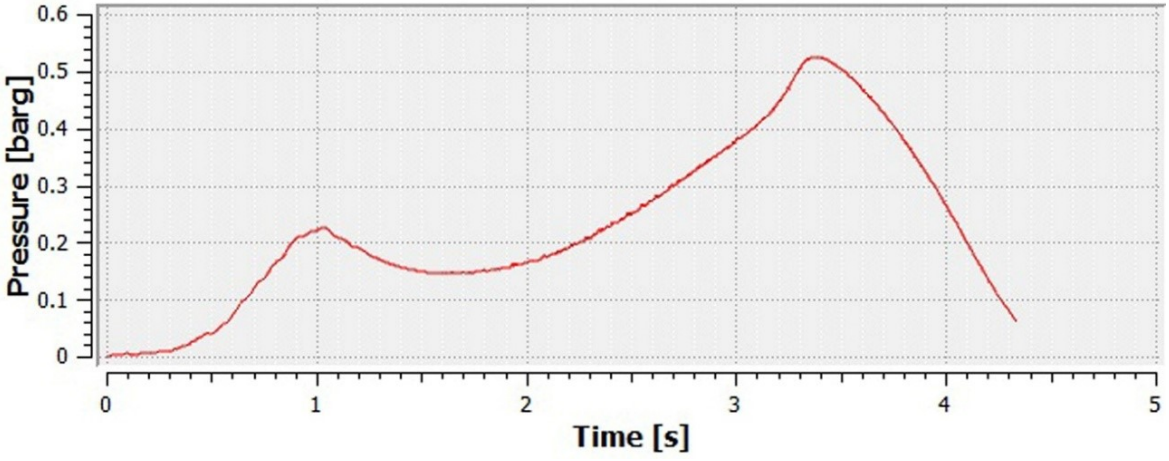

Figure 5-13 FLACS-DustEx pressure-time traces of an explosion in the spray dryer when the chamber of the dryer was filled with a dust cloud of MCC admixed with methanol and pressure panels were used as designed for MCC admixed with methanol.

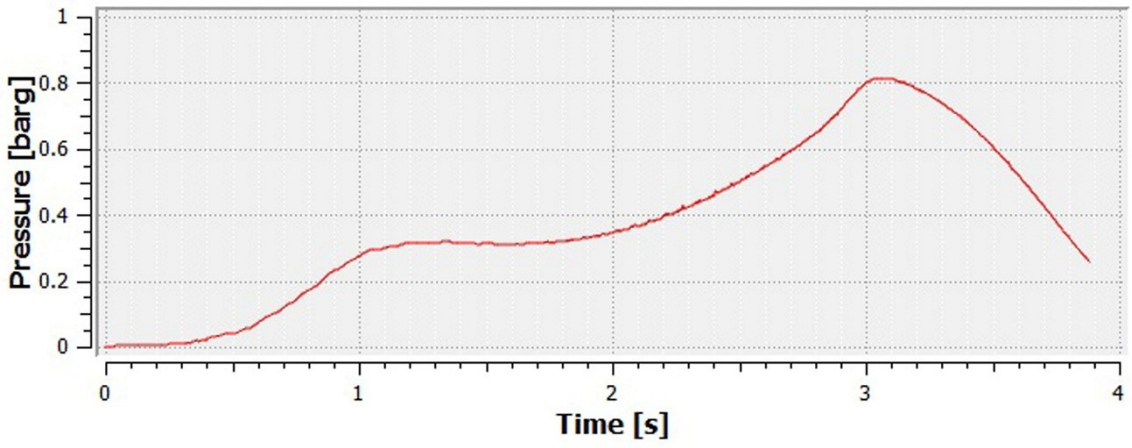

Figure 5-14 FLACS-DustEx pressure-time traces of an explosion in the spray dryer when the chamber of the dryer was filled with a dust cloud of MCC admixed with methanol, but pressure panels were used as designed for MCC.

The observation of a reduction of the pressure just after the first peak in most of the pressure-time traces in the simulation (in the cases of the vented dryer) was due to the opening of the vent and the discharge of burned and unburned material. If the volume of discharged material exceeds the volume produced by combustion, pressure usually drops. Sometimes, venting is hindered by the unburned materials flowing through the vent, which results in pressure rises. Still, combustion and subsequent burning will continue to occur, and the pressure goes up over time as the flame propagates, producing more burned material up to the next reduction after the second peak. The next reduction will occur when the flames reach the vent and the burned material is discharged from the vessel.

5.3.2 Strategies to Prevent and Mitigate Nontraditional Dust Explosions

Based on the outcomes of this research, the following strategies according to the hierarchy of controls are recommended to prevent and mitigate nontraditional dust explosions.

Inherently safer design (ISD)

Explicit incorporation of the basic ISD principles (minimization, substitution, moderation and simplification) into nontraditional dust explosion risk reduction research and practice is strongly encouraged. A few examples of such incorporation are given below.

- Minimization:

  It is critical to minimize whenever possible, the amount of dust available to participate in an explosion[99]; therefore, it is always recommended to maintain the inventory of nontraditional dusts as low as possible. Facilities that handle and process nontraditional particulate fuel systems need to be built based on the minimization principle of ISD. This applies to all units in the plant during operation as well as storage of initial, intermediate and final product. Storing a large inventory of nontraditional powder (e.g., nano-sized titanium) can lead to a more catastrophic explosion *than* the traditional ones (e.g., micron-sized titanium). If airborne dust concentrations of nontraditional fuel/particulate systems can be kept below the MEC of the materials involved, then the fuel component of the fire triangle is removed and dust explosions can in theory, be prevented.[99] As mentioned by Amyotte et al. [99], the occurrence of secondary dust explosions can be avoided by minimizing dust deposits from the workplace in a manner that limits the formation of dust suspensions (e.g. vacuuming instead of sweeping).

- Substitution:

  Substitution of nontraditional fuel particulate systems is a challenging task since most of the time, these are likely introduced for their particular uses. However, some substitutions may be possible depending on the subject matter. Considerable research is needed to find alternatives that can replace the nontraditional powders

discussed in this research. Substituting a hazardous solvent with a less hazardous one can reduce the risk in a workplace that handles combustible dusts and flammable solvents. For example, ethanol and isopropanol can provide a safer environment than methanol as a pre-wetting medium for MCC (micro crystalline cellulose). This substitution is based on both likelihood of occurrence and severity of consequences of hybrid mixture explosions as found in the current research.

- Moderation:

  Adding solid inertant can be useful to effectively decrease ignition sensitivity of nanomaterials. However, this option is not always applicable for all nanomaterials. It depends on their chemical and thermodynamic properties such as chemical composition and reaction kinetics. For example, TiO_2 powder can be used as an active suppressing chemical for nano titanium powder. Coating of nanoparticles with less hazardous substances is an application of the moderation principle of ISD and this can be useful as well to minimize the explosion risk.[100] For nanomaterials, a decreased particle size typically exhibits an increased severity of consequences and likelihood of occurrences of an explosion. So, increasing the mean diameter of a nanomaterial by any sort of surface treatment (e.g., chemical coating as mentioned earlier or vacuum plating) can be a successful application of the moderation principle of ISD. For flocculent materials (e.g., polyamide 6.6 and polyester), the short small-diameter fibers displayed a higher explosion pressure and rate of pressure rise than the long large-diameter fibers. Thus, length and diameter optimization can be achieved by applying the moderation principle of ISD as required to control the associated risks. The fibers involved in the incident that occurred at Malden Mills Industries (Malden Mills) in Massachusetts on December 11, 1995, with their high length-to-diameter ratio, illustrate the diverse

nature of shapes that combustible particulate solids can have and still pose a dust explosion hazard.[27]

- Simplification:

  The simplification principle of ISD can also be applied in nontraditional dust explosion risk reduction. For example, in some pharmaceutical applications, solvents are added in excipients or vice-versa. Adding solvents in powder through integrated mixing systems is very convenient for some equipment (e.g., a spray dryer). In this case, pre-mixing of a solvent in an additional mixing room can be avoided if integrated mixing systems give satisfactory results. This will minimize the cost as well as make the process simpler. Clear and straightforward procedures (Appendices F and G) as developed and implemented in this research for handling nano titanium powder in determining the MIT and MIE are examples of the simplification principle of ISD.

Passive Engineered Control Measures

When application of ISD principles is not a possible option, the most desirable alternative for preventing and mitigating explosion risk is to employ engineering controls.

The use of a glove bag as followed in this research for weighing activities (Figure 4-12 (Chapter 4)), is a good option for isolation of nanomaterials from the working environment. In this regard, using bench-mounted weighing enclosures (Figure 5-15), is a better option as a substitute for weighing in traditional fume hoods. A bench-mounted weighing enclosure is an integrated system that typically works at airflow rates lower than those in traditional fume hoods and this can reduce turbulence and potential for leakage.[101]

Figure 5-15 Nano containment hood.[101]

Another possible alternative engineering control is using a glove box containment system as shown in Figure 5-16. This can eliminate cleaning difficulties and provide a high degree of operator protection. [101]

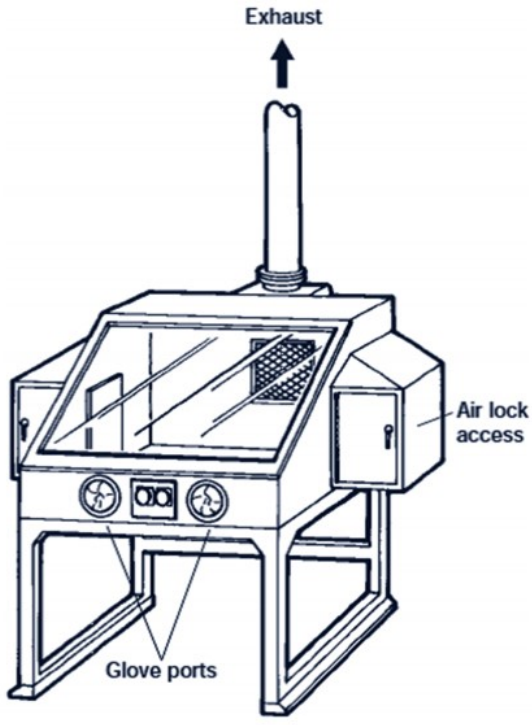

Figure 5-16 A **glove box containment system.**[101]

An explosion that occurred in a dust filter located downstream of a rotary dryer in an acrylonitrile butadiene styrene (ABS) polymer-production process at a Monsanto facility in Europe[102] is a reminder of the importance of pressure panels. Although several add-on safety features were incorporated into the polymer-production process, the only ones that worked properly during this accident were the passive vent panels.[103] Use of pressure panels for processes that involve nontraditional particulate fuel systems (e.g., hybrid mixture of a powder admixed with solvents) may not always be as simple as traditional ones (e.g., powder alone). For example, as clarified earlier, based on the simulation results found in this research, the pressure panels designed for dust explosions alone (e.g., MCC powder) cannot provide adequate protection in the case of hybrid mixture (e.g., MCC admixed with methanol) explosions. In the case of an admixed solvent, it is not really the powder itself considered but rather the composite fuel-solvent system in its entirety.

Active Engineered Control Measures

Inerting of a dust cloud by using inert gases (e.g., N_2 for dispersing nano titanium powder) can serve as an effective safety measure. Such application of inerting or partial inerting by means of a nonreactive gas would likely be viewed as an active engineered safety measure of the need for physical devices for inert gas addition and monitoring.[13] Other active devices such as dust explosion suppression systems or mechanical blocks can also be applied based on their effectiveness on the three categories of nontraditional particulate fuel systems discussed in the current research.

Procedural Safety Measures

The following procedural safety measures are recommended to prevent and mitigate explosions associated with nontraditional particulate fuel systems.

- Provide information to workers on the hazardous properties of the nanomaterials, flocculent materials and hybrid mixtures being produced or handled. For example, supplying the safety data sheets (SDS) obtained from manufacturers when using these particulate fuel systems is required.
- Train workers on the safe handling of these particulate fuel systems to minimize the likelihood of explosion occurrence.
- Store nontraditional dusts in accordance with appropriate procedures. For example, store nanomaterials in a closed hermetically-sealed condition.
- Conduct routine monitoring in facilities that handle nanomaterials, flocculent materials and hybrid mixtures to ensure that work practices are effective.
- Ensure work areas and equipment are cleaned at the end of the work period. For example, cleaning a measuring unit by wet wiping methods is very important to ensure that the unit is safe to use.

- Clean up spills of nanomaterials, flocculent materials, pharmaceutical excipients and solvents immediately and in accordance with appropriate procedures. For example, cleaning of the waste of flocculent fibers and pharmaceutical powder should be by vacuum cleaners fitted with appropriate filters. In this case, blowing with compressed air should not be used for as a cleaning method.
- Apply every precaution for introducing solvents into excipients. It is important to provide a safer environment and to ensure a dust cloud of hazardous hybrid mixture is not formed.
- Ensure housekeeping practices are adequate for controlling accumulations of dust on floors, elevated platforms, and other areas in facilities that handle nontraditional powders.
- Ensure that provisions and procedures are in place to prevent spilled solvents from entering into confined spaces.
- Ensure that eyewash stations are located near work areas.
- Use appropriately labelled and designated containers for solvents.
- Keep solvent containers tightly sealed when they are not in use.

It is important to regularly check appropriateness of work practices and the efficiency of engineering control measures. If necessary, appropriate corrective measures should be applied.

Chapter 6 Conclusions and Recommendations

In this chapter, the key findings of this research work are summarized and recommendations arising from the research for future work are given.

6.1 Summary of Conclusions

The principal conclusions which have been drawn from this study are as follows:

1. The risk management framework presented in this research is useful to assess and manage explosion risks associated with metallic nano-powder, flocculent textile materials, and hybrid mixtures of pharmaceutical excipients and solvents in industrial facilities.
2. Nano Ti powder was observed to be much more sensitive to contact with a hot surface than micron Ti powder, even when mixed with 90% nano TiO_2 powder. Such results indicate that solid inertant technology is not able to effectively reduce the ignition hazard of nano Ti powder in contact with a hot surface. However, solid inertants could effectively decrease the ignition sensitivity of micron Ti powder in contact with hot surfaces; a mixture with 70% TiO_2 could not be ignited in the BAM oven. The MIT of micron Ti powder was sharply reduced with a small amount of nano Ti powder.
3. Nano Ti powder was identified to be much more sensitive to electric sparking than micron Ti powder, even at low quantities of nano Ti powder. Inductance had almost no effect on MIE of the two pure powders (nano and micron Ti). Adding TiO_2 with micron Ti powder helped to reduce ignition sensitivity to electric sparks. Solid inertants might not be suitable for nano Ti particles because mixtures exhibited high ignition sensitivity even with 90% nano TiO_2 (10-30 nm) powder.

4. A layer fire may occur for micron Ti powder mixed with nano TiO_2 following a dust explosion with incomplete burning. Layer fires with nano Ti powder are unlikely. However, layer fires could initiate a violent dust explosion after the second dispersion, so special attention has to be taken to prevent such accidents even in situations where the potential for electric sparking is low.
5. Fine flocculent materials of polyamide 6.6 and polyester were identified to be more hazardous and easily ignitable than materials containing coarse fibers. Moreover, if the length of the fiber of flocculent materials such as polyamide 6.6 and polyester are increased, dust explosion risk reduction can be achieved. Thus, length and diameter optimization are required to control the explosion risks associated with flocculent materials.
6. Common pharmaceutical solvents such as methanol, ethanol, and isopropanol can significantly increase the explosion likelihood and explosion severity of common pharmaceutical excipients such as MCC and lactose. The influence of solvent on basic explosibility parameters of excipients is dependent on both the nature of the excipient and the method of admixture.
7. Safety measures designed for dust explosions alone cannot afford adequate protection in the case of hybrid mixture explosions.
8. Hazards involved during (i) manufacturing and processing of micron-and nano-sized titanium powders; polyamide 6.6 and polyester, and (ii) transferring solvents into excipients or vice versa should be managed as part of a comprehensive risk management plan.
9. For prevention and mitigation of nontraditional dust explosions, the control measures (inherent, passive, active, and procedural) need to be categorized along a spectrum of the process safety approaches and should not be considered to be discrete categories with clear boundaries.

6.2 Recommendations and Suggestions for Future Work

As new kinds of dust, such as nanomaterials (e.g., nano Ti), flocculent materials (e.g., polyamide 6.6 and polyester) and hybrid mixtures (e.g., MCC admixed with methanol), are widely used in industries, the adoption of safety methodologies involving new features is crucial to prevent and mitigate explosions associated with such materials. Thus, it is imperative from both a research and safety perspective to further develop various aspects of management strategies for nontraditional dust explosion risk reduction:

Based on the experience gained and conclusions drawn from this work the following list of recommendations is proposed as suggestions for future work:

1. Different types of nano-sized powders with a wide range of particle sizes should also be further investigated for their reactivity and potential explosible properties. Nano-crystalline cellulose (NCC) is being developed for its high strength and light weight. The NCC can cause dust explosions similar to micro-crystalline cellulose (MCC).[24] For future studies, more research work can be suggested on both experimental and simulation aspects of investigating the influence of particle size on explosibility parameters of NCC. Then the results can be compared with MCC as found in the current study to investigate the influence of particle sizes both experimentally and computationally. Such research work can help industries that use these kinds of materials to take adequate safety measures for preventing and mitigating explosions.
2. After adding solid inertant (nano TiO_2 powder) during MIE testing, layer fires were observed to occur for micron Ti powder following a dust explosion with incomplete burning. Layer fires could initiate a violent dust explosion

after the second dispersion, so further research is needed to improve the effectiveness of solid inertant in order to prevent such layer fires.

3. Flocculent materials with a wide range of particle sizes, considering both length and diameter should also be further investigated for their potential explosible properties. Such investigations will provide further information about the explosion behavior of flocculent materials in relation to various features including both length and diameter.
4. Because the MIKE 3 apparatus and BAM oven are not closed systems, testing of excipients admixed with solvent in atmospheric condition was not possible in the current study for MIE and MIT determination. It can be suggested for future studies, to conduct such testing in order to investigate the influence of solvents on MIE and MIT of excipients in atmospheric condition. This would require equipment modification to enable closed-system testing.
5. The qualitative fault-tree analysis of nanomaterials as developed in the current work can be considered for further development. In addition, such analysis can be extended to accommodate explosions associated with flocculent materials and hybrid mixtures.

References

1. Worsfold SM, Amyotte PR, Khan FI, Dastidar AG, Eckhoff RK. Review of the explosibility of nontraditional dusts. *Ind Eng Chem Res*. 2012;51(22):7651-7655.
2. Wu HC, Chang RC, Hsiao HC. Research of minimum ignition energy for nano Titanium powder and nano Iron powder. *J Loss Prev Process Ind*. 2009;22(1):21-24.
3. Eckhoff R. Does the dust explosion risk increase when moving from µm-particle powders to powders of nm-particles? *J Loss Prev Process Ind*. 2012;25(3):448-459.
4. Nifuku M, Koyanaka S, Ohya H, et al. Ignitability characteristics of aluminium and magnesium dusts that are generated during the shredding of post-consumer wastes. *J Loss Prev Process Ind*. 2007;20(4-6):322-329.
5. Cashdollar KL, Zlochower IA. Explosion temperatures and pressures of metals and other elemental dust clouds. *J Loss Prev Process Ind*. 2007;20(4-6):337-348.
6. Eckhoff RK. *Dust Explosions in the Process Industries*. Third ed. Boston, U.S.A: Gulf Professional Publishing/Elsevier; 2003.
7. Boilard S, Amyotte P, Khan F, Dastidar A, Eckhoff R. Explosibility of micron- and nano-size titanium powders. *J Loss Prev Process Ind*. 2013;26(6):1646-1654.
8. Bouillard J, Vignes A, Dufaud O, Perrin L, Thomas D. Explosion risks from nanomaterials. *J Phys Conf Ser*. 2009;170:012032.
9. Dobashi R. Risk of dust explosions of combustible nanomaterials. *J Phys Conf Ser*. 2009;170:012029.
10. Dufaud O, Vignes A, Henry F, Perrin L, Bouillard J. Ignition and explosion of nanopowders: something new under the dust. *J Phys Conf Ser*. 2011;304:012076.
11. CSB. *Investigation Report – Combustible Dust Hazard Study*. Report No. 2006H1, U.S. Chemical Safety and Hazard Investigation Board, Washington, USA.; 2006.
12. Amyotte PR. Some myths and realities about dust explosions. *Process Saf Environ Prot*. 2014;92(4):292-299.
13. Amyotte PR, Eckhoff RK. Dust explosion causation, prevention and mitigation: An overview. *J Chem Heal Saf*. 2010;17(1):15-28.
14. Dufaud O, Perrin L, Traoré M. Dust/vapour explosions: Hybrid behaviours? *J Loss Prev Process Ind*. 2008;21(4):481-484.
15. Dufaud O, Perrin L, Traore M, Chazelet S, Thomas D. Explosions of vapour/dust hybrid mixtures: A particular class. *Powder Technol*. 2009;190(1-2):269-273.

16. Amyotte P, Lindsay M, Domaratzki R, Marchand N, Di Benedetto A, Russo P. Prevention and mitigation of dust and hybrid mixture explosions. *Process Saf Prog*. 2010;29(1):17-21.

17. Garcia-Agreda A, Di Benedetto A, Russo P, Salzano E, Sanchirico R. Dust/gas mixtures explosion regimes. *Powder Technol*. 2011;205(1-3):81-86.

18. Perry JA, Ozog H, Murphy M, Stickles RP. Conducting process hazard analyses for dust-handling operations. *Chem Eng Prog*. 2009;105(2):28-35.

19. Pilão R, Ramalho E, Pinho C. Overall characterization of cork dust explosion. *J Hazard Mater*. 2006;133(1-3):183-195.

20. Pilão R, Ramalho E, Pinho C. Explosibility of cork dust in methane/air mixtures. *J Loss Prev Process Ind*. 2006;19(1):17-23.

21. Sanchirico R, Di Benedetto A, Garcia-Agreda A, Russo P. Study of the severity of hybrid mixture explosions and comparison to pure dust-air and vapour-air explosions. *J Loss Prev Process Ind*. 2011;24(5):648-655.

22. Abuswer M, Amyotte P, Khan F. A quantitative risk management framework for dust and hybrid mixture explosions. *J Loss Prev Process Ind*. 2013;26(2):283-289.

23. NFPA. NFPA 654: Standard for the Prevention of Fire and Dust Explosions from the Manufacturing, Processing, and Handling of Combustible Particulate Solids. *Natl Fire Prot Assoc Quincy, MA*. 2006.

24. Boilard SP. Explosibility of micron- and nano-size titanium powders. Process Engineering & Applied Science, Dalhousie University, 2013.

25. Abbasi T, Abbasi SA. Dust explosions–Cases, causes, consequences, and control. *J Hazard Mater*. 2007;140(1–2):7-44.

26. Vignes A, Muñoz F, Bouillard J, et al. Risk assessment of the ignitability and explosivity of aluminum nanopowders. *Process Saf Environ Prot*. 2012;90(4):304-310.

27. Frank WL. Dust explosion prevention and the critical importance of housekeeping. *Process Saf Prog*. 2004;23(3):175-184.

28. Glor M. A Synopsis of Explosion Hazards During the Transfer of Powders into Flammable Solvents and Explosion Preventative Measures. *ISPE, Pharm Eng*. 2010;30(1):1-8.

29. OSHA. *Combustible Dust National Emphasis Program*. Washington, DC, U.S.A; 2007.

30. CSB. *Investigation Report – Dust Explosion, West Pharmaceutical Services, Inc.,*. Report No. 2003-07-I-NC, U.S. Chemical Safety and Hazard Investigation Board, Washington, USA.; 2004.

31. The Chemical Safety Mechanism. *Lessons Learned: A Titanium Metal Fire*. Madison; 2012.

32. Hazardous Material Advisory. *Metal Fires, Health Hazardous Materials Division Emergency Operations Section.*; 2010.

33. NIOSH Report. Seven Career Fire Fighters Injured at a Metal Recycling Facility Fire. 2010. http://www.cdc.gov/niosh/fire/reports/face201030.html.

34. NIOSH Report. Tactics Factored into LA Metal Fire Explosion Injuring 7 Firefighters. 2011. http://www.firerescue1.com/fire-attack/articles/1107704-NIOSH-Tactics-factored-into-LA-metal-fire-explosion-injuring-7-firefighters/.

35. CSB. *Investigation Report – Ink Dust Explosion and Flash Fires in East Rutherford, New Jersey*. Report No. 2013-01-I-NJ, U.S. Chemical Safety and Hazard Investigation Board, Washington, USA.; 2013.

36. DEKRA Process Safety. Hazards Control & Assessment Safety Guide A strategic guide to characterisation & understanding Handling Dusts & Powders Safely. *Chilworth Technol Ltd*. 2013.

37. Occupational Safety and Health Service. Prevention of sulphur fires and explosion. *Dep Labour Wellington, New Zeal*. 1993.

38. ASTM International. ASTM E2019-03(2013): Standard Test Method for Minimum Ignition Energy of a Dust Cloud in Air. *West Conshohocken, PA*. 2013.

39. ASTM International. ASTM E1515-14: Standard Test Method for Minimum Explosible Concentration of Combustible Dusts. *West Conshohocken, PA*. 2014.

40. ASTM International. ASTM E1491-06(2012): Standard Test Method for Minimum Autoignition Temperature of Dust Clouds. *West Conshohocken, PA*. 2012.

41. ASTM International. ASTM E1226-12a: Standard Test Method for Explosibility of Dust Clouds. *West Conshohocken, PA*. 2012.

42. Woodruff JM. Consequence and likelihood in risk estimation: A matter of balance in UK health and safety risk assessment practice. *Saf Sci*. 2005;43(5-6):345-353.

43. Mannan S. *Lees' Loss Prevention in the Process Industries*. 3rd Editio. USA: Elsevier; 2005.

44. Center for Chemical Process Safety (CCPS). *Inherently Safer Chemical Processes: A Life Cycle Approach*. New York, NY: Wiley; 2009.

45. Wu HC, Ou HJ, Hsiao HC, Shih TS. Explosion characteristics of aluminum nanopowders. *Aerosol Air Qual Res*. 2010;10(1):38-42.

46. Mittal M. Explosion characteristics of micron- and nano-size magnesium powders. *J Loss Prev Process Ind*. 2014;27(1):55-64.

47. Bouillard J, Vignes A, Dufaud O, Perrin L, Thomas D. Ignition and explosion risks of nanopowders. *J Hazard Mater*. 2010;181(1-3):873-880.

48. Vignes A, Traore M, Dufaud O, Perrin L, Bouillard J. Assessing Explosion Severity of Nanopowders with the 20 L Sphere. In: *8th World Congress of Chemical Engineering*. Montreal, Canada; 2009.

49. Wu HC, Ou HJ, Peng D, Hsiao HC, Gau CY, Shih TS. Dust explosion characteristics of agglomerated 35 nm and 100 nm aluminum particles. *Int J Chem Eng*. 2010;2010.

50. Eckhoff RK, Randeberg E. Electrostatic spark ignition of sensitive dust clouds of MIE<1 mJ. *J Loss Prev Process Ind*. 2007;20(4-6):396-401.

51. Eckhoff RK. Influence of dispersibility and coagulation on the dust explosion risk presented by powders consisting of nm-particles. *Powder Technol*. 2013;239(0032):223-230.

52. Huang Y, Risha GA, Yang V, Yetter RA. Effect of particle size on combustion of aluminum particle dust in air. *Combust Flame*. 2009;156(1):5-13.

53. Dufaud O, Perrin L, Bideau D, Laurent A. When solids meet solids: A glimpse into dust mixture explosions. *J Loss Prev Process Ind*. 2012;25(5):853-861.

54. Amyotte PR, Pegg MJ, Khan FI, Nifuku M, Yingxin T. Moderation of dust explosions. *J Loss Prev Process Ind*. 2007;20(4-6):675-687.

55. Amyotte PR, Cloney CT, Khan FI, Ripley RC. Dust explosion risk moderation for flocculent dusts. *J Loss Prev Process Ind*. 2012;25(5):862-869.

56. Mintz KJ, Bray MJ, Zuliani DJ, Amyotte PR, Pegg MJ. Inerting of fine metallic powders. *J Los Prev Process Ind*. 1996;9(1):77-80.

57. Myers TJ. Reducing aluminum dust explosion hazards: Case study of dust inerting in an aluminum buffing operation. *J Hazard Mater*. 2008;159(1):72-80.

58. Amyotte PR. Solid inertants and their use in dust explosion prevention and mitigation. *J Loss Prev Process Ind*. 2006;19(2-3):161-173.

59. Ohkura Y, Rao PM, Sun Cho I, Zheng X. Reducing minimum flash ignition energy of Al microparticles by addition of WO3 nanoparticles. *Appl Phys Lett*. 2013;102(4):0-4.

60. Amyotte PR, Mintz KJ, Pegg MJ. Effectiveness of various rock dusts as agents of coal dust inerting. *J loss Prev Process Ind*. 1992;*5*(3):196-199.

61. Amyotte P, Domaratzki R, Lindsay M, MacDonald D. Moderation of explosion likelihood and consequences of non-traditional dusts. In: IChemE, ed. *Hazards XXII*. ; 2011:148-154.

62. Marmo L, Cavallero D. Minimum ignition energy of nylon fibres. *J Loss Prev Process Ind*. 2008;21(*5*):512-*517*.

63. Marmo L. Case study of a nylon fibre explosion: An example of explosion risk in a textile plant. *J Loss Prev Process Ind*. 2010;23(1):106-111.

64. Pidoll U v. Avoidance of the Ignition of Textile Fiber/Air Mixtures during the Electrostatic Flocking Process. *IEEE Trans Ind Appl*. 2002;38(2).

65. Bind VK, Roy S, Rajagopal C. CFD modelling of dust explosions: Rapid combustion in a 20 L apparatus. *Can J Chem Eng*. 2011;89(4):663-670.

66. Kosinski P, Hoffmann AC. An investigation of the consequences of primary dust explosions in interconnected vessels. *J Hazard Mater*. 2006;137(2):*752*-*761*.

67. Skjold T, Arntzen BJ, Hansen OR, Storvik IE, Eckhoff RK. Simulation of dust explosions in complex geometries with experimental input from standardized tests. *J Loss Prev Process Ind*. 2006;19(2-3):210-217.

68. Skjold T, Arntzen BJ, Hansen OR, Taraldset OJ, Storvik IE, Eckhoff RK. Simulating Dust Explosions with the First Version of DESC. *Process Saf Environ Prot*. 2005;83(2):151-160.

69. Skjold T. Review of the DESC project. *J Loss Prev Process Ind*. 2007;20(4-6):291-302.

70. Tascón A, Ruiz Á, Aguado PJ. Dust explosions in vented silos: Simulations and comparisons with current standards. *Powder Technol*. 2011;208(3):*717*-*724*.

71. Zhong S, Deng X. Modeling of maize starch explosions in a 12 m3 silo. *J Loss Prev Process Ind*. 2000;13(3-*5*):299-309.

72. Amyotte PR, Basu A, Khan FI. Reduction of dust explosion hazard by fuel substution in power plants. *Chem Eng Res Des*. 2003;81(November):*457*-462.

73. Khan FI, Amyotte PR. How to Make Inherent Safety Practice a Reality. *Can J Chem Eng*. 2003;81(February):2-16.

74. Abuswer MA. A Quantitative Risk Management Framework for Dust and Hybrid Mixture Explosions. Process Engineering & Applied Science, Dalhousie University, 2012.

75. Hendershot DC. A Summary of Inherently Safer Technology. *Process Saf Prog*. 2010;29(4):389-392.

76. Iarossi I, Amyotte PR, Khan FI, Marmo L, Dastidar AG, Eckhoff RK. Explosibility of polyamide and polyester fibers. *J Loss Prev Process Ind*. 2013;26(6):1627-1633.

77. Chunmiao Y, Amyotte PR, Hossain MN, Li C. Minimum ignition energy of nano and micro Ti powder in the presence of inert nano TiO_2 powder. *J Hazard Mater*. 2014;274:322-330.

78. Yuan C, Amyotte PR, Hossain MN, Li C. Minimum ignition temperature of nano and micro Ti powder clouds in the presence of inert nano TiO2 powder. *J Hazard Mater*. 2014;275:1-9.

79. Swicofil. Properties of Polyamide and Polyester. 2009. http://www.swicofil.com/swissflocksafetypolyamide.html.

80. Sanders A, Seager K. *Junky Styling: Wardrobe Surgery*. London: A. & C. Black; 2009.

81. Felder RM, Rousseau RW. *Elementary Principles of Chemical Processes*. 3rd ed. Hoboken: John Wiley & Sons, Inc.; 2005.

82. Kuchta JM. *Investigation of Fire and Explosion Accidents in the Chemical, Mining, and Fuel-Related Industries: A Manual*. Avondale, MD.; 1985.

83. NFPA. NFPA 68: Standard on Explosion Protection by Deflagration Venting. *Natl Fire Prot Assoc Quincy, MA*. 2007.

84. Van Lipzig JPJ, Nilsson EJK, De Goey LPH, Konnov AA. Laminar burning velocities of n-heptane, iso-octane, ethanol and their binary and tertiary mixtures. *Fuel*. 2011;90(8):2773-2781.

85. Murphy RM. *Introduction to Chemical Processes. Principles, Analysis, Synthesis*. New York, NY: McGraw-Hill; 2007.

86. Kuhner. *Operating Instructions 20-L-Apparatus 6.0.*; 2011. http://safety.kuhner.com/en/product/apparatuses/safety-testing-devices/id-20-l-apparatus.html [June 2011].

87. Kuhner. *MIKE 3 Minimum Ignition Energy.*; 2010. Retrieved from: http://safety.kuhner.com/en/product/apparatuses/safety-testing-devices/mike-3.html [June 2012].

88. Bideau D, Dufaud O, Le Guyadec F, et al. Self ignition of layers of powder mixtures: Effect of solid inertants. *Powder Technol*. 2011;209(1-3):81-91.

89. Amyotte PR, Soundararajan R, Pegg MJ. An investigation of iron sulphide dust minimum ignition temperatures. *J Hazard Mater*. 2003;97(1-3):1-9.

90. Wu HC, Kuo YC, Wang YH, Wu CW, Hsiao HC. Study on safe air transporting velocity of nanograde aluminum, iron, and titanium. *J Loss Prev Process Ind*. 2010;23(2):308-311.

91. Line LE, Rhodes HA, Gilmer TE. The spark ignition of dust clouds. *J Phys*. 1959;Chem. 2:290-294.

92. Siwek R, Cesana C. Ignition behavior of dusts: Meaning and interpretation. *Process Saf Prog*. 1995;14(2):107-119.

93. Gromov AA, Pautova YI, Lider AM, et al. Interaction of powdery Al, Zr and Ti with atmospheric nitrogen and subsequent nitride formation under the metal powder combustion in air. *Powder Technol*. 2011;214(2):229-236.

94. Hossain N, Amyotte P, Abuswer M, Dastidar A, Khan F, Eckhoff R. Influence of Liquid and Vapourized Solvents on Explosibility of Pharmaceutical Excipient Dusts. *Process Saf Prog*. 2014.

95. Flory PJ. *Principles of Polymer Chemistry*. Ithaca, NY.: Cornell University Press; 1953.

96. Russo P, Amyotte PR, Khan FI, Di Benedetto A. Modelling of the effect of size on flocculent dust explosions. *J Loss Prev Process Ind*. 2013;26(6):1634-1638.

97. Wawrzyniak P, Polańczyk A, Zbicinski I, Jaskulski M, Podyma M, Rabaeva J. Modeling of Dust Explosion in the Industrial Spray Dryer. *Dry Technol*. 2012;30(15):1720-1729.

98. Poly Processing Company. Capacity Sheet for Upright Vertical Tanks. http://www.polyprocessing.com. Accessed May 22, 2014.

99. Amyotte PR, Pegg MJ, Khan FI. Application of inherent safety principles to dust explosion prevention and mitigation. *Process Saf Environ Prot*. 2009;87(1):35-39.

100. Williams RA, Kulinowski KM, White R, Louis G. Risk Characterization for Nanotechnology. *Risk Anal*. 2010;30(11).

101. NIOSH. *Current Strategies for Engineering Controls in Nanomaterial Production and Downstream Handling Processes*. Cincinnati, OH; 2013.

102. Skinner SJ. Case Histories of Dust Explosions. In: *23rd Loss Prevention Symposium*. Houston, TX: AIChE; 1989.

103. Amyotte PR, Khan FI, Dastidar AG. Reduce Dust Explosions the Inherently Safer Way. *Chem Eng Prog*. 2003;99(10):36-43.

Appendix A Industries with combustible dusts

Table A.1 Industries that may have combustible dusts.[29]

The Standard Industrial Classification (SICS)	Industry	North American Industry Classification System (NAICS)
0723	Crop Preparation Services for Market, Except Cotton Ginning	115114, 115111
2052	Fresh cookies, crackers, pretzels, and similar "dry" bakery products.	311821
2062	Refining purchased raw cane sugar and sugar syrup.	311312
2087	Flavoring extracts, syrups, powders, and related products, not elsewhere classified.	311930
2099	Prepared foods and miscellaneous food specialties, not elsewhere classified.	311212
2221	Broadwoven Fabric Mills, Manmade Fiber and Silk	313210
2262	Finishers of Broadwoven Fabrics of Manmade Fiber and Silk	313311
2299	Textile Goods, Not Elsewhere Classified	313111
2421	Sawmills and Planing Mills, General	321113
2431	Millwork	321911
2434	Wood Kitchen Cabinets	33711
2439	Structural Wood Members, Not Elsewhere Classified	321213, 321214
2452	Prefabricated Wood Buildings and Components	321992
2493	Reconstituted Wood Products	321219
2499	Wood Products, Not Elsewhere Classified	321920, 321219
2511	Wood Household Furniture, Except Upholstered	337122
2591	Drapery Hardware and Window Blinds and Shades	337920
2819	Industrial Inorganic Chemicals, Not Elsewhere Classified	325188, 325998, 331311
2821	Plastic Materials, Synthetic Resins, and Nonvulcanizable Elastomers	325211

Table A.1 (continued)

The Standard Industrial Classification (SICS)	Industry	North American Industry Classification System (NAICS)
2823	Cellulosic Manmade Fibers	325221
2834	Pharmaceutical Preparations	325412
2841	Soap and Other Detergents, Except Specialty Cleaners	325611
2851	Paints, Varnishes, Lacquers, Enamels, and Allied Products	32551
2861	Gum and Wood Chemicals	325191
2899	Chemicals and Chemical Preparations, Not Elsewhere Classified	325510, 325998
3011	Tires And Inner Tubes	326211
3061	Molded, Extruded, and Lathe-Cut Mechanical Rubber Goods	326291
3069	Fabricated Rubber Products, Not Elsewhere Classified	326299
3081	Unsupported Plastics Film and Sheet	326113
3082	Unsupported Plastics Profile Shapes	326121
3086	Plastics Foam Products	326140, 326150
3087	Custom Compounding of Purchased Plastics Resins	325991
3089	Plastics Products, Not Elsewhere Classified	326199
3291	Abrasive Products	327910
3313	Alumina and Aluminum Production and Processing	331312
3334	Primary Production of Aluminum	331312
3341	Secondary Smelting and Refining of Nonferrous Metals	331314
3354	Aluminum Extruded Products	331316
3363	Aluminum Die-Castings	331521
3365	Aluminum Foundries	331524
3369	Nonferrous Foundries, Except Aluminum and Copper	331528
3398	Metal Heat Treating	332811
3441	Metal Cans	332431

Table A.1 (continued)

The Standard Industrial Classification (SICS)	Industry	North American Industry Classification System (NAICS)
3469	Metal Stampings, Not Elsewhere Classified	332116
3471	Electroplating, Plating, Polishing, Anodizing, and Coloring	332813
3479	Coating, Engraving, and Allied Services, Not Elsewhere Classified	332812
3496	Miscellaneous Fabricated Wire Products	332618
3499	Fabricated Metal Products, Not Elsewhere Classified	332999
3548	Lighting Equipment, Not Elsewhere Classified	335129
3714	Motor Vehicle Parts and Accessories	336322
3761	Guided Missiles and Space Vehicles	336414
3799	Transportation Equipment, Not Elsewhere Classified	333924
3995	Burial Caskets	339995
3999	Manufacturing Industries, Not Elsewhere Classified	321999, 325998, 326199
4221	Farm product warehousing and storage	493130
4911	Electric Services Establishments engaged in the generation, transmission, and/or distribution of electric energy for sale.	221112
4952	Sanitary treatment facilities	221320
4953	Refuse Systems	562920
5093	Scrap and waste materials	423930
5162	Plastics materials and basic forms and shapes	424610
3644	Noncurrent-Carrying Wiring Devices	335932

Appendix B Examples of dust explosion incidents

Table B.1 Illustrative examples of dust explosion incidents, 1911–2004 [29]

Date	Location	Material	Plant / building	Dead / injured
1785	Turin, Italy	Wheat flour	Bakery	2i
1807	Leiden, The Netherlands	Black powder	Ship	151d/2000i
1911	Glascow, UK	[a]	[a]	5d/8i
1911	Liverpool, UK	[a]	[a]	37d/100i
1911	Manchester, UK	[a]	[a]	3d/5i
1913	Manchester, UK	[a]	[a]	3d/5i
1916	Duluth, MN	Grain	Steel bin	–
1919	Cedar Rapids, IA	Corn starch	Starch plant	43d
1924	Peking, IL	Corn starch	Starch plant	42d
1924	USA	Sulphide dust	[a]	1d/6i
1924	USA	Sulphide dust	[a]	1d/1i
1924	USA	Sulphide dust	[a]	2d/1i
1926	USA	Sulphide dust	[a]	3d/1i
1930	Liverpool, UK	[a]	[a]	11d/32i
1944	Kansas City, KS	Grain dust	[a]	[a]
1949	Port Colbourne, CA	Grain	Steel bin	–
1952	Bound Brook, NJ	Phenolic resin dust	Hammer mill	5d/21i
1952	Saskatchewan	Grain dust	Shipping bin	6d/14i
1955	Waynesboro, GA	Grain dust	Feed plant	3d/13i
1956	South Chicago	Grain dust	Elevator	–

[a] : Details not available.

Table B.1 (continued)

Date	Location	Material	Plant / building	Dead / injured
1958	Kansas City	Grain dust	Elevator	–
1960	Canada	Sulphide dust	[a]	2d/–
1960	Albern, Vienna	Grain dust	[a]	–
1962	St. Louis, MO	Grain dust	Feed plant	3d/13i
1964	Paisley, UK	[a]	[a]	2d/34i
1965	London, UK	Flour	Flour mill	4d/37i
1969	Sweden	Sulphide dust	[a]	2d/1i
1970	Kiel, FRG	Grain dust	Grain silo	6d/18i
1970	Germany	Grain dust	Silos on shipping canal	6d/17i, loss $10 million
1970	Norway	Wheat grain dust	Silo	[a]
1971	New Orleans	Bushel	Elevator	[a]
1972	Norway	Silicon	Milling section	5d/4i
1973	Norway	Aluminum	Mixing vessel	5d/2i
1974	Canada	Sulphide dust	Fox mines	[a]
1974	Preska, South Africa	Sulphide dust	Mines	[a]
1975	Norway	Fish meal	Fish meal grinding plant	1d/1i
1976	Norway	Barley/oats dust	Silo	–
1976	Oslo, Norway	Malted barley dust	Silo	–
1977	Galvesto, TX	Grain dust	Grain silo	15d
1977	Westwego, Louisiana	Grain dust	Grain silo	36d/10i
1979	Lerida, Spain	Grain dust	Grain silo	7d
1979	Canada	Sulphide dust	Ruttan mines	[a]
1980	Germany	Coal	Cement factory	–
1980	Iowa, USA	Corn dust	Bucket elevator	–
1980	Minnesota, USA	Grain dust	Cross tunnel, bucket elevators	13i
1980	Naples, Italy	Grain dust	Grain silo	8i
1980	Ohama, NE, USA	Grain dust	Head house	Loss $3,300,000
1980	St. Joseph, MO, USA	Grain dust	Shipping bin	1d/4i, loss $2,000,000

Table B.1 (continued)

Date	Location	Material	Plant / building	Dead / injured
1981	Canada	Sulphide dust	Mattabi mines	[a]
1981	Corpus Christi, TX	Grain dust	Bucket elevator	9d/30i
1981	Bellwood, NE, USA	Grain dust	Bucket elevator	Loss $6,400,000
1981	Germany	Coal	Coal dust burner plant, cement works	–
1982	British Columbia, Canada	Coal	Silo	–
1983	Anglesey, UK	Aluminum	Aluminum powder production	2i
1984	USA	Caol	Silo	–
1985	Australia	Sulphide dust	Elura mines	[a]
1985	Canada	Sulphide dust	Lynn lake	[a]
1985	Germany	Coal	Silo	1i
1985	Norway	Rape seed flour pellets	Silo	–
1986	Canada	Sulphide dust	Brunswick mines	[a]
1986	Sweden	Sulphide dust	Langsele mines	[a]
1986	Canada	Sulphide dust	Dumugami mines	[a]
1986	Australia	Sulphide dust	Woodlawn	[a]
1987	Canada	Sulphide dust	GECO mines	[a]
1987	China	Textile dust	Dust collection system	58d/177i
1987	Oslo, Norway	Malted barley dust	Silo	–
1988	Norway	Wheat grain dust	Silo	–
1988	Sweden	Coal	Silo	–
1989	Sweden	Palletized wheat bran	Silo	–
1990	Japan	Benzoylperoxide	Storage	9d/17i

Table B.1 (continued)

Date	Location	Material	Plant / building	Dead / injured
1992	Moriya, Japan	Potassium chlorate and aluminum dust	Mixing operation	3d/58i
1994	Okaharu, Japan	Cotton waste	Textile mill	[a]
1994	Tokyo, Japan	Rubber waste	Shoe factory	5d/22i
1997	Japan	Tantalum dust	[a]	1d/1i
1997	Blaye, France	Grain	Storage	11d
1999	Michigan	Coal dust (cause for secondary explosion)	Powerhouse	6d/14i
1999	Massachusetts	Resin	Oven	3d/12i
2000	Japan	Mg–Al alloy		1d/1i
2000	Modesto California	Aluminum dust	[a]	[a]
2002	Mississippi	Rubber	Recycling plant	5d/[a]
2003	Kentucky	Resin	Production line	7d
2003	Kinston, NC	Polyethylene	Pharmaceutical plant	6d/38i
2004	Avon, OH	Lacquer dust	[a]	[a]

Appendix C Experimental results for micron- and nano-sized titanium powder in tabular form

Table C.1 MIT of mixtures of nano and micron Ti

Micron Ti %, by Vol.	0	50	70	90	100
MIT, °C	240	250	260	270	460

Table C.2 MIT of a mixture of nano and micron Ti (50% nano Ti and 50% micron Ti by Vol.)

Temperature, °C	Dust Volume (ml)		
	0.5 ml	1 ml	2 ml
400	-	Ignition	-
350		Ignition	
300	-	Ignition	-
290	-	Ignition	-
280	-	Ignition	-
270	-	Ignition	-
260	-	Ignition	-
250	Ignition	Ignition	Ignition
240	No ignition	No ignition	No ignition
230	No ignition	No ignition	No ignition

Table C.3 MIT of a mixture of nano and micron Ti (10% Nano Ti and 90% micron Ti by Vol.)

Temperature, °C	Dust Volume (ml)		
	0.5 ml	1 ml	2 ml
400	-	Ignition	-
350		Ignition	
300	-	Ignition	-
290	-	Ignition	-
280	-	Ignition	-
270	Ignition	Ignition	Ignition
260	No ignition	No ignition	No ignition
250	No ignition	No ignition	No ignition

Table C.4 MIT of a mixture of nano and micron Ti (30% nano Ti and 70% micron Ti by Vol.)

Temperature, °C	Dust Volume (ml)		
	0.5 ml	1 ml	2 ml
270	-	Explosion	-
260	Ignition	Ignition	Ignition
250	No ignition	No ignition	No ignition
240	No ignition	No ignition	No ignition

Table C.5 MIT of mixtures of nano TiO_2 and nano Ti powder

Nano-TiO2%, by Vol.	0	30	50	70	90
MIT, °C	240	260	280	300	310

Table C.6 MIT of a mixture of nano Ti and nano TiO_2 (70% nano Ti and 30% nano TiO_2 by Vol.)

Temperature, °C	Dust Volume (ml)		
	0.5 ml	1 ml	2 ml
300	-	Ignition	-
290		Ignition	
280	-	Ignition	-
270	-	Ignition	-
260	Ignition	Ignition	Ignition
250	No ignition	No ignition	No ignition
240	-	No ignition	-

Table C.7 MIT of a mixture of nano Ti and nano TiO2 (50% nano Ti and 50% nano TiO_2 by Vol.)

Temperature, °C	Dust Volume (ml)		
	0.5 ml	1 ml	2 ml
400	-	Ignition	-
350		Ignition	
340	-	Ignition	-
330	-	Ignition	-
320	-	Ignition	-
310	-	Ignition	-
300	-	Ignition	-
290	Ignition	Ignition	-
280	No ignition	No ignition	Ignition
270	-	No ignition	No ignition
260	-	-	No ignition

Table C.8 MIT of a mixture of nano Ti and nano TiO2 (30% nano Ti and 70% nano TiO_2 by Vol.)

Temperature, °C	Dust Volume (ml)		
	0.5 ml	1 ml	2 ml
400	-	Ignition	-
350		Ignition	
340	-	Ignition	-
330	-	Ignition	-
320	-	Ignition	-
310	-	Ignition	-
300	Ignition	No ignition	Ignition
290	No ignition	No ignition	No ignition
280	No ignition	-	No ignition

Table C.9 MIT of a mixture of nano Ti and nano TiO2 (10% nano Ti and 90% nano TiO_2 by Vol.)

Temperature, °C	Dust Volume (ml)		
	0.5 ml	1 ml	2 ml
400	-	Ignition	-
350		Ignition	
340	-	Ignition	-
330	-	Ignition	-
320	-	Ignition	-
310	Ignition	Ignition	Ignition
300	No ignition	No ignition	No ignition
290	No ignition	No ignition	No ignition

Table C.10 MIT of mixtures of nano TiO_2 and micron Ti powder

Ti/ TiO_2 (by vol.)	100%: 0%	70%: 30%	60%: 40%	50%: 50%	40%: 60%	30%:70%
MIT, °C	460	500	530	560	580	> 590

Table C.11 MIT of micron Ti powder (100% by Vol.) [24]

Temperature, °C	Dust Volume (ml)		
	0.5 ml	1 ml	2 ml
580	-	Ignition	-
560		Ignition	
540	-	Ignition	-
520	-	Ignition	-
500	-	Ignition	-
480	No Ignition	Ignition	-
460	-	Ignition	No Ignition
450	-	No Ignition	-

Table C.12 MIT of a mixture of nano TiO_2 and micron Ti powder (70% micron Ti and 30% TiO_2 by Vol.)[24]

Temperature, °C	Dust Volume (ml)		
	0.5 ml	1 ml	2 ml
550	-	Ignition	-
500	-	Ignition	-
490	No Ignition	No Ignition	No Ignition
480	-	No Ignition	-

Table C.13 MIT of a mixture of nano TiO_2 and micron Ti powder (60% micron Ti and 40% TiO_2 by Vol.)[24]

Temperature, °C	Dust Volume (ml)		
	0.5 ml	1 ml	2 ml
550	-	Ignition	-
500	-	No Ignition	-
540	-	Ignition	-
530	-	Ignition	-
520	No Ignition	No Ignition	No Ignition
510	-	No Ignition	-

Table C.14 MIT of a mixture of nano TiO_2 and micron Ti powder (50% micron Ti and 50% TiO_2 by Vol.)[24]

Temperature, °C	Dust Volume (ml)		
	0.5 ml	1 ml	2 ml
580	-	Ignition	-
570	-	Ignition	-
560	-	Ignition	-
550	No Ignition	No Ignition	No Ignition
540	-	No Ignition	-

Table C.15 MIT of a mixture of nano TiO_2 and micron Ti powder (40% micron Ti and 60% TiO_2 by Vol.)[24]

Temperature, °C	Dust Volume (ml)		
	0.5 ml	1 ml	2 ml
590	-	Ignition	-
580	-	Ignition	-
570	No Ignition	No Ignition	No Ignition
560	-	No Ignition	-

Table C.16 MIT of a mixture of nano TiO_2 and micron Ti powder (30 % micron Ti and 70% TiO_2 by Vol.)[24]

Temperature, °C	Dust Volume (ml)		
	0.5 ml	1 ml	2 ml
590	No Ignition	No Ignition	No Ignition
580	-	No Ignition	-

Table C.17 Minimum ignition energy data for 60-80 nm Ti powder

Dust Amount	Ignition Energy	Ignition Delay	Inductance	Ignition or (No Ignition)
[mg]	[mJ]	[ms]	[mH]	
600	1	120	0	1
900	1	120	0	1
300	1	120	0	1
150	1	120	0	1
100	1	120	0	1
50	3	120	0	(10)
50	1	120	0	(10)
50	10	120	1	1
50	3	120	1	5
50	1	120	1	3
50	10	120	0	1
100	1	120	0	1
100	1	120	1	1
150	1	120	1	1
300	1	120	1	1
600	1	120	1	1
900	1	120	1	1

Table C.18 Minimum ignition energy data for micron (<20 µm) Ti powder.[24]

Dust Amount	Ignition Energy	Ignition Delay	Inductance	Ignition or (No Ignition)
[mg]	[mJ]	[ms]	[mH]	
2400	10	120	1	1
2400	3	120	1	5
1800	3	120	1	(10)
3000	3	120	1	9
3600	3	120	1	5
3600	1	120	1	3
3000	1	120	1	(10)
3000	1	150	1	(10)
3000	1	90	1	(10)
3000	10	120	0	1
3000	3	120	0	(10)
3600	3	120	0	4
3600	1	120	0	(10)
3000	3	150	0	8
2400	3	150	0	8
1800	3	150	0	(10)
2400	1	150	0	(10)
3000	1	150	0	1
3600	1	150	0	(10)
3600	1	90	0	(10)
2400	1	90	0	(10)
2400	1	120	1	(10)
1800	10	120	1	2
1500	10	120	1	1
1500	3	120	1	(10)
1200	10	120	1	(10)
1200	30	120	1	8

Table C.18 (continued)

Dust Amount	Ignition Energy	Ignition Delay	Inductance	Ignition or (No Ignition)
[mg]	[mJ]	[ms]	[mH]	
900	30	120	1	1
900	10	120	1	(10)
600	30	120	1	(10)
600	100	120	1	(10)
600	300	120	1	1
300	300	120	1	(10)
300	1000	120	1	(10)
1800	10	120	0	1
2400	10	120	0	1
2400	3	120	0	(10)
1800	3	120	0	(10)
1500	3	120	0	(10)
1500	10	120	0	(10)
1500	30	120	0	6
1200	30	120	0	(10)
1200	100	120	0	4
900	100	120	0	(10)
900	300	120	0	5
600	300	120	0	1
600	100	120	0	(10)
300	300	120	0	(10)
300	1000	120	0	(10)

Table C.19 Minimum ignition energy data for a mixture of 10% TiO_2 and 90% micron (<20 µm) Ti powder

Dust Amount	Ignition Energy	Ignition Delay	Inductance	Ignition or (No Ignition)
[mg]	[mJ]	[ms]	[mH]	
2400	3	120	1	(10)
2400	10	120	1	1
3000	3	120	1	(10)
3000	10	120	1	1
3600	3	120	1	(10)
3600	10	120	1	1
1800	10	120	1	1
1800	3	120	1	(10)
1500	10	120	1	(10)
1500	30	120	1	4
1200	30	120	1	(10)
1200	100	120	1	1
900	100	120	1	2
900	30	120	1	(10)
600	100	120	1	1
600	30	120	1	(10)
300	100	120	1	(10)
300	300	120	1	(10)
300	1000	120	1	(10)
1500	10	90	1	(10)
3000	3	90	1	(10)
2400	3	90	1	(10)
1800	3	90	1	(10)
3600	3	90	1	(10)
3000	3	150	1	(10)
1500	10	150	1	(10)
1800	3	150	1	(10)
2400	3	150	1	(10)
3600	3	150	1	(10)

Table C.20 Minimum ignition energy data for a mixture of 30% TiO_2 and 70% micron (<20 µm) Ti powder

Dust Amount	Ignition Energy	Ignition Delay	Inductance	Ignition or (No Ignition)
[mg]	[mJ]	[ms]	[mH]	
3600	10	120	1	1
3600	3	120	1	(10)
2400	30	120	1	1
2400	10	120	1	3
2400	3	120	1	(10)
1800	10	120	1	(10)
1800	30	120	1	5
1500	30	120	1	(10)
1500	100	120	1	2
1200	100	120	1	1
1200	30	120	1	(10)
900	100	120	1	(10)
900	300	120	1	1
600	300	120	1	(10)
600	1000	120	1	2
300	1000	120	1	(10)
3000	10	120	1	3
3000	3	120	1	(10)
1800	10	90	1	(10)
3000	3	90	1	(10)
2400	3	90	1	(10)
3600	3	90	1	(10)
3000	3	150	1	(10)
1800	10	150	1	(10)
2400	3	150	1	(10)
3600	3	150	1	(10)
1500	10	120	1	(10)

Table C.21 Minimum ignition energy data for a mixture of 50% TiO_2 and 50% micron (<20 µm) Ti powder

Dust Amount	Ignition Energy	Ignition Delay	Inductance	Ignition or (No Ignition)
[mg]	[mJ]	[ms]	[mH]	
2400	10	120	1	(10)
2400	30	120	1	(10)
2400	100	120	1	*7*
3000	100	120	1	*5*
3000	30	120	1	(10)
3600	100	120	1	2
3600	30	120	1	(10)
1800	100	120	1	(10)
1800	300	120	1	(10)
1800	1000	120	1	1
1500	1000	120	1	(10)
1800	100	90	1	(10)
2400	30	90	1	(10)
3000	30	90	1	(10)
3600	30	90	1	(10)
3000	30	150	1	(10)
3600	30	150	1	(10)
1800	100	150	1	(10)
2400	30	150	1	(10)
1500	100	120	1	(10)
1200	1000	120	1	(10)
900	1000	120	1	(10)
600	1000	120	1	(10)
300	1000	120	1	(10)

Table C.22 Minimum ignition energy data for a mixture of 70% TiO_2 and 30% micron (<20 µm) Ti powder

Dust Amount	Ignition Energy	Ignition Delay	Inductance	Ignition or (No Ignition)
[mg]	[mJ]	[ms]	[mH]	
2400	1000	120	1	(10)
3000	1000	120	1	(10)
3600	1000	120	1	4
3600	300	120	1	(10)
3600	300	90	1	(10)
3000	1000	90	1	(10)
3000	1000	150	1	(10)
3600	300	150	1	(10)
1800	1000	120	1	(10)
1500	1000	120	1	(10)
1200	1000	120	1	(10)
900	1000	120	1	(10)
600	1000	120	1	(10)
300	1000	120	1	(10)

Table C.23 Minimum ignition energy data for a mixture of 80% TiO_2 and 20% micron (<20 µm) Ti powder

Dust Amount	Ignition Energy	Ignition Delay	Inductance	Ignition or (No Ignition)
[mg]	[mJ]	[ms]	[mH]	
3600	1000	120	1	(10)
3600	1000	90	1	(10)
3600	1000	150	1	(10)
3000	1000	120	1	(10)

Table C.24 Minimum ignition energy data for a mixture of 50% TiO_2 and 50% nano (60-80 nm) Ti powder

Dust Amount	Ignition Energy	Ignition Delay	Inductance	Ignition or (No Ignition)
[mg]	[mJ]	[ms]	[mH]	
900	30	120	1	1
900	10	120	1	1
900	3	120	1	1
900	1	120	1	1
600	3	120	1	1
600	1	120	1	1
300	3	120	1	1
300	1	120	1	1
150	3	120	1	6
150	1	120	1	10
100	3	120	1	1
100	1	120	1	1
50	10	120	1	5
50	3	120	1	(10)
50	1	120	1	(10)
900	1	120	0	1
600	1	120	0	1
300	1	120	0	1
150	1	120	0	2
100	1	120	0	1
50	10	120	0	(10)
50	30	120	0	(10)
50	100	120	0	1

Table C.25 Minimum ignition energy data for a mixture of 70% TiO_2 and 30% nano (60-80 nm) Ti powder

Dust Amount	Ignition Energy	Ignition Delay	Inductance	Ignition or (No Ignition)
[mg]	[mJ]	[ms]	[mH]	
900	10	120	1	1
900	3	120	1	1
900	1	120	1	1
600	1	120	1	1
300	1	120	1	4
150	1	120	1	(10)
150	3	120	1	2
100	3	120	1	(10)
100	10	120	1	(10)
100	30	120	1	(10)
100	300	120	1	1
100	100	120	1	(10)
50	1000	120	1	(10)

Table C.26 Minimum ignition energy data for a mixture of 90% TiO_2 and 10% nano (60-80 nm) Ti powder

Dust Amount	Ignition Energy	Ignition Delay	Inductance	Ignition or (No Ignition)
[mg]	[mJ]	[ms]	[mH]	
900	3	120	1	1
900	1	120	1	(10)
600	3	120	1	(10)
600	10	120	1	(10)
600	30	120	1	(10)
600	100	120	1	1
300	300	120	1	(10)
300	1000	120	1	(10)
150	1000	120	1	(10)
100	1000	120	1	(10)
50	1000	120	1	(10)
900	1	90	1	(10)
900	1	150	1	(10)
900	3	150	1	(10)
900	3	90	1	(10)

Appendix D Experimental results for flocculent materials in tabular form

Table D.1 Explosion likelihood parameters for polyamide 6.6 and polyester

Material	dtex	Length [mm]	MEC [g/m3]	MIE [mJ] (with inductance)	MIT, °C
Polyamide 6.6	1.7	0.5	50	540	485
Polyamide 6.6	3.3	0.5	125	>1000	485
Polyester	1.7	0.5	70	330	495
Polyester	3.3	0.5	70	390	495

Table D.2 Explosion likelihood parameters for polyamide 6.6 with changing length

dtex	Length [mm]	MEC [g/m3]	MIE [mJ] (with inductance)	MIT, °C
3.3	0.3	75	580	475
3.3	0.5	125	>1000	485
3.3	0.75	155	>1000	485
3.3	0.9	160	>1000	485
3.3	1	165	>1000	490

Appendix E Experimental results for hybrid mixtures in tabular form

Table E.1 Explosion pressure, P_m and rate of pressure rise, $(dP/dt)_m$ data for lactose

Dust Concentration	P_m	$(dP/dt)_m$
[g/m³]	[bar]	[bar/s]
250	4.9	66
500	4.2	48
750	5.6	120
1000	6.3	157
1250	6.6	171
1500	6.7	189
1750	7.0	223
2000	7.1	184
2000	7.1	208
2250	7.2	244
2500	7.0	217
2750	6.3	222
2500	6.9	245
2750	7.0	222
2250	7.0	224
1500	6.6	218
1000	6.2	175
3000	6.6	232
2000	7.1	224
1750	6.1	174
2750	6.0	185
1000	6.3	166

Table E.2 Explosion pressure, P_m and rate of pressure rise, $(dP/dt)_m$ data for lactose admixed with methanol in PW condition

Dust Concentration	P_m	$(dP/dt)_m$
[g/m³]	[bar]	[bar/s]
250	4.5	145
500	7.8	390
750	8.1	456
1000	8.0	378
1250	8.0	451
1500	8.0	591
1750	7.6	574
500	7.7	480
750	7.9	462
1000	8.1	550
1250	8.0	564
1500	7.8	500
1750	7.8	512
500	7.5	298
750	7.8	392
1000	7.9	375
1250	7.7	492
1500	7.8	487
1750	7.9	491
2000	8.3	309
2250	7.9	385
2250	7.9	409

Table E.3 Explosion pressure, P_m and rate of pressure rise, $(dP/dt)_m$ data for lactose admixed with ethanol in PW condition

Dust Concentration	P_m	$(dP/dt)_m$
[g/m³]	[bar]	[bar/s]
250	7.0	304
500	8.4	402
750	7.5	370
1000	8.3	444
1250	8.1	510
1500	8.1	550
1750	7.9	548
2000	7.6	549
500	7.9	386
750	8.0	430
1000	8.2	472
1250	8.0	462
1500	8.4	542
1750	8.0	455
500	8.2	416
750	8.4	544
1000	8.4	446
1250	8.1	446
1500	7.9	434
1750	7.7	462
2000	7.5	444

Table E.4 Explosion pressure, P_m and rate of pressure rise, $(dP/dt)_m$ data for lactose admixed with iso-propanol in PW condition

Dust Concentration	P_m	$(dP/dt)_m$
[g/m³]	[bar]	[bar/s]
250	6.8	305
500	8.8	542
750	8.4	506
1000	8.3	470
1250	8.4	466
1500	8.2	448
250	8.4	515
500	7.7	406
750	8.2	552
1000	8.3	499
1250	8.2	449
250	7.7	378
500	7.8	432
750	8.5	470
1000	8.3	447
1250	8.1	496
125	6.3	272

Table E.5 Explosion pressure, P_m and rate of pressure rise, $(dP/dt)_m$ data for lactose admixed with methanol in ATM condition

Dust Concentration	P_m	$(dP/dt)_m$
[g/m³]	[bar]	[bar/s]
750	8.1	450
1000	7.8	568
1250	7.7	458
500	7.9	486
500	6.9	302
750	7.9	496
1000	6.8	158
1000	7.6	500
1250	7.9	574
1500	7.6	540

Table E.6 Explosion pressure, P_m and rate of pressure rise, $(dP/dt)_m$ data for lactose admixed with ethanol in ATM condition

Dust Concentration	P_m	$(dP/dt)_m$
[g/m³]	[bar]	[bar/s]
500	7.2	240
750	7.3	344
1000	6.9	270
1250	7.3	376
1500	7.5	364
1750	7.3	350
1250	7.0	316
1500	7.3	280
1750	7.1	270
1000	7.3	290

Table E.7 Explosion pressure, P_m and rate of pressure rise, $(dP/dt)_m$ data for lactose admixed with iso-propanol in ATM condition

Dust Concentration	P_m	$(dP/dt)_m$
[g/m³]	[bar]	[bar/s]
500	7.7	366
750	7.6	343
1000	7.3	354
1250	7.1	334
250	5.9	228
250	6.1	315
500	8.0	400
750	7.7	340
1000	7.2	260
250	6.9	342
500	7.9	362
750	7.6	332

Table E.8 Explosion pressure, P_m and rate of pressure rise, $(dP/dt)_m$ data for MCC

Dust Concentration	P_m	$(dP/dt)_m$
[g/m³]	[bar]	[bar/s]
250	5.7	218
500	7.6	297
750	6.9	218
1000	8.2	320
1000	7.9	264
1250	8.1	322
1500	8.1	352
1750	8.7	261
2000	7.4	290
1750	7.4	280
1500	7.7	278
1250	8.8	374
1250	8.1	407
1000	7.7	240
1000	8.5	379
1500	8.0	252
750	8.4	357

Table E.9 Explosion pressure, P_m and rate of pressure rise, $(dP/dt)_m$ data for MCC admixed with methanol in PW condition

Dust Concentration	P_m	$(dP/dt)_m$
[g/m³]	[bar]	[bar/s]
250	7.4	546
750	7.4	367
1000	7.6	330
500	7.4	324
1250	7.3	341
100	5.5	177
150	6.7	312
250	7.3	394
500	8.2	565
750	8.0	488
1000	7.5	397
250	7.6	480
500	7.1	309
750	7.8	396
1000	7.7	444

Table E.10 Explosion pressure, P_m and rate of pressure rise, $(dP/dt)_m$ data for MCC admixed with ethanol in PW condition

Dust Concentration	P_m	$(dP/dt)_m$
[g/m³]	[bar]	[bar/s]
150	6.6	161
250	7.2	396
500	7.5	320
750	7.5	424
1000	7.8	457
1250	7.7	386
1500	7.5	395
250	7.6	386
750	7.5	284
1000	7.6	350
1250	7.7	421
1500	7.4	388
1250	7.9	413
1000	7.7	336
1500	7.3	350
250	7.4	352

Table E.11 Explosion pressure, P_m and rate of pressure rise, $(dP/dt)_m$ data for MCC admixed with isopropanol in PW condition

Dust Concentration	P_m	$(dP/dt)_m$
[g/m³]	[bar]	[bar/s]
750	7.6	359
500	7.6	374
1000	7.0	318
250	7.1	298
1250	7.2	325
250	6.9	314
500	7.4	390
750	7.8	432
1000	7.6	430
1250	7.5	432
500	7.7	402
750	7.7	411
1000	7.6	474

Table E.12 Explosion pressure, P_m and rate of pressure rise, $(dP/dt)_m$ data for MCC admixed with methanol in ATM condition

Dust Concentration	P_m	$(dP/dt)_m$
[g/m^3]	[bar]	[bar/s]
250	8.1	483
500	8.1	474
750	7.9	495
1000	7.8	567
1250	7.5	520
1500	7.4	522
1750	6.9	555
125	7.8	415
250	7.5	488
500	7.8	468
750	7.6	512
1000	7.7	666
1250	7.6	616
250	7.3	394
500	8.0	594
750	7.8	624
1000	7.8	610
1250	7.5	620

Table E.13 Explosion pressure, P_m and rate of pressure rise, $(dP/dt)_m$ data for MCC admixed with ethanol in ATM condition

Dust Concentration	P_m	$(dP/dt)_m$
[g/m³]	[bar]	[bar/s]
250	6.8	260
500	7.9	386
750	8.2	540
1000	8.2	526
1250	7.8	412
250	7.2	230
500	8.0	262
1000	8.2	586
1250	8.2	480
500	8.3	518
750	8.0	458
1000	7.8	514
250	7.5	374
750	8.3	452

Table E.14 Explosion pressure, P_m and rate of pressure rise, $(dP/dt)_m$ data for MCC admixed with iso-propanol in ATM condition

Dust Concentration	P_m	$(dP/dt)_m$
[g/m^3]	[bar]	[bar/s]
250	7.5	426
500	8.5	500
750	8.1	592
1000	7.8	551
1250	7.3	481
250	8.2	516
500	8.3	509
750	8.0	640
1000	7.9	532
250	7.9	591
500	8.3	517
750	8.0	671
1000	7.6	664

Table E.15 Minimum ignition energy data for lactose

Dust Amount	Ignition Energy	Ignition Delay	Inductance	Ignition or (No Ignition)
[mg]	[mJ]	[ms]	[mH]	
1200	1000	120	1	1
600	1000	120	1	1
150	1000	120	1	(10)
300	1000	120	1	1
3600	1000	120	1	2
600	100	120	1	(10)
600	300	120	1	5
300	300	120	1	(10)
1200	300	120	1	3
1200	100	120	1	(10)
1500	100	120	1	1
1500	30	120	1	(10)
1800	30	120	1	(10)
1800	100	120	1	3
3000	30	120	1	(10)
3000	100	120	1	(10)
2400	100	120	1	9
2400	30	120	1	(10)
3600	100	120	1	3
3600	30	120	1	(10)
2400	1000	120	1	3
1500	30	90	1	(10)
1200	100	90	1	4
900	100	90	1	6
600	100	90	1	6
300	100	90	1	(10)
600	30	90	1	(10)
3000	100	90	1	(10)

Table E.15 (continued)

Dust Amount	Ignition Energy	Ignition Delay	Inductance	Ignition or (No Ignition)
[mg]	[mJ]	[ms]	[mH]	
3000	30	90	1	(10)
300	100	150	1	(10)
600	30	150	1	(10)
1200	1000	120	0	4
900	1000	120	0	(10)
900	300	120	0	(10)
1200	300	120	0	(10)
1500	1000	120	0	2
1500	300	120	0	(10)
1800	1000	120	0	2
1800	300	120	0	(10)
2400	1000	120	0	2
2400	300	120	0	10
2400	100	120	0	(10)
3000	300	120	0	(10)
3000	1000	120	0	2
1800	300	90	0	(10)
2400	100	90	0	(10)
3000	300	90	0	(10)
3000	300	150	0	(10)
2400	100	150	0	(10)
1800	300	150	0	(10)

Table E.16 Minimum ignition energy data for lactose admixed with methanol in PW condition

Dust Amount	Ignition Energy	Ignition Delay	Inductance	Ignition or (No Ignition)
[mg]	[mJ]	[ms]	[mH]	
600	100	120	1	2
300	100	120	1	(10)
600	30	120	1	(10)
900	30	120	1	(10)
900	100	120	1	1
1500	100	120	1	1
1500	30	120	1	(10)
2400	100	120	1	3
2400	30	120	1	8
2400	10	120	1	(10)
1800	30	120	1	2
3000	30	120	1	1
3600	10	120	1	(10)
3600	30	120	1	2
3000	10	120	1	(10)
1800	10	120	1	(10)
300	10	90	1	(10)
300	100	90	1	(10)
600	30	90	1	(10)
1500	30	90	1	(10)
1800	10	90	1	(10)
3600	10	90	1	(10)
3600	10	150	1	(10)
1800	10	150	1	(10)
600	30	150	1	(10)
300	100	150	1	(10)
600	1000	120	0	9

Table E.16 (continued)

Dust Amount	Ignition Energy	Ignition Delay	Inductance	Ignition or (No Ignition)
[mg]	[mJ]	[ms]	[mH]	
600	300	120	0	(10)
300	1000	120	0	(10)
900	300	120	0	7
900	100	120	0	(10)
1200	100	120	0	(10)
1200	300	120	0	2
1500	300	120	0	1
1800	300	120	0	(10)
1500	100	120	0	(10)
1800	1000	120	0	1
1800	300	150	0	2
1800	100	150	0	(10)
900	100	150	0	(10)
600	300	150	0	(10)
300	1000	150	0	(10)
300	1000	90	0	(10)
900	100	90	0	(10)
2400	300	150	0	1
3000	300	150	0	2
3600	300	150	0	6
2400	100	150	0	(10)
3000	100	150	0	(10)
3600	100	150	0	(10)
1800	100	90	0	(10)
3600	100	90	0	(10)

Table E.17 Minimum ignition energy data for lactose admixed with ethanol in PW condition

Dust Amount	Ignition Energy	Ignition Delay	Inductance	Ignition or (No Ignition)
[mg]	[mJ]	[ms]	[mH]	
300	300	120	1	(10)
600	300	120	1	1
600	100	120	1	(10)
900	300	120	1	1
900	100	120	1	1
900	30	120	1	(10)
1200	30	120	1	(10)
1800	100	120	1	2
1800	30	120	1	(10)
3000	100	120	1	4
3000	30	120	1	(10)
3600	30	120	1	(10)
3600	100	120	1	3
600	100	90	1	1
300	100	90	1	(10)
600	30	90	1	(10)
1800	30	90	1	(10)
3600	30	90	1	(10)
3600	30	150	1	1
3600	10	150	1	(10)
3000	30	150	1	2
2400	30	150	1	(10)
600	30	150	1	(10)
300	100	150	1	(10)
900	1000	120	0	3
600	1000	120	0	(10)
900	300	120	0	(10)

Table E.17 (continued)

Dust Amount	Ignition Energy	Ignition Delay	Inductance	Ignition or (No Ignition)
[mg]	[mJ]	[ms]	[mH]	
1200	300	120	0	6
1200	100	120	0	(10)
1500	100	120	0	(10)
1500	300	120	0	1
2400	300	120	0	(10)
1800	300	120	0	(10)
1800	1000	120	0	5
2400	1000	120	0	2
600	1000	90	0	2
300	1000	90	0	(10)
600	300	90	0	(10)
1200	100	90	0	(10)
2400	300	90	0	(10)
300	1000	150	0	(10)
1500	100	150	0	(10)
2400	300	150	0	(10)

Table E.18 Minimum ignition energy data for lactose admixed with isopropanol in PW condition

Dust Amount	Ignition Energy	Ignition Delay	Inductance	Ignition or (No Ignition)
[mg]	[mJ]	[ms]	[mH]	
600	1000	120	1	1
300	1000	120	1	2
300	300	120	1	(10)
600	300	120	1	6
600	100	120	1	2
600	30	120	1	(10)
900	30	120	1	(10)
900	100	120	1	2
1200	100	120	1	1
1200	30	120	1	2
1200	10	120	1	(10)
1800	30	120	1	1
1800	10	120	1	(10)
3000	30	120	1	1
3000	10	120	1	(10)
3600	10	120	1	(10)
3600	30	120	1	1
2400	30	120	1	2
2400	10	120	1	(10)
1500	30	120	1	2
1500	10	120	1	(10)
300	300	90	1	1
300	100	90	1	1
300	30	90	1	(10)
900	30	90	1	(10)
1200	10	90	1	(10)
3600	10	90	1	(10)

Table E.18 (continued)

Dust Amount	Ignition Energy	Ignition Delay	Inductance	Ignition or (No Ignition)
[mg]	[mJ]	[ms]	[mH]	
3600	10	150	1	(10)
300	30	150	1	(10)
900	30	150	1	(10)
1200	10	150	1	(10)
600	1000	120	0	(10)
900	1000	120	0	5
900	300	120	0	1
900	100	120	0	(10)
1200	100	120	0	(10)
1200	300	120	0	1
1500	300	120	0	3
1500	100	120	0	(10)
1800	300	120	0	(10)
1800	1000	120	0	2
2400	1000	120	0	2
2400	300	120	0	(10)
600	300	90	0	1
600	100	90	0	(10)
300	300	90	0	(10)
1500	100	90	0	(10)
1800	300	90	0	(10)
300	300	150	0	(10)
600	100	150	0	(10)
1500	100	150	0	(10)
1800	300	150	0	(10)

Table E.19 Minimum ignition energy data for MCC

Dust Amount	Ignition Energy	Ignition Delay	Inductance	Ignition or (No Ignition)
[mg]	[mJ]	[ms]	[mH]	
1200	100	120	1	(10)
1200	1000	120	1	1
1200	300	120	1	8
900	300	120	1	8
900	100	120	1	(10)
600	300	120	1	1
600	100	120	1	(10)
300	300	120	1	5
1500	100	120	1	(10)
1500	300	120	1	(10)
300	100	120	1	(10)
300	100	150	1	1
900	100	150	1	(10)
300	30	150	1	(10)
600	100	150	1	(10)
300	30	180	1	(10)
600	100	180	1	(10)
300	30	180	1	(10)
600	100	90	1	(10)
300	30	90	1	(10)
1200	1000	120	0	(10)
900	1000	120	0	(10)
600	1000	120	0	(10)
300	1000	120	0	(10)
1500	1000	120	0	(10)
2400	1000	120	0	2
1800	1000	120	0	(10)
1800	300	120	0	(10)

Table E.19 (continued)

Dust Amount	Ignition Energy	Ignition Delay	Inductance	Ignition or (No Ignition)
[mg]	[mJ]	[ms]	[mH]	
3000	1000	120	0	1
3600	1000	120	0	3
3000	300	120	0	(10)
3600	300	120	0	(10)
2400	300	90	0	(10)
1800	1000	90	0	5
1500	1000	90	0	1
1800	1000	90	0	(10)
1200	1000	90	0	(10)
1500	300	90	0	(10)
3600	300	90	0	(10)
3600	1000	90	0	10
1500	300	150	0	(10)
2400	300	150	0	(10)
3600	300	150	0	(10)
3600	1000	150	0	1
1200	1000	150	0	10
900	1000	150	0	(10)

Table E.20 Minimum ignition energy data for MCC admixed with methanol in PW condition

Dust Amount	Ignition Energy	Ignition Delay	Inductance	Ignition or (No Ignition)
[mg]	[mJ]	[ms]	[mH]	
1200	100	120	1	5
1200	30	120	1	(10)
900	100	120	1	(10)
900	300	120	1	1
600	300	120	1	1
600	100	120	1	(10)
300	300	120	1	2
300	100	120	1	(10)
1500	100	120	1	6
1200	30	120	1	(10)
1500	30	120	1	(10)
2400	100	120	1	(10)
1800	100	120	1	10
1800	30	120	1	(10)
2400	30	120	1	(10)
2400	300	120	1	(10)
2400	1000	120	1	1
900	100	150	1	1
900	30	150	1	(10)
600	30	150	1	(10)
600	100	150	1	4
300	100	150	1	7
300	30	150	1	(10)
2400	100	150	1	(10)
1800	30	150	1	(10)
150	100	150	1	(10)
150	100	90	1	(10)
300	30	90	1	(10)
1800	30	90	1	(10)

Table E.20 (continued)

Dust Amount	Ignition Energy	Ignition Delay	Inductance	Ignition or (No Ignition)
[mg]	[mJ]	[ms]	[mH]	
2400	100	90	1	*5*
2400	30	90	1	(10)
3000	100	90	1	(10)
900	100	120	0	(10)
900	1000	120	0	(10)
1200	1000	120	0	1
1200	300	120	0	(10)
1500	1000	120	0	1
1500	300	120	0	(10)
1800	1000	120	0	1
1800	300	120	0	(10)
2400	300	120	0	(10)
2400	1000	120	0	1
3000	1000	120	0	1
3000	300	120	0	(10)
3600	300	120	0	(10)
3600	1000	120	0	1
900	1000	90	0	1
900	300	90	0	(10)
600	1000	90	0	1
600	1000	90	0	1
600	300	90	0	(10)
300	1000	90	0	*5*
300	300	90	0	1
3600	300	90	0	(10)
3600	1000	90	0	2
3600	1000	150	0	3
3600	300	150	0	(10)
300	300	150	0	(10)

Table E.20 (continued)

Dust Amount	Ignition Energy	Ignition Delay	Inductance	Ignition or (No Ignition)
[mg]	[mJ]	[ms]	[mH]	
300	1000	150	0	1
300	100	90	0	7
300	30	90	0	(10)
600	100	90	0	(10)
300	30	90	0	(10)
300	30	120	0	(10)
300	30	90	0	(10)
300	30	120	1	(10)

Table E.21 Minimum ignition energy data for MCC admixed with ethanol in PW condition

Dust Amount	Ignition Energy	Ignition Delay	Inductance	Ignition or (No Ignition)
[mg]	[mJ]	[ms]	[mH]	
300	300	90	1	1
300	100	90	1	1
300	30	90	1	9
300	10	90	1	(10)
600	30	90	1	(10)
600	100	90	1	2
900	100	90	1	4
900	30	90	1	(10)
1200	100	90	1	5
1200	30	90	1	(10)
1500	100	90	1	1
1500	30	90	1	(10)
2400	100	90	1	(10)
1800	100	90	1	(10)
300	10	120	1	(10)
300	30	120	1	(10)
600	30	120	1	(10)
1500	30	120	1	(10)
1800	100	120	1	3
1800	30	120	1	(10)
2400	100	120	1	(10)
300	10	150	1	(10)
150	30	90	1	(10)
150	30	120	1	(10)
150	30	150	1	(10)
1800	30	150	1	(10)
2400	100	150	1	6

Table E.21 (continued)

Dust Amount	Ignition Energy	Ignition Delay	Inductance	Ignition or (No Ignition)
[mg]	[mJ]	[ms]	[mH]	
2400	30	150	1	(10)
3000	100	150	1	(10)
600	1000	120	0	(10)
900	1000	120	0	(10)
1200	1000	120	0	1
1200	300	120	0	(10)
1500	1000	120	0	1
1500	300	120	0	(10)
1800	1000	120	0	1
2400	1000	120	0	2
3000	1000	120	0	1
3600	1000	120	0	1
3600	300	120	0	(10)
3000	300	120	0	(10)
2400	300	120	0	(10)
1200	300	120	0	(10)
1800	300	120	0	(10)
900	1000	90	0	1
600	1000	90	0	*5*
300	1000	90	0	1
300	300	90	0	(10)
600	300	90	0	(10)
900	300	90	0	(10)
3600	1000	90	0	1
3600	300	90	0	(10)
3600	300	150	0	(10)
3600	1000	150	0	3
300	1000	150	0	(10)
600	300	150	0	(10)
300	30	90	1	(10)
300	30	90	1	(10)

Table E.22 Minimum ignition energy data for MCC admixed with isopropanol in PW condition

Dust Amount	Ignition Energy	Ignition Delay	Inductance	Ignition or (No Ignition)
[mg]	[mJ]	[ms]	[mH]	
1200	1000	120	1	1
1200	300	120	1	1
1200	100	120	1	1
1200	30	120	1	(10)
1500	100	120	1	(10)
300	300	120	1	1
300	100	120	1	*5*
300	30	120	1	(10)
900	100	120	1	1
900	30	120	1	(10)
150	100	120	1	1
150	30	120	1	(10)
600	30	120	1	(10)
600	100	90	1	1
600	30	90	1	(10)
150	100	90	1	(10)
150	30	150	1	(10)
150	30	90	1	(10)
1500	30	90	1	(10)
1500	100	90	1	(10)
1500	30	150	1	(10)
1500	100	150	1	(10)
150	100	150	1	(10)
600	300	150	1	1
600	100	150	1	8
600	100	120	1	6
600	100	120	0	(10)

Table E.22 (continued)

Dust Amount	Ignition Energy	Ignition Delay	Inductance	Ignition or (No Ignition)
[mg]	[mJ]	[ms]	[mH]	
600	300	120	0	(10)
600	1000	120	0	7
300	1000	120	0	(10)
900	1000	120	0	6
900	300	120	0	(10)
1200	1000	120	0	2
1200	100	120	0	(10)
1500	300	120	0	2
1500	100	120	0	(10)
1800	300	120	0	2
2400	300	120	0	(10)
1800	100	120	0	(10)
1800	100	90	0	(10)
2400	300	90	0	(10)
2400	300	150	0	(10)
1800	100	150	0	(10)
300	1000	150	0	(10)
600	300	150	0	(10)
300	1000	90	0	8
300	300	90	0	(10)
150	1000	90	0	(10)

Table E.23 Test results for MIT of pharmaceutical lactose powder

Temperature, °C	Dust Volume (ml)		
	1 ml	2 ml	0.5 ml
530	Ignition		
520	Ignition		
510	Ignition		
500	Ignition		
490	Ignition		
480	Ignition		
470	Ignition	Ignition	
460	Ignition	Ignition	
450	Ignition	Ignition	Ignition
440	Ignition	Ignition	Ignition
430	Ignition	Ignition	No Ignition
420	No Ignition	Ignition	No Ignition
410	No Ignition	No Ignition	No Ignition
400		No Ignition	

Table E.24 Test results for MIT of MCC Powder

Temperature, °C	Dust Volume (ml)		
	1 ml	2 ml	0.5 ml
530	Ignition		
520	Ignition		
510	Ignition		
500	Ignition		
490	Ignition		
480	Ignition		
470	Ignition		
460	Ignition	Ignition	
450	Ignition	Ignition	Ignition
440	No Ignition	Ignition	No Ignition
430	Ignition	Ignition	Ignition
420	No Ignition	No Ignition	No Ignition
410	No Ignition	No Ignition	No Ignition

Table E.25 Test results for MIT of MCC powder with methanol

Temperature, °C	Dust Volume (ml)		
	1 ml	2 ml	0.5 ml
450	Ignition		
440	Ignition	Ignition	Ignition
430	Ignition	Ignition	Ignition
420	Ignition	Ignition	Ignition
410	Ignition	Ignition	Ignition
400	Ignition	Ignition	Ignition
390	No Ignition	Ignition	No Ignition
380	Ignition	No Ignition	No Ignition
370	No Ignition	No Ignition	No Ignition
360	No Ignition		

Table E.26 Test results for MIT of MCC powder with ethanol

Temperature, °C	Dust Volume (ml)		
	1 ml	**2 ml**	**0.5 ml**
450	Ignition		
440	Ignition	Ignition	Ignition
430	Ignition	Ignition	Ignition
420	Ignition	No Ignition	Ignition
410	No Ignition	Ignition	No Ignition
400	No Ignition	No Ignition	No Ignition
390		No Ignition	

Table E.27 Test results for MIT of MCC powder with isopropanol

Temperature, °C	Dust Volume (ml)		
	1 ml	**2 ml**	**0.5 ml**
450	Ignition		Ignition
440	Ignition	Ignition	Ignition
430	Ignition	Ignition	Ignition
420	No Ignition	Ignition	Ignition
410	No Ignition	No Ignition	Ignition
400		No Ignition	Ignition
390			No Ignition
380			No Ignition

Table E.28 Test results for MIT of pharmaceutical lactose powder with methanol

Temperature, °C	Dust Volume (ml)		
	1 ml	2 ml	0.5 ml
450	Ignition		
440	Ignition		
430	Ignition	Ignition	Ignition
420	Ignition	Ignition	Ignition
410	Ignition	Ignition	Ignition
400	Ignition	Ignition	Ignition
390	Missed	Ignition	Ignition
380	Ignition	Ignition	Ignition
370	Ignition	Ignition	Ignition
360	Ignition	Ignition	Ignition
350	No Ignition	Ignition	No Ignition
340	No Ignition	No Ignition	No Ignition

Table E.29 Test results for MIT of pharmaceutical lactose powder with ethanol

Temperature, °C	Dust Volume (ml)		
	1 ml	**2 ml**	**0.5 ml**
450	Ignition		
440	Ignition		Ignition
430	Ignition	Ignition	Ignition
420	Ignition	Ignition	Ignition
410	Ignition	Ignition	Ignition
400	Ignition	Ignition	Ignition
390	No Ignition	Ignition	Ignition
380	No Ignition	No Ignition	Ignition
370		No Ignition	No Ignition
360			No Ignition

Table E.30 Test results for MIT of pharmaceutical lactose powder with isopropanol

Temperature, °C	Dust Volume (ml)		
	1 ml	2 ml	0.5 ml
450	Ignition		
440	Ignition	Ignition	Ignition
430	Ignition	Ignition	Ignition
420	Ignition	Ignition	Ignition
410	Ignition	Ignition	Ignition
400	Ignition	Ignition	Ignition
390	No Ignition	No Ignition	No Ignition
380	No Ignition	No Ignition	No Ignition

Appendix F MIT test procedures for titanium powders

1) Turn on the fume hood, close the elephant trunk, and turn on the BAM Oven. Set the temperature of oven at the predetermined value.

2) Wait for desired temperature.

3) Open a glass vial, and place 1 ml of premeasured sample with one percentage of TiO_2 and Ti powder in the dispersion nozzle. (One day, only one sample concentration tested.)

4) Connect dispersion nozzle to the rubber bulb.

5) Insert the dispersion nozzle into the oven inlet and disperse the sample with a blast of air by squeezing the rubber bulb.

6) Observe there exist a flame exiting the flap at the rear of the oven or not.

7) If a flame is seen, the temperature is recorded and reduced by 10 °C and then tested at the lower temperature until no flames occurs.

8) Repeat step 2-7 for 2 ml and 0.5 ml premeasured sample of the same concentration.

9) Cool down and clean BAM oven.

10) Collect post-test material from oven and fume hood into a clean open container using clean spatula.

11) Stabilize the left over test material as per "Powder Titanium Combustion Test Procedure."

12) Leave neutralized Ti powder in waste containers with lids on, but not screwed closed tight in the fume hood (turned on) over night. Next day close waste container and remove to chemical waste storage locker.

Appendix G MIE test procedures for titanium powders

1) Turn on the vent hood and MIKE 3.
2) Set and enter experiment conditions (sample mass, inductance, ignition energy, and delay time) using MIKE 3.3 software.
3) Open glass vial, and place premeasured sample into the dispersion cup.
4) Initiate the dispersion and ignition sequence in glass tube using MIKE 3.3 software.
5) Observe there exist a flame in the glass tube or not.
6) Whether sample is ignited or not, collect post-test material from the dispersion cup by using clean spatula and put it in a clean open container. Take the container to the fume hood and stabilize powder titanium material inside by adding 2 g of Ti powder to 150 ml of water, mix solution and then dispense solution in to waste container.
7) Do MIKE 3 test at another experiment condition until all schedule MIE test are finished for the day.
8) After all scheduled MIE tests are finished for the day, shut down the test apparatus, and close the compressed air cylinder.
9) Stabilize the left over test material as per "Powder Titanium Combustion Test Procedure."
10) Leave neutralized Ti powder in waste containers with lids on, but not screwed closed tight in the fume hood (turned on) over night. Next day close waste container and remove to chemical waste storage locker.